

An investigation into the subcellular localisation of nonstructural protein NS3 of African horsesickness virus

by

Tracey-Leigh Hatherell

Submitted in partial fulfilment of the requirements for the degree

Magister Scientiae

in the Faculty of Natural and Agricultural Science

University of Pretoria

Pretoria

April 2007

Under the supervision of Dr. V. van Staden and Prof. H. Huisman



Declaration

I, the undersigned, hereby declare that the dissertation submitted herewith for the degree *Magister Scientiae* to the University of Pretoria contains my own independent work and has not been submitted for any degree at any other university.

Tracey-Leigh Hatherell

April 2007

ACKNOWLEDGEMENTS

I would like to express my gratitude to the following people for assisting me in the completion of this project:

- To Dr V. van Staden for her professional leadership of this project. Thank you for your unlimited patience and excellent advice.
- To Prof H. Huismans for teaching me to think scientifically and to critically assess my own work.
- To the Genetics Department of the University of Pretoria for providing a sound academic environment.
- To the sequencing facility at the University of Pretoria, Renate Zipfel, Gladys Shabangu and Mia Beyleveld for fast and efficient service, dedication and valuable advice during the course of this project.
- To the National Research Foundation of South Africa (NRF) for funding supplied by the grant holder-linked scholarship.
- To Mr Alan Hall at the Laboratory for Microscopy and Microanalysis at the University of Pretoria for hours of assistance with both the Fluorescent microscope and the Confocal microscope.
- To Mr Flip Wege for helping out with everything related to cell culture.
- To all past and present members of Team Viro, especially Michelle van Niekerk, Tracy Meiring, Tumelo Seameco, Rencia Appelgryn, Britta Heinbockel, Tamlyn Cramer, Carel Smit, Mia Beyleveld, Karen De Lange, Jeanne Korsman, Eshchar Mizrachi and Luisa Teixeira for maintaining a stimulating and productive environment in which to work.
- To my family: Dad, Mom, Bruce, Nick, Mike and David, thank you for always being there for me, for the financial and emotional support you have given me and for moulding me into the person I am today.
- To my friends, especially Alex, Ouma, Vin, Joha, Rencia, Esh and Jo Jo, for all of the good times we've shared and for keeping me sane (I think) during this process.
- To Karl, for all of the love and support you have given me over the past two years.



UNIVERSITEIT VAN PRETORIA
UNIVERSITY OF PRETORIA
YUNIBESITHI YA PRETORIA

Dedicated to my parents, Thelton and Pam Hatherell



List of Buffers

Hypotonic buffer:

10 mM Tris, 0.2 mM MgCl₂ [pH 7.4]

NTE:

100 mM NaCl, 10 mM Tris, 1 mM EDTA [pH 7.4]

PBS:

137 mM NaCl, 2.7 mM KCl, 4.3 mM Na₂HPO₄·7H₂O, 1.4 mM KH₂PO₄ [pH 7.3]

Protein solvent buffer (PSB) (2×):

0.125 M Tris-HCl [pH 6.8], 4% SDS, 20% glycerol, 10% 2-mercaptoethanol

TAE buffer:

0.04 M Tris-acetate, 0.002 M EDTA [pH 8.5]

TE buffer:

0.01 M Tris-HCl [pH 7.6], 0.001 M EDTA

TGS buffer:

0.025 M Tris-HCl [pH 8.3], 0.192 M glycine, 0.1% SDS



Abbreviations

aa/AA	amino acids
AHS	African horsesickness
AHSV	African horsesickness virus
AHSV-3	African horsesickness virus serotype 3
AHSV-2	African horsesickness virus serotype 2
ATCC	American type culture collection
bp	base pairs
BTV	bluetongue virus
°C	degrees Celsius
CLP	core-like particle
Da	Dalton
DAPI	4'6'-diamidino-2-phenylindole
ddH ₂ O	deionised distilled water
dNTP	deoxynucleotidyl-triphosphate
DMSO	dimethyl sulphoxide
DNA	deoxyribonucleic acid
DRMs	detergent resistant membrane fractions
ds	double-stranded
dsRNA	double-stranded ribonucleic acid
EDTA	ethylenediaminetetra-acetic acid
eGFP	enhanced Green Fluorescent Protein
e.g.	<i>exempli gratia</i> (for example)
EHDV	epizootic hemorrhagic disease virus
ER	endoplasmic reticulum
<i>et al.</i>	<i>et alia</i> (and others)
etc.	<i>et cetera</i> (and so forth)
EtBr	ethidium bromide
FCS	fetal calf serum
FITC	α -rabbit-fluorescein isothiocyanate
g	gravitational force
G	gauge
Gent	gentamycin
GFP	Green Fluorescent Protein
h	hour/s
HD	hydrophobic domain

h.p.i.	hours post infection
ICTV	International Committee for the Taxonomy of Viruses
i.e.	<i>id est</i> (that is to say)
IPTG	isopropyl- β -D-thiogalactopyranoside
k	kilo
kan	kanamycin
kb	kilobasepairs
kDa	kilodalton
L1-L3	large segments 1 to 3 (refers to orbiviruses)
LB	Luria broth
M4-M6	medium segments 4 to 6 (refers to orbiviruses)
M	molar
ml	millilitre
mM	millimolar
mmol	millimole
MOI	multiplicity of infection
mRNA	messenger ribonucleic acid
MTT	3-[4,5-dimethylthiazol-2-yl]-2,5-diphenyltetrazolium bromide
ng	nanograms
nm	nanometers
NS	non-structural
NS1, NS2, NS3, NS3A	nonstructural proteins 1,2, 3 or 3A (refers to orbivirus)
NSP4	nonstructural protein 4 (refers to rotavirus)
OVI	Onderstepoort Veterinary Institute
PAGE	polyacrylamide gel electrophoresis
PBS	phosphate buffered saline
pBS	BlueScribe plasmid
PCR	polymerase chain reaction
pFB	FastBac plasmid
pfu	plaque forming units
p.i.	post infection
pmol	picomole
PSB	protein solvent buffer
RFU	Relative Fluorescent Units
RNA	ribonucleic acid
rpm	revolutions per minute
S7-S10	small segments 7 to 10 (refers to orbiviruses)

SA	South Africa
SDS	sodium dodecyl sulphate
Sf9	<i>Spodoptera frugiperda</i> insect cells
ss	single-stranded
ssRNA	single-stranded ribonucleic acid
TE	Tris EDTA
tet	tetracycline-hydrochloride
TM	transmembrane
Tris	Tris-hydroxymethyl-aminomethane
µg	microgram
µl	microlitre
µm	micrometers
U	units
UP	University of Pretoria
UV	ultraviolet
V	volts
VIB	viral inclusion body
VLP	virus-like particle
VMP	viral membrane protein
VP1-7	virus protein 1 to 7 (refers to orbiviruses)
X-Gal	5-Bromo-4-chloro-3-indolyl-β-D-galactopyranoside

An investigation into the subcellular localisation of nonstructural protein NS3 of African horsesickness virus

Tracey-Leigh Hatherell

Supervisor: Dr. V. van Staden

Co-supervisor: Prof. H. Huismans

Department of Genetics

Submitted in partial fulfilment of the requirements for the degree *Magister Scientiae*

Summary

African horsesickness virus (AHSV) is a double-stranded RNA virus belonging to the *Orbivirus* genus in the *Reoviridae* family (Bremer *et al.*, 1990; Calisher and Mertens, 1998). The virus is highly pathogenic and its mortality rate in horses, the most susceptible species, may be as high as 95% (House, 1993). S10, the smallest genome segment of AHSV, codes for two proteins (NS3 and NS3A) from in-phase overlapping reading frames. The C-terminal sequences of these proteins are identical, but NS3A lacks the first 10 amino acids present on the N-terminal of NS3 (Van Staden and Huismans, 1991).

Nonstructural protein NS3 is a membrane protein, associated with both smooth intracellular membranes and the plasma membrane. NS3 has pleiotropic roles in the viral life cycle including the transport and release of mature virions and viroporin-like alteration of cell membrane permeability. NS3 is cytotoxic when expressed in bacterial or insect cells, and is speculated to play a vital role in viral virulence and disease pathogenesis (Stoltz *et al.*, 1996; Van Staden *et al.*, 1995).

A number of different domains that could mediate the membrane interaction or intracellular trafficking of NS3 have been identified. The relative contributions of these domains in insect and mammalian cells are not known, but could differ, as there are distinct differences in NS3 expression levels, cytopathic effects and virus release mechanisms in these two cell types.

In order to investigate the subcellular localisation of NS3, a number of full-length, truncated or mutant versions of AHSV-3 NS3 were constructed as C-terminal eGFP (enhanced green fluorescent protein) fusion proteins. These proteins were used to generate recombinant baculoviruses for expression in *Spodoptera frugiperda* (Sf9) insect cells and were compared in terms of their subcellular localisation by conventional fluorescence microscopy. Confocal laser

microscopy was used to investigate co-localisation with the nucleus, the Golgi apparatus and the Endoplasmic Reticulum (ER). Subcellular fractionations and membrane flotation analyses were used to confirm membrane interactions and to identify detergent-resistant membrane fractions.

NS3 as well as a C-terminal deletion of NS3 targeting a putative dileucine motif both localised to cellular/nuclear membrane components. In contrast, site-specific mutations to either of the transmembrane domains abolished membrane association and resulted in cytoplasmic localisation. NS3A showed mixed results, displaying both membrane localisation and a cytoplasmic distribution. The 11 amino acid region unique to NS3 and absent from NS3A, which has been shown to bind to cellular exocytosis proteins in bluetongue virus (Beaton *et al.*, 2002), did not display membrane interaction. These results indicate that both of the hydrophobic domains as well as the N11 region are required to be present for NS3 to be properly targeted to the plasma/nuclear membrane. In addition, NS3 was shown to be present in detergent-resistant membrane fractions, indicative of a possible localisation within lipid rafts.

The above results indicate that the NS3 protein contains specific signals involved in membrane targeting, confirming a potential role for NS3 in viral localisation and release in the AHSV replication cycle.



Contents

<u>Chapter 1: Literature Review</u>	1
1.1. Introduction	1
1.2. African Horsesickness Virus	2
1.2.1. Pathology of African Horsesickness	2
1.2.2. Prevention and Control	3
1.2.3. African Horsesickness Virus Structure	3
1.2.3.1. Structural Proteins	5
1.2.3.1.1. Outer capsid proteins	5
1.2.3.1.2. Inner capsid proteins	6
1.2.3.2. Nonstructural Proteins	8
1.3. Orbivirus entry, replication and release	12
1.4. African Horsesickness Virus NS3 protein analogues in the <i>Reoviridae</i> family	14
1.4.1. Rotavirus NSP4	14
1.5. General mechanisms for subcellular trafficking and localisation of proteins	17
1.5.1. Viral membrane proteins	21
1.6. Green Fluorescent Protein (GFP)	25
1.7. Aims of this study	29
<u>Chapter 2</u>	30
2.1. Introduction	30
2.2. Materials and Methods	31
2.2.1. Construction of fusion proteins	31



2.2.1.1. Materials obtained	31
2.2.1.2. Agarose gel electrophoresis	32
2.2.1.3. Plasmid DNA isolation	32
2.2.1.4. PCR amplification	33
2.2.1.5. Construction of the N11 region	34
2.2.1.6. Restriction endonuclease digestions	35
2.2.1.7. Purification of DNA fragments	35
2.2.1.8. Ligation of DNA fragments	36
2.2.1.9. Preparation of competent XL1Blue <i>E. coli</i> cells	36
2.2.1.10. Transformation of recombinant DNA into competent cells	36
2.2.1.11. Sequencing	37
2.2.1.12. Long-term storage of clones	37
2.2.2. Expression and analysis of fusion proteins	38
2.2.2.1. Preparation of competent DH10Bac™ cells	38
2.2.2.2. Transposition of recombinant proteins into Bacmid DNA	38
2.2.2.3. Isolation of Bacmid DNA	38
2.2.2.4. Transfection of Sf9 cells with Bacmid DNA	39
2.2.2.5. Titration of viruses	40
2.2.2.6. Amplification of baculovirus recombinants	40
2.2.2.7. Analysis of protein expression	40
2.2.2.7.1. SDS-PAGE	41
2.2.2.7.2. Western blots	41
2.2.2.8. [³⁵ S]-methionine labelling of proteins	42
2.2.2.9. Isolation of viral DNA from Sf9 cells	42
2.2.2.10. Glycosylation assay	43
2.2.2.11. Cytotoxicity assay	43
2.2.2.12. Fluorescent microscopy	43
2.2.2.13. Protein release assay	43
2.2.2.14. Subcellular fractionation	44
2.2.2.15. Membrane flotation analysis	44
2.2.2.16. Brefeldin A treatment	45
2.2.2.17. Confocal microscopy	45
2.3. Results	46
2.3.1. Production of constructs in pFastBac	46
2.3.1.1. Generation of different AHSV-3 S10 fragments	48
2.3.1.2. Production of different NS3-eGFP fusions by cloning into the pFB-eGFP vector	50



2.3.1.3. Sequence verification of recombinant pFB constructs	54
2.3.2. Baculovirus expression of fusion proteins	56
2.3.3. Glycosylation assay	62
2.3.4. Cytotoxicity assay	63
2.3.5. Fluorescent microscopy	64
2.3.6. Protein release assay	66
2.3.7. Subcellular fractionation	69
2.3.8. Membrane flotation analysis	75
2.3.9. Use of a drug treatment to block ER to Golgi transport in cellular trafficking pathways	82
2.3.10. Confocal microscopy	83
2.4. Discussion	89
<u>Chapter 3: Concluding Remarks</u>	101
<u>References</u>	103
<u>Appendix 1</u>	121



Chapter 1: Literature Review

1.1. Introduction

The field of virology is only about a hundred years old, but viruses have probably been present in living organisms since just after the origin of life. Viruses are continually being discovered in many different species. Because of this, one could almost conclude that every species on this planet carries viruses. The occurrence of double-stranded RNA (dsRNA) was discovered fairly recently in members of the *Reoviridae* family in 1963 (Levy *et al.*, 1994). These double-stranded RNA viruses are harmful to their hosts and have become the focus of many studies due to their economic importance (Levy *et al.*, 1994).

Eight families of dsRNA viruses are recognised by the International Committee for the Taxonomy of Viruses (ICTV) (Mertens, 2004). These viruses range from the simple viruses of the *Hypoviridae* family, which contain a single, unpackaged dsRNA segment, to the more complex viruses of the *Reoviridae* family, which contain 10 to 12 dsRNA segments (Jayaram *et al.*, 2004). In all of the well-characterised dsRNA viruses, the capsid structure is based on icosahedral symmetry (Jayaram *et al.*, 2004). With the exception of the *Cystoviridae* family, in which members use bacteria as hosts, all dsRNA viruses are non-enveloped (Mindich, 1988).

The *Reoviridae* family has 12 distinct genera, including *Rotavirus* and *Orbivirus* (Mertens and Diprose, 2004). Viruses of the *Rotavirus* genus are the major global cause of infantile diarrhoea, and are associated with sporadic outbreaks of diarrhoea in the elderly and in immunocompromised patients (Ball *et al.*, 2005). The *Orbivirus* genus includes 19 serogroups with multiple serotypes (Calisher and Mertens, 1998; Roy, 2001). They are primarily viruses of insects but also infect many mammals with occasional high morbidity and mortality (Levy *et al.*, 1994). These viruses are transmitted by hematophagous arthropods of the genus *Culicoides* e.g. *Culicoides imicola* and *Culicoides variipennis* and possibly by other biting insects e.g. mosquitoes, ticks or phlebotomine flies (Boorman *et al.*, 1975; Coetzer and Erasmus, 1994). Orbiviruses are economically important and are generally found in Africa, Australia, South East Asia, South America and Central America (Roy, 2001). Bluetongue virus (BTV) is the prototype virus of the *Orbivirus* genus and has 24 serotypes (Verwoerd and Erasmus, 1994). African horsesickness virus (AHSV) is also a member of the *Orbivirus* genus (Verwoerd *et al.*, 1979).

The first known historical reference to a disease resembling African horsesickness was in an Arabian document entitled “Le Kitâb El-Akouâ El-Kâfiyah Wa El Chafiâh”. This document reported an outbreak of the disease in Yemen in 1327 (Moule, 1896). Sir Arnold Theiler identified African

horsesickness virus as the etiological agent of the disease around 1901 (Theiler, 1921).

1.2. African Horsesickness Virus

African horsesickness virus (AHSV) is the etiological agent of African horsesickness (AHS), an infectious but non-contagious gnat transmitted disease of horses (Maurer and McCully, 1963). African horsesickness occurs throughout sub-Saharan Africa, although periodic epizootics have caused severe outbreaks of the disease outside of its enzootic regions i.e. North Africa, the Middle East and southern Europe (Awad et al., 1981; Lubroth, 1988; Mellor and Boorman, 1995). Transmission occurs mainly by *Culicoides imicola* (Wetzel *et al.*, 1970; Meiswinkel, 1998), but recently a second species, *Culicoides bolitinos*, has been implicated in the transmission of AHSV into areas where *Culicoides imicola* is rarely found (Meiswinkel and Paweska, 2003). The antigenic plurality of strains has been documented and, to date, 9 AHSV serotypes are known (Howell, 1962). Serotypes 1 - 8 are highly virulent, whereas serotype 9 is less virulent (Coetzer and Erasmus, 1994).

1.2.1. Pathology of African Horsesickness

African horsesickness is highly pathogenic. Its mortality rate in horses, the most susceptible species, may be as high as 95%. AHSV infects endothelial cells and targets organs such as the lymph nodes and lungs. There are four forms of African horsesickness. These are the cardiac form, the pulmonary form, the mixed form and the fever form. The main symptoms of each form are similar, but there are differences in the time of onset, clinical presentation, mortality and organs affected by the disease (Maurer and McCully, 1963).

The cardiac or 'dikkop' form of African horsesickness is subacute. This form is characterized by a fever and time course of several weeks. Main symptoms include pronounced oedema of the subcutaneous and intermuscular tissues of the head and neck. Large amounts of fluid are also present in the pericardial sac, while multifocal haemorrhages of the epi-, endo-, and myocardium are observed. Although some animals do recover, the mortality rate is high (50-80%). The incubation period is variable, usually between 7 and 14 days (Coetzer and Erasmus, 1994; Mellor and Hamblin, 2004). The pulmonary or 'dunkop' form is peracute. This form develops so rapidly that an animal may die without any previous indication of illness. It is characterized by marked depression, high fever, severe pulmonary oedema and pleural effusion. This form affects the lungs, spleen, hydrothorax, bronchial and mediastinal nodes. Its mortality rate commonly exceeds 95% and it has an incubation period of 4 to 5 days (Mellor, 1994). The mixed form is the most common form of AHS. It displays features of both the pulmonary form and the cardiac form. The mortality

rate of this form is approximately 70% and it has an intermediate incubation period of 5 to 7 days (Coetzer and Erasmus, 1994; Mellor and Hamblin, 2004). The last form, horsesickness fever, is always mild. In this form, affected horses develop a mild to moderate fever, some scleral infection and mild depression. The incubation period is 5 to 14 days and there is no mortality (Howell, 1963).

1.2.2. Prevention and Control

AHSV is non-contagious and can only be spread through the bites of infected vector species of *Culicoides*. Methods of control therefore include husbandry modification, quarantine and slaughter of infected animals, destruction of cadavers, control of insect vectors and vaccination (Mellor and Hamblin, 2004). Polyvalent live attenuated vaccines are currently produced in South Africa. These vaccines are administered as two quadravalent vaccines consisting of serotypes 1, 3 and 4 and serotypes 2, 6, 7 and 8 (Mirchamsy and Taslimi, 1964; Coetzer and Erasmus, 1994; Mellor and Hamblin, 2004). Serotype 9 is not included in the South Africa AHS vaccine as it rarely occurs in southern Africa and serotype 6 affords sufficient cross-protection (Coetzer and Erasmus, 1994). AHSV 5 was withdrawn in the 1990s following cases of encephalitis and chorioretinitis in laboratory workers (Van der Meyden *et al.*, 1992). There are a number of problems associated with live virus vaccine use. These include insect transmission, interference by the maternal antibody and the potential for reversion and gene reassortment with wild-type viruses (Roy, 2001).

An alternative approach would be to develop a non-infectious, safe subunit virus vaccine. A number of possibilities exist for such a vaccine. Stone-Marschat *et al.* (1996) found that AHSV VP2 alone is sufficient to induce a protective immune response in horses. The major neutralization domain of VP2 has been narrowed down to a central region from amino acid 200 to amino acid 413 (Martinez-Torrecuadrada and Casal, 1995). Wade-Evans *et al.* (1997) have demonstrated VP7 to be effective as a subunit vaccine in mice. In addition, Martinez-Torrecuadrada *et al.* (1999) found that recombinant VP5 expressed in insect cells and used for rabbit immunization was able to elicit significant neutralizing activity. The N-terminal of VP5 was found to be the most immunodominant region. An amino-terminal region of VP5 could, therefore, be of special interest for inclusion in a new generation of subunit vaccines for AHSV (Martinez-Torrecuadrada *et al.*, 1999).

1.2.3. African Horsesickness Virus Structure

All members of the *Orbivirus* genus share certain morphological characteristics and molecular composition (Levy *et al.*, 1994). Because of this, the prototype orbivirus, BTV, is often used to describe other orbiviruses that are not as well characterized, such as AHSV. In the same way, I will

use some information relating to BTV structure to describe the structure of AHSV.

Orbiviruses are nonenveloped and have 2 protein shells surrounding a double-stranded RNA genome. This protein bilayer makes up a double icosahedral capsid (Roy, 2001). A number of obvious reasons exist for these viruses having evolved a separate container, the icosahedral viral capsid (Bamford, 2000). Because their host cells do not possess the enzymatic machinery needed to convert dsRNA into a translatable mRNA molecule, these viruses have to provide for a mechanism to synthesize mRNA from their genomic dsRNA (Bamford, 2000; Jayaram *et al.*, 2004). Both transcription and the subsequent synthesis of progeny dsRNA have to be carried out in confined environments so as to avoid degradation of the genome by cellular nucleases and to prevent unfavourable antiviral responses in host cells that could be triggered by increased concentrations of dsRNA e.g. interferon induction, gene silencing, induction of apoptosis and modification of host cell translation mechanisms (Jacobs and Langland, 1996; Gitlin and Andino, 2003; Bamford, 2000; Jayaram *et al.*, 2004)).

Orbiviruses consist of 7 structural proteins (denoted VP1-VP7 in order of decreasing size), 4 nonstructural proteins (denoted NS1, NS2, NS3 and NS3A) and 10 dsRNA segments (L1-L3, M4-M6, S7-S10) (Grubman and Lewis, 1992; Roy, 1996). Each of these genome segments encodes one viral protein except the smallest segment, S10, which codes for two related proteins from in-frame overlapping reading frames (NS3 and NS3A). The virion is divided into the outer capsid layer, consisting of VP2 and VP5, and an icosahedral core consisting of VP1, VP3, VP4, VP6 and VP7, where VP3 and VP7 are the major core proteins (Verwoerd *et al.*, 1972; Verwoerd and Huismans, 1972; Els, 1973; Huismans *et al.*, 1987, Figure 1.1).

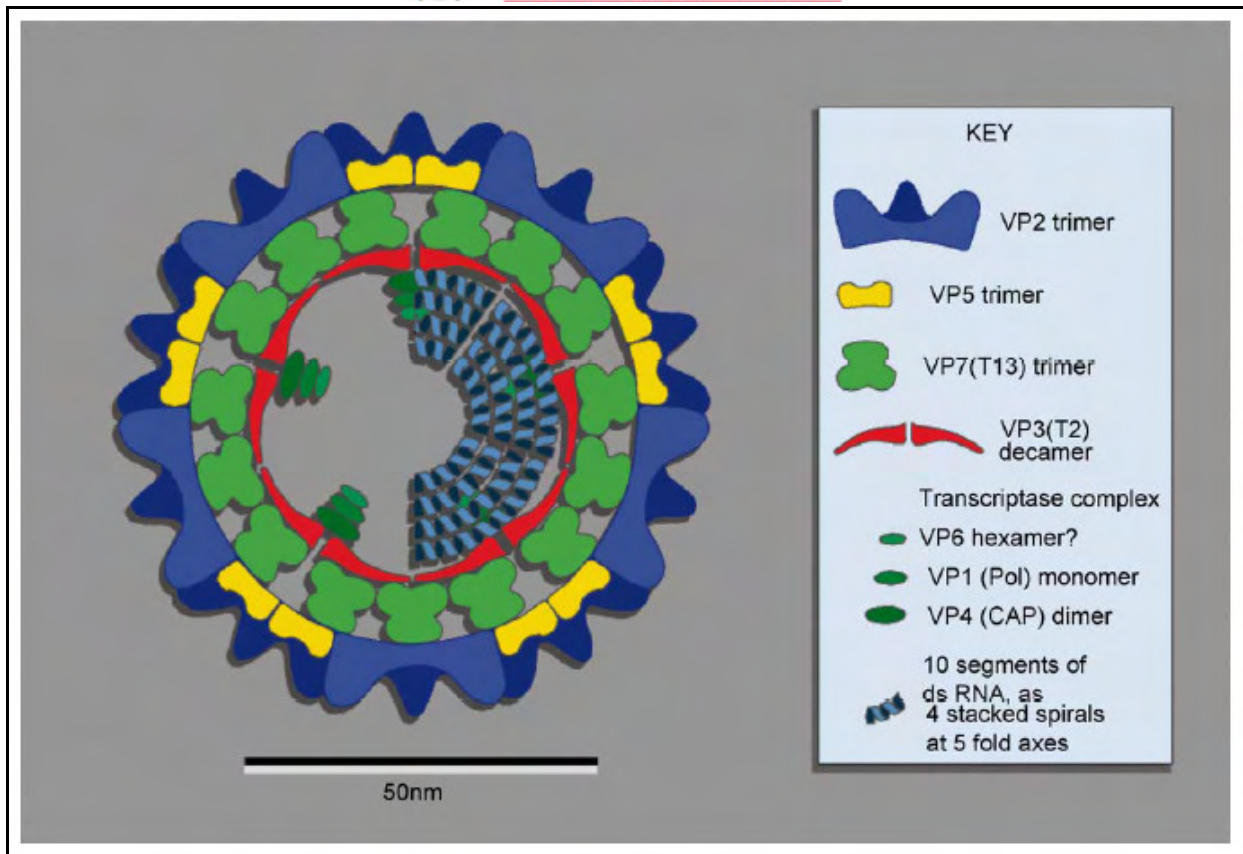


Figure 1.1. Schematic diagram of the structure of the bluetongue virus particle (Mertens and Diprose, 2004).

1.2.3.1. Structural Proteins

1.2.3.1.1. Outer capsid proteins

VP2 and VP5 are the outer capsid proteins of African horsesickness virus (Verwoerd *et al.*, 1972; Els, 1973). These proteins are involved in the attachment of the virus particles to target cells and are responsible for virus entry and penetration during the initial stages of infection. They, therefore, have a potentially large influence on the replication efficiency and virulence of the virus (Roy, 2001). Mortola *et al.* (2004) found that, in BTV, the viral outer capsid proteins (VP2 and VP5) alone are sufficient to trigger apoptosis.

VP2, the most variable protein of AHSV, is encoded by genome segment L2. This protein forms sail-shaped spikes in BTV (French *et al.*, 1990; Roy, 2001). VP2 is directly involved in the attachment of BTV to cells and in the entry of virions (Hassan and Roy, 1999). This protein is the principal antigen that determines serotype specificity and also elicits serotype-specific neutralizing antibodies that confer protection against homologous virus infection in vertebrate hosts (Huisman and Erasmus, 1981; Burrage *et al.*, 1993). BTV VP2 has hemagglutination activity (Cowley and Gorman, 1987). BTV VP2 has recently been found to associate with the intermediate filament protein vimentin, which seems to play a key role in intracellular trafficking. Amino acids 65 - 114 of

VP2 were found to be responsible for this association, which was found to contribute to virus release (Bhattacharya *et al.*, 2007).

VP5, a relatively conserved protein of AHSV, is encoded by genome segment M6 (Du Plessis and Nel, 1997). BTV VP5 is a globular, almost spherical protein, existing as 360 molecules beneath a layer of VP2 trimers (Hewat *et al.*, 1992a). This protein is involved in cell attachment and virus penetration during the initial stages of infection. It possesses characteristic structural features compatible with virus penetration activity i.e. 2 amino-terminal amphipathic helices. BTV VP5 has been shown to readily form trimers in solution, a feature of many proteins involved in membrane penetration (Hassan *et al.*, 2001). This protein has a role in viral penetration of the endosomal membrane and is responsible for the release of the virus core into the cell cytoplasm. This is due to its ability to induce membrane destabilization and permeabilization of endocytosed vesicles (Hassan *et al.*, 2001; Roy, 2001). The purified BTV VP5 protein is able to permeabilize mammalian and *Culicoides* insect cells, inducing cytotoxicity (Hassan *et al.*, 2001). Although present in the outer shell of the virus particle, AHSV VP5 is mostly unexposed on the surface of the virus. Despite this, it is one of the earliest serological markers in AHSV infections (Martinez-Torrecuadrada *et al.*, 1997). AHSV VP5 is also involved in eliciting an immune response, although it is less exposed on the surface than VP2 and does not contain neutralizing epitopes (Martinez-Torrecuadrada *et al.*, 1999).

1.2.3.1.2. Inner capsid proteins

The 2 major inner capsid proteins, which make up the outer layer of the core, are VP3 and VP7 (Huismans and Erasmus, 1981). VP3 and VP7 of BTV, when coexpressed in *Spodoptera frugiperda* insect cells, have been shown to spontaneously aggregate into core-like particles (CLP). They do not require the presence of any other proteins for assembly (French and Roy, 1990). Maree *et al.* (1998) have shown that co-expression of AHSV VP3 and VP7 also results in the intracellular formation of core-like particles, which structurally resemble AHSV cores. VP3 and VP7 are serogroup-specific antigens (Huismans and Erasmus, 1981). Both of these proteins are highly conserved amongst members of the *Orbivirus* genus (Roy, 1996).

VP3, encoded by genome segment L3, is a disk-shaped protein that is usually dimeric (Hewat *et al.*, 1992b). This protein is present in the core in the form of 120 copies arranged as 60 dimers (Monastyrskaya *et al.*, 1997). VP3 forms the “skeleton” of the icosahedral core by forming an inner scaffold for the deposition of the surface layer of VP7 (Tanaka *et al.*, 1995). VP3 has a very specific role in the determination of virus capsid morphology and in the organization of the viral genome (Roy, 2001). The VP3 N-terminus has been shown to be important for the binding and encapsidation of the transcription complex components. The dimerization domain (amino acids 699 - 854) is involved in VP3-VP3 interactions in the core (Kar *et al.*, 2004).

VP7, encoded by genome segment S7, is present in the core in the form of 780 molecules that are arranged as 260 trimers (Verwoerd *et al.*, 1972; Roy, 2001). This protein interacts with VP3 and the 2 outer capsid proteins, VP2 and VP5 (Hewat *et al.*, 1992b). There are also VP7 trimer-trimer interactions in the core, most likely involving the VP7 C-termini, which extend out of the side of the trimer arrangement (Monastyrskaya *et al.*, 1997). The upper domain of VP7 is composed of β -sheets while its lower domain is composed of α -helices (Monastyrskaya *et al.*, 1997). In contrast to the cognate protein in BTV, AHSV VP7 is highly insoluble and hydrophobic (Roy *et al.*, 1991). AHSV VP7 forms flat, hexagonal crystals in the cytoplasm of infected cells and large disc-shaped crystals when expressed by a recombinant baculovirus (Chuma *et al.*, 1992; Burroughs *et al.*, 1994). VP7 is the most accessible protein of the BTV core and, therefore, may participate in vector cell entry (Xu *et al.*, 1997; Tan *et al.*, 2001). Xu *et al.* (1997) reported evidence for the involvement of VP7 in the binding of BTV to membrane preparations of vector insects and cultured cells. This protein has an RGD motif, which is responsible for *Culicoides* cell binding activity (Tan *et al.*, 2001). RGD-integrin binding may be an initial step of BTV core attachment to insect cells (Tan *et al.*, 2001).

The three minor inner capsid proteins are VP1, VP4 and VP6. These proteins are found inside the inner shell with the dsRNA and are all highly conserved (Roy, 2001). The core particles exhibit RNA-dependant RNA polymerase activity, which allows the virus to synthesize mRNA from virion RNA templates (Roy, 2001).

VP1, encoded by genome segment L1, is the largest viral protein and is the virion RNA-dependant RNA polymerase in AHSV (Roy *et al.*, 1988; Roy *et al.*, 1994). BTV VP1 interacts with VP3 on the inside of the core and is responsible for single-stranded RNA (ssRNA) elongation (Loudon and Roy, 1991; Roy, 1996).

VP4, encoded by genome segment M4, modifies (caps) the 5' termini of positive stranded RNA. This protein has guanyltransferase activity in BTV, where it is responsible for the capping and methylation of mRNA (Le Blois *et al.*, 1992; Ramadevi *et al.*, 1998). It may have a similar function in AHSV.

VP6, encoded by genome segment S9, is a basic protein that binds RNA (ssRNA and dsRNA) (Stauber *et al.*, 1997). BTV VP6 is thought to be a helicase enzyme that unwinds the dsRNA substrate (Stauber *et al.*, 1997). Roy (1996) postulated that BTV VP6 might act as a chaperone for RNA incorporation into new virus particles. Kar and Roy (2003) characterized BTV VP6 activity and showed that, like other known helicases, BTV VP6 is hexameric and forms discrete ring-like structures when complexed with its substrate. De Waal and Huisman (2005) recently showed that baculovirus expressed AHSV VP6 can bind both single-stranded and double-stranded DNA and RNA. The efficiency of binding was found to be dependant on the salt concentration. Their results

suggest that the presence of charged amino acids seems to be important for binding activity (De Waal and Huismans, 2005).

1.2.3.2. Nonstructural Proteins

There are at least 4 nonstructural proteins in BTV and AHSV, which are involved in viral replication and morphogenesis and are only seen in virally infected cells (Roy, 1996). The major nonstructural proteins, NS1 and NS2, are synthesized abundantly whereas the smallest nonstructural proteins, NS3 and NS3A, are synthesized at barely detectable levels (Roy, 2001; Bansal *et al.*, 1998). NS1 and NS2 are highly conserved between the different virus serotypes, whereas NS3 is the second most variable of all AHSV proteins (Roy *et al.*, 1994).

Nonstructural protein NS1 is encoded by genome segment M5 (Roy, 2001). BTV NS1 is present in large amounts in infected cells as polymeric tubules with a ladder-like structure, mostly in perinuclear locations (Huismans and Els, 1979). These tubules have also been identified in AHSV infected cells and are entirely composed of NS1 protein. The characteristic tubule structure is maintained when expressed in insect cells, but the absence of the ladder-like structure and a lower sedimentation value distinguishes them from bluetongue virus NS1 tubules (Maree and Huismans, 1997). The tubules attach to the cytoskeleton and are thought to play a role in viral transport and replication (Eaton and Hyatt, 1989; Roy, 1996). BTV NS1 has also been shown to be a major cross-reactive immunogen for cytotoxic T-lymphocytes (Andrew *et al.*, 1995). Results of Owens *et al.* (2004) suggest that NS1 tubules play a direct role in the cellular pathogenesis and morphogenesis of BTV.

NS2, encoded by genome segment S8, is an abundantly expressed viral phosphoprotein, which assembles into multimers and has non-specific ssRNA binding ability (Taraporewala *et al.*, 2001). Sequence comparisons of AHSV and BTV NS2 indicate that this protein has a high helical content and is predominantly hydrophobic (Van Staden *et al.*, 1991). NS2 is the major protein of large electron-dense structures called granular viral inclusion bodies (VIBs) in infected cells (Thomas *et al.*, 1990). These structures are observed in areas in the cytoplasm where viral replication and assembly are localised (Brookes *et al.*, 1993). Phosphorylation of NS2 occurs at two serine residues at positions 249 and 259. This phosphorylation is not necessary for RNA binding or for the ability to interact with viral polymerase VP1, but has been found to control VIB formation and is, therefore, probably necessary for viral assembly (Modrof *et al.*, 2005). The RNA-binding domain of BTV NS2 has been mapped to the protein's N-terminal (Zhao *et al.*, 1994). NS2 has a preference for BTV ssRNA over nonspecific RNA. It has been shown to recognize a specific region of RNA with a defined stem-loop structure in BTV segment S10. This implies a possible function for BTV

NS2 in recruiting virus mRNAs selectively from other RNAs within the infected cytosol of the cell during virus replication (Lymeropoulos *et al.*, 2003). Lymeropoulos *et al.* (2006) recently demonstrated that the interaction between NS2 and BTV S10 RNA is abolished by mutations predicted to disrupt the stem-loop structure. In addition, RNA regions in three other genomic segments of BTV that are bound preferentially by NS2 were mapped. Upon further analysis, these regions did not seem to form stem-loop structures. In addition, the specific binding by NS2 of two different viral RNAs was found to occur independently. These data support the hypothesis that recognition of different RNA structures by NS2 may be the basis for discrimination between viral RNAs during virus assembly (Lymeropoulos *et al.*, 2006).

S10, the smallest genome segment of AHSV, codes for two proteins from in-phase overlapping reading frames. These proteins are NS3 and NS3A (Van Staden and Huismans, 1991). As NS3 and NS3A are derived from alternative in-frame methionine initiation codons, the C-terminal sequences of these two proteins are identical, but NS3A lacks the 10-11 amino acids present on the NS3 N-terminal (Van Staden and Huismans, 1991). Both initiation codons are in suboptimal orientation for translation initiation, which may explain the low levels of expression of the two proteins (Van Staden *et al.*, 1995).

The NS3 protein of AHSV is 217 amino acids in length and is highly variable when compared across all AHSV serotypes, showing only 64% conservation (Van Niekerk *et al.*, 2001b). NS3 of BTV is 229 amino acids long and is far less variable, showing approximately 91% conservation (Bansal *et al.*, 1998; Van Niekerk *et al.*, 2001b). Specific conserved domains of AHSV and BTV NS3 have been identified and well characterized (Van Staden *et al.*, 1995; Bansal *et al.*, 1998; Beaton *et al.*, 2002) and are shown in Figure 1.2. These domains include i) the second AUG initiation codon (Wu *et al.*, 1992); ii) the 2 conserved hydrophobic domains (between amino acids 116-137 and 154-170 in AHSV and between amino acids 118-141 and 162-182 in BTV), which are predicted transmembrane domains (Bansal *et al.*, 1998); iii) a conserved amphipathic helix at the N-terminus; iv) a proline rich region (between amino acids 22 and 34 in AHSV and between amino acids 36 and 50 in BTV) and v) a conserved domain (between amino acids 43 and 93 in AHSV and between amino acids 46 and 96 in BTV) that shows high conservation of identical amino acids (Van Niekerk *et al.*, 2003). These features have been shown to be common in the NS3 protein of other orbiviruses such as epizootic hemorrhagic disease virus (EHDV), Palyam viruses and Chuzan viruses, but generally the S10 protein products of these viruses are more conserved within a serogroup (Van Staden *et al.*, 1995). In addition to the above-mentioned domains, BTV NS3 has two potential asparagine-linked glycosylation sites (at amino acids 63 and 150). The latter of these glycosylation sites is located between the two hydrophobic domains and is responsible for N-linked glycosylation of BTV NS3 (Bansal *et al.*, 1998). In the case of AHSV NS3, most of the sequence

variation between different NS3 proteins is located in Hydrophobic Domain 1 and the adjacent variable region between Hydrophobic Domain 1 (HD1) and Hydrophobic Domain 2 (HD2).

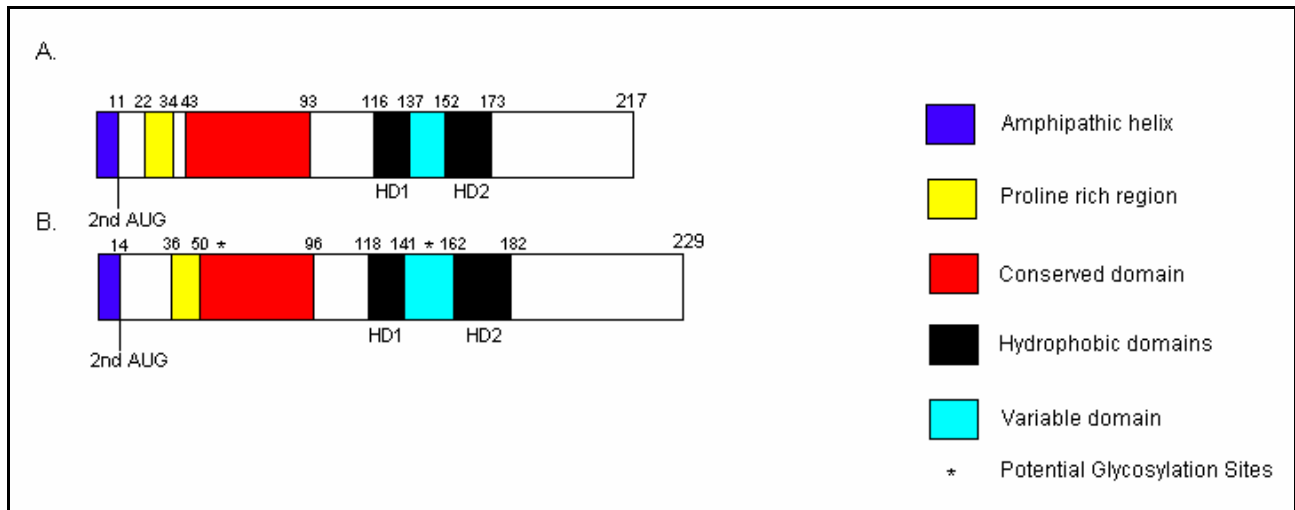


Figure 1.2. Conserved domains of AHSV (A) and BTV (B) NS3.

In the case of BTV, maturation of NS3 occurs in the endoplasmic reticulum (ER). The protein is then transported through the Golgi apparatus to the cell plasma membrane (Wu *et al.*, 1992). BTV NS3 is associated with intracellular smooth-surfaced vesicles and the cell plasma membrane. Hyatt *et al.* (1993) found that BTV NS3/NS3A mediate the release of virus-like particles (VLPs), but not core-like particles (CLPs), from infected cells. These proteins are therefore believed to be involved in the final stages of BTV morphogenesis and in the release of virions (Hyatt *et al.*, 1993). AHSV NS3 is present in membrane components of infected Vero cells, where it is specifically localised to sites of virus release. This finding confirms that AHSV NS3 is also membrane associated and could have an involvement in the final stages of viral morphogenesis and release (Stoltz *et al.*, 1996). A general model predicting the membrane orientation of AHSV NS3 has been proposed. In this model, the two hydrophobic domains span the membrane and the N- and C-termini are cytoplasmic (Van Staden *et al.*, 1995). A similar model has been proposed for BTV NS3 (Bansal *et al.*, 1998).

Recently, Beaton *et al.* (2002) found that BTV NS3 interacts with a cellular protein, p11 of the calpactin light chain. This protein is part of the annexin II complex that is involved in exocytosis. BTV NS3 interacts with p11 through a 13-residue peptide located at its N-terminus. It competes with another component of the complex (p36) for p11 ligand binding. The C-terminal domain of BTV NS3 was found to interact with VP2, the outermost protein of the fully assembled virus particle. These findings suggest that BTV NS3 forms a bridging molecule that draws the assembled virus into contact with the cellular export machinery i.e. may be part of an active extrusion process (Figure 1.3) (Beaton *et al.*, 2002).

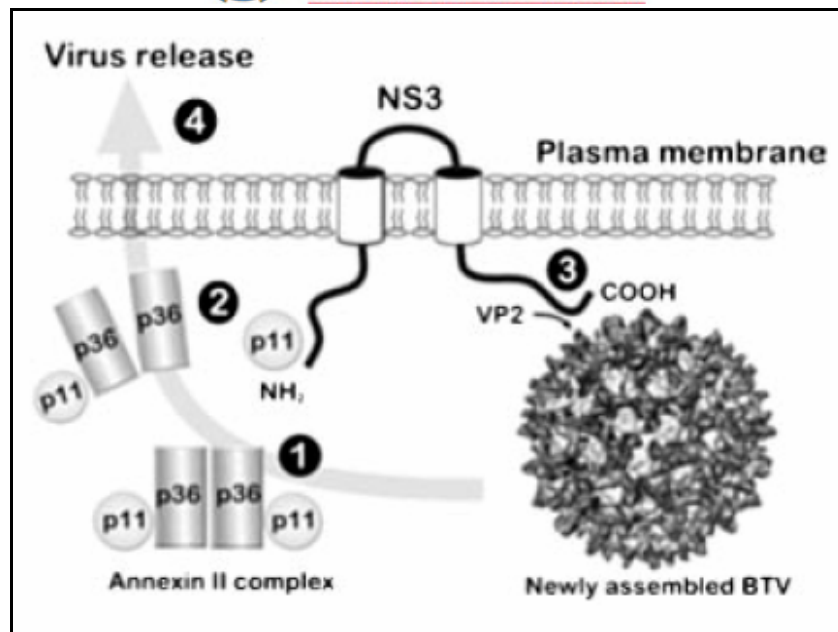


Figure 1.3. A model for the role of BTV NS3 in viral release. (1) The host protein, p11, is present in cells with p36 as part of the annexin II complex involved in cellular exocytosis. (2) NS3 is synthesized in the infected cell and localises to the secretory pathway, where it engages with p11 either alone or in a partial annexin II complex by the displacement of one copy of p36 via a sequence at the N terminus. (3) Assembled virions formed in cytosolic viroosomes similarly bind to NS3 via interaction between virion protein VP2 and a sequence in the NS3 carboxyl domain. (4) Assembled virions are drawn into contact with the p11/annexin II complex and engage to cellular exocytic machinery to affect nonlytic virus release (Beaton *et al.*, 2002).

The annexins are a family of proteins that bind acidic phospholipids in the presence of Ca^{2+} . The interaction of these proteins with biological membranes has led to the suggestion that they may be involved in membrane trafficking events such as exocytosis, endocytosis and cell-cell adhesion (Waisman, 1995). Annexin II is a member of the annexin family that has been found to bridge secretory granules to the plasma membrane. This finding led researchers to believe that annexin II may play a role in Ca^{2+} dependent exocytosis (Waisman, 1995). Various interactions exist between annexin II and a number of mammalian pathogens. To date, the best-documented interactions are those between human cytomegalovirus and annexin II (Depla, 2000). For example, Raynor *et al.* (1999) found that annexin II enhances cytomegalovirus (CMV) binding and fusion to phospholipid membranes. As mentioned previously, Beaton *et al.* (2002) recently found that BTV NS3 interacts with a part of the annexin II complex.

Wirblich *et al.* (2006) recently found that BTV NS3 and NS3A bind to cellular protein Tsg101, a component of the ESCRT-I (endosomal sorting complex required for transport) complex. The ESCRT proteins form three distinct complexes, ESCRT-I, II and III, that act sequentially to form the budding multivesicular body (MVB) vesicle (Katzmann *et al.*, 2001; Babst *et al.*, 2002a; Babst *et al.*, 2002b). The interaction between NS3 and Tsg101 is mediated by a conserved PSAP motif, which is a part of the "proline rich region" of NS3 (Figure 1.2) and appears to play a role in virus release. The depletion of Tsg101 inhibited the release of both BTV and AHSV. These results

indicate that NS3 recruits Tsg101, thereby facilitating virus release (Wirblich *et al.*, 2006).

An interesting feature of baculovirus expressed AHSV NS3 is that it is cytotoxic when expressed in insect cells. This cytotoxicity results from an alteration of cell membrane permeability and has raised the question of NS3's involvement in other virus attributes such as virulence and pathogenicity (Van Staden *et al.*, 1995). Mutation analyses of the conserved region of NS3 suggest that this region has no effect on cytotoxicity. However, mutations in the two hydrophobic domains have been shown to greatly decrease the cytotoxic effect (Van Staden *et al.*, 1998). Interestingly, these changes do not affect membrane targeting of the mutant proteins. Rather, such mutations seem to abolish membrane anchoring (Van Niekerk *et al.*, 2001a). This prevents the localisation of the mutant proteins to the cell surface, and obviates their cytotoxic effect. The cytotoxicity of NS3 is therefore dependent on its membrane topography and involves both hydrophobic domains (Van Niekerk *et al.*, 2001a). Re-assortment studies have shown that NS3 influences the virulence of AHSV by altering the timing of virus release (Martin *et al.*, 1998). NS3 has many of the characteristics of lytic viral proteins that play a central role in viral pathogenesis through modifying membrane permeability (Van Niekerk *et al.*, 2001a).

Many aspects of the functioning and role of NS3 and NS3A in the viral life cycle, as well as reasons for their conservation, remain unclear. In addition, the exact roles of these proteins in the cytotoxicity, virulence and pathogenesis of AHSV remain to be determined. Since NS3 and NS3A are the focus of this investigation, a clearer perspective of these proteins must be gained. In order to do this, it is essential to gain a greater understanding of a number of aspects. Important aspects include the viral life cycle, AHSV NS3 analogues in the *Reoviridae* family and viral membrane proteins. Each of these aspects will be discussed in the following sections.

1.3. Orbivirus entry, replication and release

In order to gain a clearer understanding of the role of NS3 and NS3A in virus maturation and release, a brief overview of the orbivirus life cycle (as shown in Figure 1.4) is discussed. Information concerning the replication cycle of BTV will be used in order to give a generalized overview of the orbivirus life cycle.

For nonenveloped viruses, separate coat proteins are often involved in the activities of virus attachment, entry and penetration. In the case of BTV, initial binding to erythrocytes and vertebrate cells is mediated by VP2 (Hassan and Roy, 1999). After this, the endosome invaginates and detaches i.e. the virus is taken up by phagocytic vacuoles through coated pits. This results in the formation of clathrin-coated vesicles containing virus particles (Eaton *et al.*, 1990; Roy, 2001). Due

to a low pH, either within the endosome or inside the cell, VP2 is degraded and VP5 undergoes an altered conformation. Transcriptionally active core particles (inner cores) are then released into the cytoplasm (Huisman *et al.*, 1987; Eaton *et al.*, 1990). The precise mechanisms of cytoplasm penetration remain unclear, but it is thought that VP5 could play a role in the membrane destabilization required for core access to the cytoplasm (Hassan *et al.*, 2001).

Once in the cytoplasm, the core is immediately activated to transcribe viral mRNA using dsRNA genome segments as templates. This is possibly done by VP1 (Roy *et al.*, 1988; Roy *et al.*, 1994; Roy, 2001). Newly synthesized mRNA strands leave the core through the VP7 capsomers, where they are methylated and capped by VP4 (Le Blois *et al.*, 1992; Ramadevi *et al.*, 1998). These strands are used to direct protein synthesis for the assembly of virions or as genomic precursors that are packaged into newly formed particles (Bamford, 2000). For the assembly of virions, the viral mRNA is translated by the host's own machinery to form the viral proteins. These viral proteins assemble into new particles and localise to the viral inclusion bodies (VIBs), which are formed by NS2 and ssRNA (Brookes *et al.*, 1993). One copy of each of the ten ssRNA segments is packaged into a new core particle inside the VIB (Bamford, 2000). The ssRNA segments inside the particle are then converted to double-stranded molecules by VP1 (Roy *et al.*, 1988; Roy *et al.*, 1994). VP3 provides protection for the viral enzymes and genome from degradation by cytosolic enzymes and VP7 strengthens the core, as it is highly insoluble. During the final stages of assembly, VP2 and VP5 are acquired through interactions with the core surface. The viral capsid is then released from the VIB and the core is no longer transcriptionally active (Roy, 2001). Intracellular core particles eventually lose their surface VP7 and subcores fail to transcribe RNA (Roy, 2001).

Depending on the host cell type, virus-like particles exit the cell by one of two possible processes. One of these processes is virion budding, where the particle temporarily acquires a lipid membrane (Roy, 2001). The other process is virion extrusion, where particles move through a disrupted plasma membrane (Roy, 2001). NS3 may be involved in both of these processes, by mediating the transport of the virus to the membrane and disrupting the plasma membrane in order to release the virus.

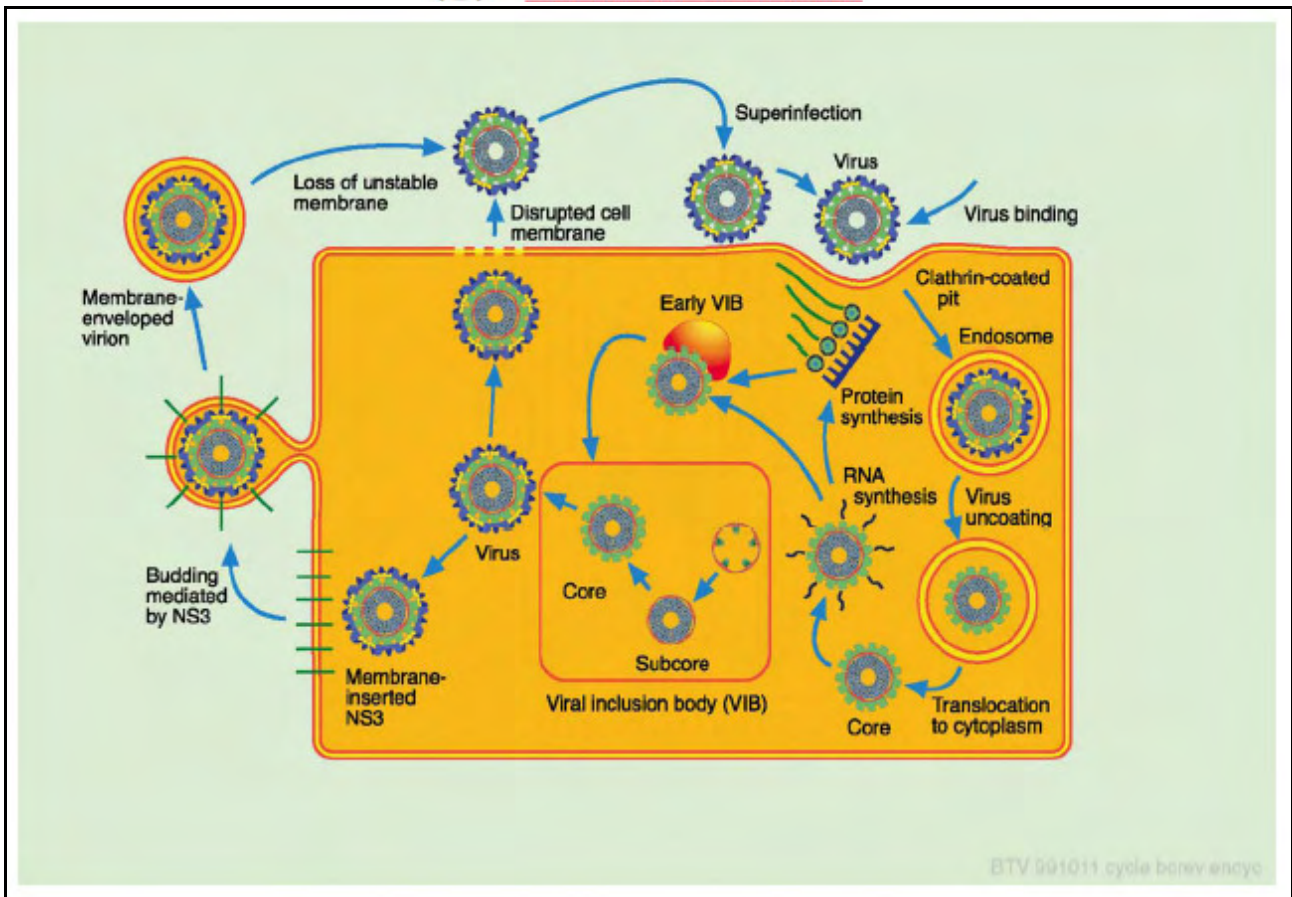


Figure 1.4. Schematic diagram representing the lytic replication cycle of BTV (Mertens and Diprose, 2004).

1.4. African Horsesickness Virus NS3 protein analogues in the Reoviridae family

One way to gain a greater understanding of the AHSV NS3/NS3A proteins is by making comparisons to analogous viral proteins that have been the focus of many studies and are well characterized. Two examples of viruses containing AHSV NS3 analogues that have been well studied and can be used in comparisons are BTV and rotavirus. As discussed above, BTV has NS3/NS3A proteins that are similar to NS3/NS3A of AHSV. Rotavirus has been the focus of many studies as it is a virus that infects humans. Rotavirus NSP4 is a possible functional analogue of BTV NS3 (Bansal *et al.*, 1998).

1.4.1. Rotavirus NSP4

NSP4, which was previously known as NS28, is a nonstructural glycoprotein encoded by rotavirus gene 10 (Ball *et al.*, 2005). NSP4 is a relatively small protein of 175 amino acids (Lin and Tian, 2003). This protein has a number of conserved features, including i) a single transmembrane domain, ii) three hydrophobic domains (denoted H1, H2 and H3), iii) two glycosylation sites within a short luminal domain (at amino acids 8 and 18) and iv) a large cytoplasmic tail (Taylor *et al.*, 1996;

Mirazimi *et al.*, 2003; Ball *et al.*, 2005). In addition to these domains, there are fourteen amino acids that are absolutely conserved throughout Group A rotaviruses. Of these residues, two are glycosylation sites, one is in the middle of the transmembrane region, seven span the VP4 binding domain and five are clustered in the middle of the toxic peptide region (Lin and Tian, 2003).

NSP4 plays an important role in the final stages of virus morphogenesis and is also a key factor in rotavirus pathogenesis. Structural changes between amino acids 131 and 140 have proved to be extremely important in its pathogenesis (Zhang *et al.*, 1998). NSP4 matures and remains in the endoplasmic reticulum (ER) (Mirazimi *et al.*, 2003). Classical ER retention signals are lacking in the NSP4 sequence and the mechanism of retention in the ER is unknown (Ball *et al.*, 2005). Glycosylated NSP4 has been shown to interact with calnexin, an ER-associated molecular chaperone. Calnexin has been proposed to promote folding and assembly of glycoproteins that pass through the secretory pathway in eukaryotic cells (Mirazimi *et al.*, 1998). Mirazimi *et al.* (2003) found that a cytoplasmic region on the NSP4 C-terminus, between amino acids 85 and 123, is responsible for its retention in the ER. Deletion of this domain results in the normal vesicular trafficking pathway to the cell surface. A number of models have been proposed for the membrane topology of NSP4. In one model, H3 is the membrane-spanning domain, while H1 and H2 are partly imbedded in lipid bilayers on the luminal side of the ER (Chan *et al.*, 1988). In another model, H2 serves as a signal sequence and as a membrane-spanning domain, while H3 is embedded in lipid bilayers on the cytoplasmic side of the ER (Estes and Cohen, 1989). A third model has H2 as the transmembrane domain with the C-terminal domain (amino acid 45 to 175) on the cytoplasmic side and the N-terminal 24 amino acids in the ER lumen (Taylor *et al.*, 1992; Ball *et al.*, 2005). This third model is the generally accepted model for the membrane topology of NSP4 (Lin and Tian, 2003).

Berkova *et al.* (2006) recently showed that intracellular NSP4-eGFP localises in novel vesicular structures, which contain an autophagosomal marker. These vesicles associate with viroplasm in virus-infected cells. They hypothesize that three pools of intracellular NSP4 exist. The first pool consists of NSP4 in the ER membrane and is present throughout the course of infection. This pool serves as a receptor for the budding of immature viral particles into the ER. The second pool enters the ER-Golgi intermediate compartment (ERGIC) and can be recycled back to the ER or may form a part of the predicted nonclassical secretion pathway. The third pool is distributed in the cytoplasmic vesicular structures and is proposed to be involved in the regulation of virus replication (Berkova *et al.*, 2006).

Rotavirus assembly is initiated in the cytoplasm of the infected cell and is completed in the lumen of the endoplasmic reticulum (ER) (Newton *et al.*, 1997). NSP4 acts as an intracellular receptor for

immature particles (i.e. particles without the outer capsid proteins, VP4 and VP7) (Au *et al.*, 1989). Targeting of the immature inner capsid particle (ICP) to the ER is mediated by a domain, between amino acids 161 and 175, on the cytoplasmic tail of NSP4 (Taylor *et al.*, 1996). This region has distinct viral binding and coiled coil domains, which represent a novel structural motif amongst proteins known to interact with icosahedral viruses (Taylor *et al.*, 1996). A second domain, between amino acids 112 and 148, is responsible for the binding of the spike protein, VP4 (Tian *et al.*, 1994; Kirkwood and Palombo, 1997). The association between the receptor and the particle is transient and NSP4, with its associated membranes, is not incorporated into the mature particle, which assembles within the ER lumen (Newton *et al.*, 1997).

Once the double-shelled particles are assembled, they bud from the cytoplasmic viroplasm structures into the adjacent ER. During this process, which is mediated by the interaction of the double-shelled particles with NSP4, the particles acquire a temporary lipid bilayer. This lipid bilayer is removed by an unknown mechanism to yield the mature triple-layered virions (Gonzalez *et al.*, 2000). Glycosylation of NSP4 is required for the removal of the transient envelope from budding particles (Kirkwood and Palombo, 1997).

From the ER, mature rotavirus virions follow an atypical pathway, bypassing the Golgi apparatus to the plasma membrane. The exact nature of this pathway is unclear, but it is thought that lipid rafts are involved in the process (Sapin *et al.*, 2002). Sapin *et al.* (2002) found high proportions of VP4, the outermost protein of the triple-layered structure, to be associated with rafts within the cell as early as 3 hours post infection. At 6 hours post infection, high proportions of NSP4 were found to be associated with rafts within the cell. These findings support the conclusion that infectious rotavirus virions use rafts as assembly platforms and are transported to the cell surface using a raft-dependent pathway i.e. a non-conventional vesicular transport mechanism. This leads to question whether NSP4 could perhaps act as a “raft receptor” that transiently binds double-layered particles for their translocation into lipid microdomains where viral particles are assembled (Cuadras and Greenberg, 2003). Cuadras *et al.* (2006) recently found that silencing of VP4 and NSP4 reduced the association of rotavirus particles with rafts, confirming a possible role for NSP4 as a “raft receptor”. Parr *et al.* (2006) recently showed colocalisation between NSP4 and caveolin-1, a marker for detergent resistant membrane fractions, in NSP4-transfected and rotavirus infected mammalian cells. Amino acids 114 to 135 were found to be directly involved in this association, which most likely contributes to the intracellular trafficking of NSP4 from the ER to the cell surface (Parr *et al.*, 2006).

Because NSP4 is known to associate with VP7 and VP4 to form an ER-localised, heterotrimeric complex, silencing of NSP4 has been employed to examine rotavirus morphogenesis (Ball *et al.*,

2005). Recent reports show that the inhibition of NSP4 expression by small interfering RNAs leads to alteration of the production and distribution of other viral proteins and mRNA synthesis, suggesting that NSP4 affects virus replication (Lopez *et al.*, 2005; Silvestri *et al.*, 2005). These results point to a multifaceted role of NSP4 in virus replication, including influencing the development of viroplasms, linking genome packaging with particle assembly and acting as a modulator of viral transcription (Silvestri *et al.*, 2005).

NSP4 can induce diarrhoea and has thus been recognized as the first viral enterotoxin (Ball *et al.*, 1996). An NSP4 peptide fragment, from amino acid 114 to 135 is predicted to fold as an amphipathic helix. This peptide, localised in the cytoplasmic domain of NSP4, mobilizes intracellular calcium in eukaryotic cells and constitutes part of the active site for enterotoxigenic activity (Ball *et al.*, 1996). Rotaviruses bind to and penetrate enterocytes and replicate in these cells. NSP4 expressed in these cells is then released in the lumen of the intestine. This NSP4 interacts with surrounding enterocytes, resulting in the facilitation of chloride secretion through a calcium-dependent signal transduction pathway, thus causing diarrhoea (Kirkwood and Palombo, 1997). Expression of NSP4 results in a loss of plasma membrane integrity. A sustained increase in Ca^{2+} in response to NSP4 expression may lead to changes in cellular metabolism, deregulated activation of enzymes and ultimately cell death (Newton *et al.*, 1997). It remains unclear if the enterotoxigenic effects of NSP4 are due to a single signaling event or if the activation of multiple pathways is required for NSP4-induced diarrhoea (Ball *et al.*, 2005). Berkova *et al.* (2007) recently found that the expression of rotavirus NSP4 causes actin reorganization through activation of the actin remodelling protein cofilin. This reorganization may contribute to rotavirus pathogenesis by interfering with cellular processes dependent on actin remodelling such as endocytosis, exocytosis, channel activity and ion transport. The cofilin activation was found to be calcium dependent (Berkova *et al.*, 2007).

A novel, soluble form of NSP4 was recently identified. This soluble form is secreted from virus-infected cells and has the potential to carry out the enterotoxic effects. The secretion of NSP4 was accompanied by a selective posttranslational modification of the protein characteristic of transit through the Golgi apparatus during maturation (Bugarcic and Taylor, 2006).

A number of pleiotropic roles of NSP4 have been discussed above. It is easy to see that NSP4 is a single protein that has a number of different regions involved in conferring different functionalities.

1.5. General mechanisms for subcellular trafficking and localisation of proteins

Protein trafficking and localisation are of critical importance in determining the correct site of

protein activity and function. In order to fully understand the role of NS3 within a cell, a clear understanding of its movement and localisation is required. Such an understanding may be gained by investigating general trafficking pathways that may be used by NS3 as well as specific sorting signals and topogenic sequences that may be carried by NS3.

A number of general trafficking pathways exist within a cell. Although many ordinary cellular processes rely on these trafficking events, pathogens often gain entry by “hijacking” and utilizing these pathways (Altschuler *et al.*, 2003). In this way, NS3 may be utilizing one or more of the host cells general trafficking pathways to carry out its functions in the viral life cycle. General trafficking pathways within a cell include secretory pathways, endocytic pathways and nuclear and mitochondrial pathways (Lodish *et al.*, 2004). Proteins that are destined for the nucleus or mitochondria are transported there directly, while others are initially transferred by ribosomes across the endoplasmic reticulum (ER) (Lodish *et al.*, 2004).

The secretory pathway is used by nearly all proteins destined for extracellular or membrane-bound destinations within the eukaryotic cell (Hegde and Lingappa, 1997). In this pathway, transport of membrane and soluble proteins from one membrane-bound compartment to another is mediated by transport vesicles that collect proteins in buds arising from the membrane of one compartment. These transport vesicles then deliver the proteins to the next compartment by fusing with its membrane. As these transport vesicles bud from one membrane and fuse with the next the same face of the membrane always remains oriented towards the cytosol (Lodish *et al.*, 2004).

After synthesis has begun on free ribosomes in the cytosol, proteins that are transported and sorted by the secretory pathway begin their journey at the ER membrane (Hegde and Lingappa, 1997; Lodish *et al.*, 2004). A 16 to 30-residue ER signal sequence, typically located at the N-terminus of the nascent protein, directs the ribosome to the ER membrane (Lodish *et al.*, 2004). The transport of most secretory proteins into the ER lumen occurs while the nascent protein is still bound to the ribosome and being elongated (cotranslational translocation) (Lodish *et al.*, 2004). The signal recognition particle (SRP) on the ribosome binds simultaneously to the ER signal sequence in the nascent protein, the large ribosomal unit and the SRP receptor in the ER membrane. This particle ensures the correct interaction of the ribosome and the ER membrane and only permits elongation and synthesis of complete proteins when the ER membrane is present (Lodish *et al.*, 2004). Once the SRP and its receptor have targeted a ribosome synthesizing a secretory protein to the ER membrane, the ribosome and nascent chain are rapidly transferred to a complex macromolecular machine, termed the translocon (Walter and Lingappa, 1986; Lodish *et al.*, 2004). The translocon is responsible for the proper transport and biogenesis of proteins at the ER membrane (Hegde and Lingappa, 1997). The elongating chain then passes through the

translocon into the ER (Lodish *et al.*, 2004). As the growing polypeptide chain enters the lumen of the ER, the signal sequence is cleaved by signal peptidase, which is a transmembrane ER protein associated with the translocon (Lodish *et al.*, 2004).

Once membrane proteins have been targeted to the membrane, they need to be integrated into the membrane. According to the signal hypothesis, membrane proteins are integrated into the membrane by independent topogenic sequences (signal sequences, stop-transfer sequences and signal-anchor sequences) (Dalbey *et al.*, 2000). The final orientation of membrane proteins is established during their biosynthesis on the ER membrane and is preserved. Topogenic sequences direct the insertion and orientation of various classes of integral proteins into the membrane and membrane-spanning domains determine their topology. These membrane-spanning domains usually contain 20 to 25 hydrophobic amino acids. Each such segment forms an α -helix that spans the membrane, with the hydrophobic amino acids anchored to the hydrophobic interior of the phospholipid bilayer. Internal stop-transfer and signal-anchor sequences determine the topology of single-pass proteins, while multipass proteins have multiple internal topogenic sequences (Lodish *et al.*, 2004).

Membrane proteins are divided into two major classes, peripheral membrane proteins and integral membrane proteins. Peripheral membrane proteins are proteins that are associated with membranes but are generally not integrated into the hydrophobic region of the membrane bilayer. Peripheral membrane proteins can be further divided into two subclasses; associated membrane proteins or skeletal membrane proteins. Associated membrane proteins bind to some of the integral membrane proteins of the membrane through portions that are exposed on the surface of the membrane. Skeletal membrane proteins form membrane skeletons, which are cytoplasmic membrane networks intimately associated with the membrane. With integral membrane proteins, a portion of the mass is integrated into the structure of the lipid bilayer. Integral membrane proteins can be further subdivided into two classes; transmembrane proteins and anchored proteins. Transmembrane proteins span the lipid bilayer of the membrane. At least some of the protein appears on each of the sides of the membrane. Anchored proteins bury a portion of their mass in the hydrophobic interior of the lipid bilayer; this portion serves as an anchor to hold the protein in the membrane (Yeagle, 1987). Topologically, transmembrane proteins can be classified into three groups. Type 1 proteins span the lipid bilayer once with their N-termini located towards the ER lumen and their C-termini on the cytoplasmic side. Type 2 proteins span the membrane in the opposite orientation with their N-termini in the cytoplasm and their C-termini in the ER lumen. Type 3 membrane proteins span the membrane more than once (Garoff, 1985).

Proteins that have been translocated into the lumen of the ER begin to fold before translation is

completed (co-translationally). Folding occurs in three topologically and biochemically distinct environments: the ectodomain folds in the ER lumen, the transmembrane domain folds in the ER membrane and the cytoplasmic domain folds within the cytosol (Doms *et al.*, 1993). The ER provides a unique, specialized, high-capacity folding environment in which polypeptides can efficiently attain their complex three-dimensional structures (Doms *et al.*, 1993). Improperly folded proteins are prevented from progressing through the ER (Fewell *et al.*, 2001). Folding is not a spontaneous process. It requires the participation of numerous folding enzymes and molecular chaperones e.g. calnexin and calreticulin (Doms *et al.*, 1993; Fewell *et al.*, 2001; Schrag *et al.*, 2003). These enzymes and chaperones are necessary to prevent irreversible aggregation and to catalyse rate-limiting steps such as disulphide bond formation and proline isomerization. By doing this, they increase the efficiency of the folding process. This is especially important for large, complex molecules such as viral membrane proteins, which typically fold slowly and inefficiently *in vitro* (Doms *et al.*, 1993; Fewell *et al.*, 2001).

Many of the steps in the abovementioned trafficking pathways require specific signal sequences that carry the necessary information to target a protein to a specific destination within the cell (Lodish *et al.*, 2004). For example, signal sequences are required for retention in the endoplasmic reticulum, sorting to mitochondria, sorting to the plasma membrane, sorting to the nucleus, sorting to lysosomes and sorting to chloroplasts (Lodish *et al.*, 2004). Signal peptides are generally between 20 and 50 amino acids in length and usually contain a short basic region at the amino-terminus as well as a hydrophobic “core” region that helps anchor the protein in the membrane (Lodish *et al.*, 2004). Each organelle carries a set of receptor proteins that bind only to specific kinds of signal sequences, thus assuring that the information encoded in a specific signal sequence controls the specificity of targeting (Lodish *et al.*, 2004). Examples of known sorting signals are KDEL in ER-resident luminal proteins, a dilysine motif (KKXX) in ER-resident membrane proteins, a di-acidic (Asp-X-Glu) signal in cargo membrane proteins in the ER, the Mannose 6-phosphate motif in soluble lysosomal enzymes after processing in the *cis* Golgi, NPXY in the low density lipoprotein (LDL) receptor in the plasma membrane, YXX Φ in membrane proteins in the *trans* Golgi and in plasma membrane proteins and the dileucine motif (D/EXXXLL) in plasma membrane proteins (Brown and Breton, 2000; Fernandez-Salas *et al.*, 2004; Lodish *et al.*, 2004). A three-residue motif, RxR, has been described as a signal sequence for targeting of transmembrane proteins to the nuclear membrane (Meyer and Radsak, 2000; Meyer *et al.*, 2002).

Much evidence exists to suggest that lipid rafts are sorting centers that also play a huge role in the targeting of proteins to the plasma membrane (Brown and Breton, 2000). Plasma membranes of all eukaryotic cells consist of a mix of dynamic membrane domains in which raft microdomains coexist with fluid domains (Slimane and Hoekstra, 2002). These raft microdomains (lipid rafts) are

relatively small structures formed by the dynamic clustering of glycosphingolipids, cholesterol and associated proteins. Lipid rafts are able to move within the fluid bilayer (Simons and Ikonen, 1997; Briggs *et al.*, 2003; Helms and Zurzolo, 2004). It is generally accepted that raft formation takes place in the Golgi apparatus. The synthesis of glycerolipids starts in the ER and the headgroups of the sphingolipids are added in the Golgi complex (Simons and Ikonen, 1997). Simons and Ikonen (1997) proposed that these rafts function as platforms for the attachment of proteins when membranes are moved around inside the cell during signal transduction. A few proteins are permanent residents of rafts. These are important for maintaining a specific raft organization and include the caveolins. Many other proteins are transient passengers that use rafts for intracellular targeting or specific signal transduction processes (Briggs *et al.*, 2003). At present, lipid rafts provide one of the most defined systems to study lipid-mediated protein trafficking. However, in most cases, the precise function of rafts in the transport process remains to be elucidated.

1.5.1. Viral membrane proteins

A broad overview of viral membrane proteins will be discussed in order to gain an understanding of the diversity, synthesis, localisation and roles of these proteins in the viral life cycle, which may be relevant to AHSV NS3.

The functions of viral membrane proteins are diverse. They include binding virus particles to receptors on the host cell plasma membrane, mediating membrane fusion and penetration into cells, directing virus morphogenesis at the budding site and serving as receptor-destroying enzymes necessary for virus release (Doms *et al.*, 1993). The majority of these proteins are also important antigens to which neutralizing antibodies are directed (Doms *et al.*, 1993). Pinto *et al.* (1992) discovered another function of viral membrane proteins. They found that M2, the small integral membrane protein of the influenza A virus, had ion channel activity that allowed the protein to modify the permeability of the membrane into which it was inserted. This membrane permeabilisation may play a critical role in viral pathogenesis.

Viral membrane proteins are typically complex, high molecular weight, transmembrane oligomers (Doms *et al.*, 1993). Most commonly, these proteins have a single transmembrane domain and the large majority of their mass is located outside the viral envelope (the ectodomain) (Doms *et al.*, 1993). Like most cellular glycoproteins, viral membrane proteins are translated on membrane-bound ribosomes and inserted into the ER in an unfolded form (Doms *et al.*, 1993). Only correctly and completely folded molecules are transported out of the ER. Defective proteins are retained in the ER or other early compartments of the secretory pathway, where they accumulate and are eventually degraded (Doms *et al.*, 1993).

Viral membrane proteins often “hijack” and utilize general trafficking pathways within a cell for their own purposes (Altschuler *et al.*, 2003). Unless the protein contains additional sorting signals, post-translational targeting occurs via the default pathway used by cellular membrane proteins. This pathway is from the ER through the Golgi apparatus and on to the cell surface. Further modifications such as glycosylation and oligomerisation may occur in the Golgi apparatus (Bassel-Duby *et al.*, 1985; Hegde and Lingappa, 1997). Glycosylation generally occurs by the addition of N-linked carbohydrate chains, although some proteins contain only O-linked carbohydrate chains and others have both N- and O-linked chains (Doms *et al.*, 1993). Oligomerisation may be as a result of disulphide bond formation or, more commonly, non-covalent interactions (Bassel-Duby *et al.*, 1985). These modifications generally take place either before or during folding (Doms *et al.*, 1993). Once correctly folded, modified, assembled and targeted to the cell membrane the viral membrane protein is ready to perform its specific function.

A number of pathogen proteins have been found to contain examples of known sorting signals that carry the relevant information to target them to a specific location within the cell. For example, the first viral protein carrying a functional KDEL-like ER-retention signal was found by Vennema *et al.* (1993). This retention signal (KTEL) was found at the C-terminus of protein 6b of feline infectious peritonitis virus (FIPV) and caused the protein’s slow export from the cell. An example of a group of viral proteins containing a dilysine motif (KKXX) is the envelope glycoproteins of foamy viruses (FV), a group of retroviruses. This dilysine motif functions to localise these envelope glycoproteins to the ER (Goepfert *et al.*, 1995). An example of a di-acidic signal sequence (Asp-X-Glu) exists on the cytoplasmic tail of the vesicular stomatitis virus glycoprotein (VSV-G) This signal is required for efficient recruitment to vesicles mediating export from the ER (Nishimura and Balch, 1997). Fernandez-Salas *et al.* (2004) recently found that Botulinum neurotoxin type A light chain (BoNT/A-LC) has an active dileucine motif (FEFYKLL) on its C-terminus that is likely to be involved in membrane trafficking. Disruption of this motif results in a periplasmalemmal distribution with some protein in the cytoplasm. These findings suggest that, without this motif, the protein is able to reach the target membrane, but remains loosely anchored (Fernandez-Salas *et al.*, 2004). An example of a viral protein containing a dileucine motif (EXXXLL) is human immunodeficiency virus-1 (HIV-1) Nef, a multifunctional regulatory protein. Greenberg *et al.* (1998) found that this dileucine motif is required for sorting to clathrin-coated vesicles, resulting in this viral proteins involvement in the clathrin-mediated pathway. This dileucine motif was also found to be essential for the downregulation of CD4. Upon analysis of the AHSV NS3 sequence, we have identified a putative dileucine motif (DTSVLL) on its C-terminal. This dileucine motif may be involved in the targeting of NS3 to the cell membrane.

Over the past years, increasing evidence has accumulated to support the idea that many pathogens, such as viruses, use lipid rafts for their own benefit. Due to their role in membrane sorting and intracellular trafficking, raft domains also provide sites for the assembly or budding of a number of viruses (Briggs *et al.*, 2003). For example, because of the detergent insolubility of the lipid and protein constituents of influenza fowl plaque virus (FPV), it has been proposed that FPV selectively incorporates lipid rafts into its envelope during its assembly process (Scheiffele *et al.*, 1999). The hemagglutinin (HA) and neuraminidase of influenza virus are also recovered in lipid rafts during their transport to the cell surface (Kundu *et al.*, 1996). In addition, rafts are used by viruses for the intracellular trafficking of viral proteins e.g. echovirus types 1 and 11 and as platforms for cell entry e.g. HIV and rotavirus (Lopez and Arias, 2004). Cuadras and Greenberg (2003) recently characterized the association of rhesus rotavirus (RRV) with lipid rafts during the rotavirus replication cycle. Their results confirmed the association of rotavirus infectious particles with rafts during replication *in vitro* and *in vivo* and strongly supported the prediction that this virus uses these microdomains for transport to the cell surface during replication (Cuadras and Greenberg, 2003). Lindwasser and Resh (2001) have shown that the HIV-1 Gag protein is associated with what they term barges. Barges are raft-like membrane microdomains that have a higher density than standard rafts, most likely due to the presence of oligomeric Gag-Gag assembly complexes. These results imply that the association of Gag with barge-like raft microdomains plays an important role in the HIV-1 assembly process.

Quite a number of viral membrane proteins have been shown to be membrane damaging and could be involved in viral pathogenesis. NS3 is an example of such a viral membrane protein as it is able to modify cell membrane permeability in insect cells, thus inducing cytotoxicity (Van Staden *et al.*, 1995). Animal viruses are able to alter cell membrane permeability either early, when the virus gains access to the cytoplasm, or later in the replication cycle following viral gene expression (Carrasco, 1995). Early membrane permeabilization is induced by isolated virus particles or by the co-entry of toxins with virus particles during infection. Late membrane permeabilization requires the expression of viral genes and, therefore, one or more viral protein is responsible for the leakiness observed (Carrasco, 1995). Membrane leakiness is required for the efficient release of nonenveloped virus particles from infected cells (Carrasco, 1995).

The most common change that occurs in the plasma membrane during infection of a susceptible cell by a cytolytic virus is enhanced permeability to monovalent cations. This effect is obviously accomplished by a drastic drop in membrane potential. Sodium ions accumulate in the cell while potassium ions leak out. Viral mRNAs translated late during infection are, therefore, adapted with special structures for optimum translation under these altered conditions (Carrasco, 1995). The concentrations of protons and calcium ions also change at about the same time that monovalent

ion concentrations are affected. In addition to ions, other low-molecular-weight compounds readily diffuse through the membranes of virus-infected cells. Nucleotides and sugars leak from cells and a number of hydrophilic antibiotics that do not permeate the plasma membrane of normal cells selectively enter virus-infected cells (Carrasco, 1995).

Viroporin is the name given to a family of virus proteins that alter membrane permeability (Carrasco, 1995). Viroporins are small, highly hydrophobic, virus-encoded proteins that interact with membranes, thus modifying the cells permeability to ions or other small molecules (Gonzalez and Carrasco, 2003). These proteins contain between 50 and 120 amino acids and possess a hydrophobic stretch of about 20 amino acids. This hydrophobic region is a transmembrane domain that interacts with the lipid bilayer and may form an amphipathic α -helix (Carrasco, 1995; Gonzalez and Carrasco, 2003). Some viroporins contain an additional hydrophobic region that interacts with membranes (Gonzalez and Carrasco, 2003). Viroporins usually contain basic amino acids, which may participate in membrane permeabilization by acting as detergents and destabilizing the lipid bilayer (Carrasco, 1995; Gonzalez and Carrasco, 2003). They contain a higher than average content of leucine and isoleucine residues and a lower than average content of glycine residues (Carrasco, 1995). Viroporins tend to form oligomers, most frequently tetramers, thus leaving a hydrophilic pore through which ions and low-molecular-weight hydrophilic compounds pass in a non-specific manner (Carrasco, 1995). All of the abovementioned features of viroporins contribute to their role in membrane destabilization (Gonzalez and Carrasco, 2003). This leads to changes in the metabolism and morphology of the cell and promotes the release of viral particles (Gonzalez and Carrasco, 2003). Viroporins also affect cellular functions, including the cell vesicle system and glycoprotein trafficking (Gonzalez and Carrasco, 2003). The presence of these proteins enhances virus growth (Gonzalez and Carrasco, 2003).

Agirre *et al.* (2002) found the first evidence of viroporin activity shown by a protein from a naked animal virus, non-structural protein 2B of poliovirus. Han and Harty (2004) recently found that cells expressing BTV NS3 were permeable to the translational inhibitor, hygromycin-B, in a dose-dependent manner. This finding suggests that NS3 may be capable of permeabilizing or destabilizing lipid membranes; a property shared by viroporins. They went on to demonstrate a number of characteristics of NS3 that are commonly associated with viroporins. For example, NS3 was able to form homo-oligomers when expressed in mammalian cells. NS3 is also a transmembrane protein with two transmembrane domains. Mutations in transmembrane region 1 (TM1) to disrupt the hydrophobic nature of this region abolished the ability of NS3 to permeabilize the plasma membrane. Deletion of amino acids in transmembrane region 2 (TM2) did not result in disruption of NS3-induced membrane permeability. Enhanced permeability to hygromycin-B correlated with the ability of NS3 to target predominantly to the Golgi apparatus. These results are

consistent with a possible role for NS3 as a viroporin, which may facilitate the release of virus particles and contribute to pathogenesis of BTV infections (Han and Harty, 2004). The rotavirus protein NSP4 and the influenza virus protein M2 discussed above are also examples of viroporins. All of these proteins play an integral role in the viral replication cycle and possibly in the pathogenesis of the disease.

As can be seen from the information provided, viral membrane proteins represent an extremely diverse group of proteins. These proteins have been found to fulfill a vast number of roles within virus infected cells. For example, viral membrane proteins are involved in entry and exit processes, targeting of virus particles to various compartments within the cell and permeabilisation of the cell membrane. NS3 and NS3A of AHSV are viral membrane proteins that are involved in some of these processes. However, many aspects of the functioning and role of NS3 and NS3A in the viral life cycle remain unclear. In addition, the exact roles of these proteins in the cytotoxicity, virulence, pathogenesis, trafficking and release of AHSV remain to be determined.

At the outset of this project, no reverse genetics system existed for members of the *Reoviridae* family. Boyce and Roy (2007) have recently found a way to recover infectious BTV from ssRNA. This suggests a means for establishing a reverse genetics system for members of the *Reoviridae* family. At the start of this project, however, it was necessary to find another method to investigate the roles of NS3 and NS3A in the life cycle of AHSV. Green Fluorescent Protein (GFP) serves as an ideal tool with which to investigate these roles.

1.6. Green Fluorescent Protein (GFP)

Green fluorescent protein (GFP) was originally isolated from the light-emitting organ of the jellyfish *Aequorea victoria* (Chalfie *et al.*, 1994). This 27kDa protein absorbs both UV and blue light and emits green light (Lippincott-Schwartz and Smith, 1997). GFP has revolutionized studies into the localisation of proteins by allowing their visualization in living cells (Lippincott-Schwartz and Smith, 1997). This means that it can be used to determine protein location, mobility, interactions and concentration (Chalfie *et al.*, 1994).

GFP has a number of advantages that make it an excellent Biological tool. The most important of these advantages is that it is non-invasive. Because of this, proteins can be tagged with GFP on either end and generally behave as untagged proteins (Chalfie *et al.*, 1994). GFP is also simple to use because its visualization does not require time-consuming fixation and tissue processing steps (Ehrhardt, 2003). Additional advantages are that GFP is relatively bright, particularly stable, inert, species-independent and spontaneously fluorescent when expressed in prokaryotic or eukaryotic

cells and in cell-free expression systems (Ehrhardt, 2003; Miyawaki *et al.*, 2003; Ashby *et al.*, 2004). GFP fusion proteins have been used in a wide variety of applications including time-lapse-imaging, double-labelling and photobleaching experiments. As such, they have become powerful tools in the analysis of membrane trafficking pathways, membrane protein mobility and the biogenesis of secretory and endocytic organelles (Lippincott-Schwartz *et al.*, 1999).

The tertiary structure of GFP makes it extremely stable (Lippincott-Schwartz and Smith, 1997; Ashby *et al.*, 2004). A “barrel” structure, formed by 11 β -sheets, surrounds and protects the fluorophore. The fluorophore, an α -helix, runs diagonally across the inside of this barrel (Lippincott-Schwartz and Smith, 1997; Ashby *et al.*, 2004). The fluorophore is a hexapeptide that is formed by an autocatalytic process that entails structurally driven, post-translational cyclization of residues Ser65, Tyr66 and Gly67 (Lippincott-Schwartz and Smith, 1997; Ashby *et al.*, 2004). It is excited at a specific wavelength of light, which causes it to fluoresce. Optimal fluorophore formation is dependent on temperature and pH (Lippincott-Schwartz and Smith, 1997). Very little can be deleted without affecting the proper folding and activity of GFP. Residues 2 to 232 are essential for its fluorescence (Lippincott-Schwartz and Smith, 1997).

The most widely used form of GFP is the commercially available enhanced GFP (eGFP) (Ashby *et al.*, 2004). eGFP has a number of improved characteristics elucidated from mutational studies. These include improved stability, folding properties and expression, low levels of photobleaching and the ability to visualize tagged proteins over many hours. eGFP folds properly at all temperatures, but the pH should be above 7 (Lippincott-Schwartz and Smith, 1997). The identification of other variants with differing absorbance and emission spectra, such as blue fluorescent protein (BFP), cyan fluorescent protein (CFP) and red fluorescent protein (dsRed), has allowed multispectral imaging of different tagged proteins simultaneously (Lippincott-Schwartz and Smith, 1997). This allows simultaneous imaging of more than one protein, which provides a method for studying protein-protein interactions (Rieder and Khodjakov, 2003).

Some factors must be taken into account when designing fusion proteins involving GFP. For example, all constructs should be designed so as not to disrupt the structure and function of the fluorescent protein or the host protein (Ashby *et al.*, 2004). Three important factors should be taken noted i) a fluorescent protein must fold correctly to fluoresce; ii) the host protein must fold correctly to be functional and iii) the integrity of the chimeric protein must be maintained (Miyawaki *et al.*, 2003). A particular terminus may need to be preserved in order to retain proper protein function or to ensure correct localisation. Therefore, when using fusion proteins for functional studies, constructs that represent fusions at both the N and the C termini of the protein should be evaluated (Miyawaki *et al.*, 2003; Mohan *et al.*, 2003).

GFP has a floppy carboxy terminal tail of approximately 10 amino acids, which makes its fusion to the amino terminus of other proteins possible without the addition of a linker (Miyawaki *et al.*, 2003). However, when fusing GFP to the carboxy terminus of another protein, a linker may be required. If a linker is used and it is not sufficiently long and flexible, there may be steric hindrance or folding interference (Miyawaki *et al.*, 2003). The best linker would consist of a small number of glycine residues (because of their high flexibility) interspersed with serine (to improve the solubility) (Miyawaki *et al.*, 2003). In rare cases in which neither end of a host protein can be modified, it is possible to insert the fluorescent protein into the middle of the protein (Miyawaki *et al.*, 2003). A highly flexible portion e.g. a β -turn should, theoretically, be tolerant to such an insertion (Miyawaki *et al.*, 2003). In general, to preserve the original structure of a host protein, the resulting amino and carboxyl termini of the inserted fluorescent protein should be in close proximity. This allows efficient folding of the fluorescent protein (Miyawaki *et al.*, 2003).

The use of GFP as a molecular tag has allowed the identification of viral proteins in live infected cells. This has provided valuable information regarding viral protein function and intracellular trafficking patterns. It has even facilitated the monitoring of more than one viral protein within an infected cell simultaneously (Zamyatnin *et al.*, 2002). The fluorescence of some mutant GFP molecules displays marked pH-dependence. These mutants may be used to measure the pH of different cellular environments (Ashby *et al.*, 2004). Hack *et al.* (2000) have shown how GFP can be used as a quantitative tool. They developed a simple method for measuring the concentration of an overexpressed protein in single cells and for measuring the covariation of particular physiological properties with a protein's expression.

Green fluorescent protein (GFP) serves as an ideal tool with which studies of viral genomes can be carried out. GFP has previously been used to visualize proteins of BTV and a number of rotaviruses in order to study the molecular biology of these viruses.

For example, Ghosh *et al.* (2002) used GFP as a tool to show that BTV NS1 retains the capacity to form tubules when carrying large inserts. Since these recombinant tubules can be purified in large quantities from insect cells, they have the potential to develop as a safe vaccine delivery system (Ghosh *et al.*, 2002). An example of the use of GFP in studying targeting in rotaviruses was in a study performed by Mohan *et al.* (2002). In this study, a tripeptide sequence (CRL) was investigated as a type of PTS1 (type 1 peroxisomal targeting sequencing). Results showed that cellular expression of GFP-fused VP4CRL resulted in the transport of VP4 to peroxisomes. Expression of the chimera lacking the PTS1 signal resulted in diffuse cytoplasmic staining, suggesting CRL-dependent targeting of the protein. In this study, GFP proved to be a good tool to

use in studying the targeting of VP4 by a PTS1 signal (Mohan *et al.*, 2002).

The use of eGFP in the study of viral membrane proteins has also provided some interesting results regarding the intracellular trafficking and localisation of these proteins within infected cells (Zamyatnin *et al.*, 2002). Research has been done using NSP4, the rotavirus enterotoxin, linked to eGFP to study the role of this protein in viral release and its effect on intracellular calcium levels (Berkova *et al.*, 2003). Berkova *et al.* (2003) effectively showed that intracellular expression of an NSP4-eGFP fusion protein elevates basal intracellular calcium levels by a phospholipase C (PLC) independent mechanism. This facilitates chloride secretion through a calcium-dependent signal transduction pathway, thus causing diarrhoea. As mentioned above, Berkova *et al.* (2006) recently used eGFP to show that intracellular NSP4 localises in novel vesicular structures, which contain an autophagosomal marker.

The potential use of eGFP as a molecular reporter molecule to determine the subcellular localisation patterns of different domains of AHSV NS3 will be investigated in this study.

1.7. Aims of this study

The smallest genome segment of African horsesickness virus (AHSV), S10, encodes two non-structural proteins (NS3 and NS3A) from in-phase overlapping reading frames. The C-terminal sequences of these proteins are identical, but NS3A lacks the first 10 amino acids present on the N-terminal of NS3 (Van Staden and Huismans, 1991). NS3 is a membrane protein that has been found to be associated with both smooth intracellular membranes and the plasma membrane. This protein has pleiotropic roles in the viral life cycle including the transport and release of mature virions and viroporin-like alteration of cell membrane permeability. NS3 is cytotoxic when expressed in bacterial or insect cells, and is speculated to play a vital role in viral virulence and disease pathogenesis (Van Staden *et al.*, 1995; Stoltz *et al.*, 1996).

Many aspects of the functioning and role of NS3 and NS3A in the viral life cycle, as well as reasons for their conservation, remain unclear. In addition, the exact roles of these proteins in the cytotoxicity, virulence and pathogenesis of AHSV remain to be determined. Long-term aims of this project are to identify functional domains of AHSV NS3 that play a role in the viral life cycle. These domains could, for example, affect viral pathogenesis, cytotoxicity, virulence, localisation, trafficking or release.

Short-term aims were to address the following questions:

1. Can eGFP be used to monitor the localisation of NS3 within a cell?
2. How do the different domains of NS3 affect its subcellular localisation and/or trafficking to specific compartments?

Chapter 2

2.1. Introduction

The smallest genome segment of African horsesickness virus (AHSV), S10, codes for two non-structural proteins (NS3 and NS3A) from in-phase overlapping reading frames. The C-terminal sequences of these proteins are identical, but NS3A lacks the first 10 amino acids present on the N-terminal of NS3 (Van Staden and Huisman, 1991). NS3 is a membrane protein, associated with both smooth intracellular membranes and the plasma membrane. NS3 has pleiotropic roles in the viral life cycle including the transport and release of mature virions and viroporin-like alteration of cell membrane permeability. NS3 is cytotoxic when expressed in bacterial or insect cells, and is speculated to play a vital role in viral virulence and disease pathogenesis (Van Staden *et al.*, 1995; Stoltz *et al.*, 1996).

Mutation analyses of the conserved region of NS3 suggest that this region has no effect on the protein's cytotoxicity. However, mutations in the two hydrophobic domains have been shown to greatly decrease the cytotoxic effect (Van Staden *et al.*, 1998). Interestingly, these changes do not affect membrane targeting of the mutant proteins. Rather, such mutations seem to abolish membrane anchoring (Van Niekerk *et al.*, 2001a). This prevents the localisation of the mutant proteins to the cell surface, and obviates their cytotoxic effect. The cytotoxicity of NS3 is therefore dependent on its membrane topography and involves both hydrophobic domains (Van Niekerk *et al.*, 2001a).

A number of domains that could mediate the membrane interaction or intracellular trafficking of NS3 have been identified. These domains include a conserved amphipathic helix at the N-terminus that binds to a cellular exocytosis protein in BTV, the two hydrophobic domains and a putative dileucine motif (DTSVLL) on the C-terminus. The relative contributions of these domains in insect and mammalian cells are not known, but could differ, as there are distinct differences in NS3 expression levels, cytopathic effects and virus release mechanisms in these two cell types.

In order to identify particular regions of NS3 that are involved in subcellular localisation and movement, it is necessary to visualize the effects of the different domains of NS3 within a cell. Green fluorescent protein (GFP) serves as a powerful tool that can be used as a molecular tag to identify the cellular location and to observe the movement of proteins within a single cell. eGFP is an enhanced version of the GFP protein (Ashby *et al.*, 2004) that will be used to address the aims of this project.

In order to investigate the subcellular localisation of NS3, a number of full-length, truncated or mutant versions of AHSV-3 NS3 will be constructed as C-terminal eGFP (enhanced green fluorescent protein) fusion proteins. These proteins will be used to generate recombinant baculoviruses for expression in *Spodoptera frugiperda* (Sf9) insect cells and will be compared in terms of their subcellular localisation by conventional fluorescence microscopy. Confocal laser microscopy will be used to investigate nuclear/endoplasmic reticulum (ER)/Golgi colocalisation. Membrane flotation analysis will be used to confirm membrane interactions and to identify detergent-resistant membrane fractions.

2.2. Materials and Methods

2.2.1. Construction of fusion proteins

2.2.1.1. Materials obtained

Plasmids:

Clones of pFB-eGFP were obtained from Michelle Victor (Department of Genetics, University of Pretoria). pFB-eGFP contains the eGFP gene cloned into the *EcoRI* and *HindIII* sites of pFastBac 1.

Clones of pUC-S10 were obtained from Dr. V. van Staden (Department of Genetics, University of Pretoria). pUC-S10 contains AHSV-3 genome segment S10 cloned into the *BamHI* site of pUC13.

Clones of pBS-HD1 and pBS-HD2 were obtained from Dr. M. van Niekerk (Department of Genetics, University of Pretoria). pBS-HD1 contains AHSV-3 NS3, with amino acids 124 to 128 in its first hydrophobic domain mutated from VTMAT to RTRDK (five non polar amino acids substituted with polar amino acids), cloned into the *BamHI* site of pBlueScribe. pBS-HD2 contains AHSV-3 NS3, with amino acids 165 to 169 in its second hydrophobic domain mutated from MLLA to KRDV (four non polar amino acids substituted with polar amino acids), cloned into the *BamHI* site of pBlueScribe.

Plasmids had been transformed into XL1-Blue (pFB-eGFP and pFB-NS3-eGFP) or DH5 α (pUC-S10, pBS-HD1 and pBS-HD2) *E. coli* cells.

Recombinant baculoviruses:

Bac-NS3, a recombinant baculovirus expressing AHSV-3 NS3 from a polyhedrin promoter, was obtained from Carel Smit (Department of Genetics, University of Pretoria).

Bac 82/61, a recombinant baculovirus expressing AHSV-2 NS3 from a polyhedrin promoter, was obtained from Dr. V. van Staden (Department of Genetics, University of Pretoria).

Antisera:

Anti- β -gal-NS3, a polyclonal antiserum raised in rabbits to a denatured form of a bacterially expressed β -galactosidase-NS3 fusion protein, was obtained from Dr. M. van Niekerk (Department of Genetics, University of Pretoria).

2.2.1.2. Agarose gel electrophoresis

Agarose gel electrophoresis was used to separate and visualise DNA fragments and to verify that they were of the expected size. To visualise purified plasmids, PCR products and restriction enzyme digest products, 1% agarose in TAE (0.04 M Tris-acetate, 1 mM EDTA, pH 8.5) was used. To visualise the products of restriction enzyme digests used to verify clones as well as the annealed N11 oligonucleotides, 2% agarose in TAE was used. Ethidium bromide was added to the gel to a final concentration of 1%, so that the DNA bands would be visible under UV light. The plastic tray containing the gel was submerged in 1 \times TAE buffer in a horizontal electrophoresis tank, and run at \pm 80 - 100 V constant current. Gels were visualised on a UV transilluminator and the sizes of the DNA fragments were estimated by comparing their migration during electrophoresis with standard molecular weight size markers. Size markers used include the Lambda DNA/*EcoRI*+*HindIII* Marker (SM0191), the O'RangeRuler™ 100 bp + 500 bp DNA ladder (SM0653) and the O'GeneRuler™ 100 bp DNA ladder plus (SM1153) purchased from Fermentas as well as the 100 bp ladder (G2101) purchased from Promega.

2.2.1.3. Plasmid DNA isolation

All plasmids were isolated using a protocol based on the alkaline-lysis method described by Sambrook and Russell (2001). Using a sterile toothpick, a single bacterial colony was selected and transferred from an agar plate to a 3 ml liquid culture of LB-Broth (1% Bacto-Tryptone, 0.5% Bacto-Yeast extract, 1% NaCl pH 7.4) containing the appropriate antibiotics (100 μ g/ml ampicillin, 12.5 μ g/ml tetracycline). Cultures were grown overnight at 37°C with shaking. Cells were collected from 1.5 ml of the overnight culture by centrifugation at 13 000 rpm for 5 min. Pellets were resuspended in 200 μ l of ice-cold lysis buffer (50 mM glucose, 10 mM EDTA, 25 mM Tris) and incubated on ice for 5 min. To denature proteins and double-stranded DNA as well as to solubilise the bacterial membrane and release plasmid DNA into the supernatant, 400 μ l of 0.2 M NaOH, 1% SDS was added and the tubes were incubated on ice for 5 min. To precipitate double-stranded DNA,

proteins and high molecular weight RNA, 300 µl of 3 M NaAc, pH 4.8 was added and the tubes were incubated on ice for 5 min. Precipitates were collected by centrifugation for 13 000 rpm for 10 min. Supernatants were transferred to clean Eppendorf tubes and 500 µl of Propan-2-ol (isopropanol) was added to precipitate the plasmid DNA. Tubes were incubated on ice for 20 min, where after DNA was pelleted by centrifugation at 13 000 rpm for 10 min. The resulting pellet was washed with 70% ethanol (EtOH), allowed to air dry and resuspended in 30 µl ddH₂O (Sambrook and Russell, 2001). Isolated plasmids were visualized by 1% agarose gel electrophoresis.

If required, plasmids were further purified using the GFX PCR and Gel Band Purification kit (Amersham Biosciences) or the High Pure PCR Product Purification kit (Roche) described below (2.2.1.7).

2.2.1.4. PCR Amplification

The Polymerase Chain Reaction (PCR) was used to obtain the different fragments of NS3 and eGFP that were used for the production of the seven constructs. PCR primers (Table 2.1) were designed according to the full-length gene sequences of the genes to be amplified and were obtained from either Inqaba Biotechnical Industries (South Africa) or Invitrogen Life Technologies (South Africa). Additional sequences that were added to the ends of the primers include two nucleotides to stabilize the ends and restriction enzyme sites (*Bam*HI, *Eco*RI or *Hind*III, as indicated by underlining) to facilitate cloning.

Table 2.1. Oligonucleotide primers used for PCR and sequencing reactions. *Bam*HI (GGATCC), *Eco*RI (GAATTC) and *Hind*III (AAGCTT) sites used for cloning and for the verification of clones are underlined. The regions on the NS3 gene (primers 1 - 5), the eGFP gene (primers 6 - 8) or pFB (primers 9 - 10) to which the primers had complementarity are indicated.

	Primer	Sequence	Length	T _m	Complementary region on gene (nt)
1.	NS3pBam	5'- <u>GCGGATCC</u> GTTTAAATTATCCCTTG-3'	25 bases	44°C	1 - 18
2.	NS3StopEcoR	5'- <u>GCGAATTC</u> GCTGTCGCCATATTTTAC-3'	26 bases	52°C	653 - 670
3.	NS3ABamF	5'- <u>GCGGATCC</u> ATGATGCATAATGGAAATC-3'	27 bases	50°C	50 - 68
4.	NS3DileucR	5'- <u>GCGAATTC</u> CCCCACTCCAAGACATAC-3'	25 bases	52°C	612 - 628
5.	NS3pEco	5'- <u>CGGAATTC</u> GTAAGTCGTTATCCCGG-3'	25 bases	52°C	742 - 758
6.	eGFPEcoF	5'- <u>GCGAATTC</u> ATGGTGAGCAAGGCGAG-3'	26 bases	58°C	1 - 18
7.	eGFPHindR	5'- <u>GCAAGCTT</u> TTACTTGTACAGCTCGTC-3'	26 bases	52°C	703 - 720
8.	eGFPinternal	5'-GGGCATGGCGGACTTGAAGAAG-3'	22 bases	70°C	249 - 270
9.	PFB1 POLH FW	5'-TTCCGGATTATTCATACC-3'	18 bases	60°C	3997-4014
10.	PFB1 RV	5'-GTGGTATGGCTGATTATGATCCTC-3'	24 bases	72°C	4156 - 4180

PCR reactions were set up as follows: 50 µl reactions containing 50 ng of appropriate template

DNA, 100 pmol of each oligonucleotide primer, 10 μ l of 10 \times Taq polymerase buffer (500 mM KCl, 100 mM Tris.HCl, 1% Triton X-100) (TaKaRa), and 2 μ l of a 2.5 mM dNTP mixture (TaKaRa). Hot-start PCR reactions were performed using the Perkin-Elmer 9600 Gene Amp PCR system. The reaction conditions were as follows: Template denaturation occurred at 95°C for 5 min, with 2.5 U of *Ex Taq* DNA polymerase (TaKaRa) added to the mixture just before primer annealing was allowed to occur for 45 s at a temperature determined by the primer sequence. Primer extension and polymerization occurred at 72°C for 2 min. Amplification was allowed to proceed for 30 cycles followed by a final elongation at 72°C for 5 min.

For the verification of clones, bacterial colonies were resuspended in 10 μ l ddH₂O and heated to 95°C for 5 min to break open the cells and release the DNA. Cellular debris was removed by centrifugation at 13 000 rpm for 1 min after which 5 μ l of this sample was used as a template in a PCR reaction set up as described above.

For the verification of viral DNA, DNA isolated in 2.2.2.8. was diluted 1/100 and 1 μ l of this dilution was used as the template in a reaction set up as described above.

PCR products were analysed by 1% agarose gel electrophoresis.

2.2.1.5. Construction of the N11 region

The DNA sequence encoding the first 11 N-terminal amino acids of NS3 (NS3-N11) that were used for the construction of pFB-N11-eGFP were ordered as two separate oligonucleotides that were modified by the addition of 5' *Bam*HI and 3' *Eco*RI sites to allow for cloning (Table 2.2). These oligonucleotides are 49 bp in length and were purchased from Inqaba Biotechnical Industries (South Africa). NS3-N11A and NS3-N11B were annealed in a 60 μ l reaction containing 500 pmol of each oligonucleotide and 6 μ l 10 \times RE buffer B (Roche). This mixture was heated to 95°C for 5 min to ensure complete denaturation and then placed at 65°C for 1 h. It was gradually cooled to room temperature to allow annealing and placed on ice before being digested overnight with 25 U *Eco*RI and 25 U *Bam*HI at 37°C. The annealed oligonucleotides were then purified either directly by ethanol precipitation or by phenol/chloroform extraction followed by ethanol precipitation. For ethanol precipitation, oligonucleotides were precipitated in 2.5 volumes 96% EtOH for 1 h at -70°C. They were then washed with 70% EtOH and resuspended in 10 μ l ddH₂O. For phenol/chloroform extraction, oligonucleotides were made up to a final volume of 500 μ l with 1 \times TE buffer. An equal volume of a 1:1 phenol/chloroform mixture was added to denature any proteins present. DNA was separated from the denatured proteins in phenol by centrifugation at 13 000 rpm for 5 min, after

which the upper aqueous layer containing the DNA was transferred to a new tube. Residual phenol was removed by the addition of 1 volume chloroform. Precipitation of DNA occurred by the addition of 2 volumes 96% EtOH and 1/10 volume 3 M NaAc followed by a -20°C incubation for 60 min. Oligonucleotides were washed with 70% EtOH, air-dried and resuspend in 10 µl ddH₂O.

Table 2.2. Oligonucleotides used for the construction of pFB-N11-eGFP. *Bam*HI (GGATCC), *Eco*RI (GAATTC) and *Pvu*II (CGATCG) sites that were used for cloning and for the verification of clones are underlined.

1.	NS3-N11A	5'-GCGGATCCATGAGTCTAGCTACGATCGCCGAAAATTATATGGAATTCCG-3'
2.	NS3-N11B	5'-CGGAATTCATATAATTTTCGGCGATCGTAGCTAGACTCATGGATCCGC-3'

2.2.1.6. Restriction endonuclease digestions

Restriction endonuclease digestions were performed in the appropriate buffers at 37°C according to the manufacturer's instructions (Roche). Large-scale digestions of PCR products and plasmids were carried out in a total volume of 120 µl containing approximately 4 µg DNA, 12 µl of the appropriate 10 × RE buffer and 32 U of the appropriate restriction enzyme. These reactions were allowed to take place at 37°C overnight. Small-scale digestions of plasmids were carried out in a total volume of 30 µl containing approximately 1 µg of DNA, 3 µl of the appropriate 10 × buffer and 8 U of the appropriate restriction enzyme. These reactions were allowed to take place at 37°C for 1 h.

2.2.1.7. Purification of DNA fragments

PCR products were purified from solution through the use of one of two commercially available purification kits, the GFX PCR and Gel Band Purification kit (Amersham Biosciences) or the High Pure PCR Product Purification kit (Roche). The GFX kit uses a chaotropic agent that denatures proteins and promotes the binding of dsDNA to a glass fibre matrix. Once bound, DNA is washed with ethanol to remove salts and other contaminants before being eluted in ddH₂O. In the Roche kit, DNA amplified by PCR binds selectively to glass fibres, which are pre-packed in the High Pure filter tube. Bound DNA is then washed with ethanol to remove contaminating primers, nucleotides and salts before being eluted in ddH₂O.

Plasmid DNA fragments to be purified from gels were excised from 0.8% agarose gels with a razor blade and purified using one of two commercially available purification kits, the GFX PCR and Gel Band Purification kit (Amersham Biosciences) or the GeneClean[®] III kit. (BIO 101[®] Systems). The GFX kit uses a chaotropic agent that denatures proteins, dissolves agarose and promotes the

binding of dsDNA to a glass fibre matrix. The gel slice is incubated with an equal volume of capture buffer at 60°C for approximately 60 min until the agarose has dissolved completely. DNA is then captured on glass fibres within a spin column and washed with ethanol to remove salts and other contaminants before being eluted in ddH₂O. The GeneClean[®] kit utilizes an aqueous silica matrix suspension (EZ-GLASSMILK[®]) that binds DNA in high concentrations of chaotropic salt. The gel slice is incubated with 3 volumes NaI at 55°C for approximately 5 min until the agarose has completely dissolved. The appropriate amount of glassmilk is then mixed into the DNA/NaI solution. The glassmilk, with its bound DNA, is pelleted by centrifugation and washed with ethanol before being resuspended in ddH₂O and pelleted by centrifugation once again. The supernatant containing the DNA is then removed.

2.2.1.8. Ligation of DNA fragments

Constructs (vector + insert) were ligated using the standard ligation protocol. Ligation reactions were carried out in a final volume of 20 µl containing 2 µl 10 × ligase buffer, 2 U T4 DNA ligase (Roche), and an insert: vector ratio of 10:1. Ligations were allowed to take place at 16°C for 16 h.

2.2.1.9. Preparation of competent XL1Blue *E. coli* cells

Competent XL1Blue *E. coli* cells were prepared by treatment with CaCl₂ in the early log phase of growth as described by Sambrook and Russell (2001). Using a sterile toothpick, an XL1Blue colony was transferred from an agar plate to a 3 ml culture of LB-Broth containing tetracycline (12.5 µg/ml) and grown at 37°C with shaking overnight. A 1 ml sample of this overnight culture was added to a 100 ml culture of LB Broth, which was allowed to grow to log phase (OD₅₅₀ of 0.5) at 37°C with shaking. Cells were collected by centrifugation at 5000 rpm for 5 min at 4°C and resuspended in half the original volume of ice-cold 50 mM CaCl₂. Cells were collected again by centrifugation and resuspended in 1/20 of the original volume of ice-cold 50 mM CaCl₂. Competent cells were left at 4°C on ice overnight prior to use in transformation (Sambrook and Russell, 2001).

2.2.1.10. Transformation of recombinant DNA into competent cells

Ligation mixtures were used to transform competent XL1Blue *E. coli* cells according to the protocol of Sambrook and Russell (2001). A volume of 10 µl of the appropriate ligation mixture was added to 100 µl of competent cells in a glass test tube on ice. The ligation mixture and the cells were mixed gently and incubated on ice for 30 min to allow the DNA to bind to the membranes of the cells. The cells were made more permeable by heat shock at 42°C for 90 s, followed by a 2 min

incubation on ice. Following this incubation, 800 μl of pre-warmed LB broth was added and cells were allowed to grow at 37°C for 1 h with shaking. Quantities of 150 μl of the transformation mixture were plated on agar plates containing the correct selection media for growth (100 $\mu\text{g}/\text{ml}$ ampicillin, 12.5 $\mu\text{g}/\text{ml}$ tetracycline) and allowed to grow at 37°C overnight (Sambrook and Russell, 2001).

2.2.1.11. Sequencing

Sequencing was performed to ensure the genes were inserted in the correct orientation and that no mutations were present. Plasmid DNA was isolated from resultant recombinant colonies using the method described above (2.2.1.3.) and purified using one of two commercially available purification kits described above (2.2.1.7); the High Pure PCR product purification kit (Roche) or the GFX PCR and Gel Band Purification kit (Amersham biosciences).

Sequencing was carried out by means of dye-terminator cycle sequencing using the ABI Prism™ 310 Genetic analyser. The reactions were carried out according to the manufacturer's instructions using an ABI Prism Big Dye Terminator Cycle Sequencing Ready Reaction kit, version 3.0 (Perkin Elmer Applied Biosciences). Sequencing reactions were set up as follows: a 10 μl reaction containing approximately 500 ng plasmid DNA, 1.6 pmol of the appropriate primer (Table 1) and 4 μl Big Dye. Sequencing reactions were performed using the Perkin-Elmer 9600 Gene Amp PCR system. The reaction conditions were as follows: template denaturation occurred at 96°C for 10 s, followed by primer annealing at 50°C for 10 s and extension at 60°C for 4 min. This was allowed to continue for a further 25 cycles, followed by cooling to 4°C.

Excess dye terminators were removed through ethanol precipitation as follows: 16 μl ddH₂O and 64 μl 99% EtOH were added to sequencing reactions. Reactions were left at room temperature for 15 min and pelleted by centrifugation at maximum speed for 20 min. Reactions were washed with 70% EtOH after which the supernatant was removed and the pellet was allowed to air dry.

Sequences were analysed using the Chromas program (www.technelysium.com.au). Sequences were compared to known sequences using Blast (www.ncbi.nlm.nih.gov) and the ClustalX (www.ncbi.nlm.nih.gov) program.

2.2.1.12. Long-term storage of clones

Bacterial cultures were stored in LB-broth containing 15% glycerol at -70°C.

2.2.2. Expression and analysis of fusion proteins

2.2.2.1. Preparation of competent DH10Bac™ cells

Competent DH10Bac™ *E. coli* cells were prepared using the DMSO method described by Chung and Miller (1988). Using a sterile toothpick, a DH10Bac™ colony was transferred from an agar plate to a 5 ml culture of LB-Broth containing tetracycline (10 µg/ml) and kanamycin (50 µg/ml) and grown at 37°C with shaking overnight. A 1 ml sample of this overnight culture was added to a 100 ml culture of LB Broth, which was allowed to grow to early log phase (OD₆₀₀ of 0.6) at 37°C with shaking. Cells were collected by centrifugation at 5000 rpm for 5 min at 4°C and resuspended in 1/10 of the original volume of ice-cold TSB (1.6% Peptone, 1% yeast extract, 0.5% NaCl, 10% polyethyleneglycol, 1 M MgCl₂, 1 M MgSO₄). Competent cells were left at 4°C on ice overnight prior to use in transformation (Chung and Miller, 1988).

2.2.2.2. Transposition of recombinant proteins into Bacmid DNA

Recombinant pFastBac constructs were used to transform competent DH10Bac™ *E. coli* cells according to the BAC-to-BAC™ Baculovirus expression system manual (Invitrogen Life Technologies). Approximately 100 ng of the appropriate pFB construct was added to 100 µl of competent DH10Bac™ *E. coli* cells in a glass test tube on ice. The pFB construct and the cells were mixed gently and incubated on ice for 30 min to allow the DNA to bind to the cell membranes. Cells were made more permeable by heat shock at 42°C for 45 s without shaking, followed by 2 min incubation on ice. This was followed by the addition of 900 µl of room temperature S.O.C. medium (1.6% Peptone, 1% yeast extract, 0.5% NaCl, 10% polyethyleneglycol, 1 M MgCl₂, 1 M MgSO₄, 20 mM glucose) and cells were allowed to grow at 37°C for 4 h. Quantities of 100 µl of the transformation mixture were plated on agar plates containing the correct selection media for growth (50 µg/ml kanamycin, 7 µg/ml gentamycin, 10 µg/ml tetracycline, 100 µg/ml X-gal, 40 µg/ml IPTG) and allowed to grow for 48 h at 37°C. White colonies were restreaked and grown overnight at 37°C to verify the white phenotype.

2.2.2.3. Isolation of Bacmid DNA

Bacmid DNA was isolated according to the protocol for the isolation of high molecular weight Bacmid DNA provided in the BAC-to-BAC™ Baculovirus expression system manual (Invitrogen Life Technologies). Recombinant colonies identified in 2.2.2.2 were used to inoculate a 2 ml culture of LB broth containing the appropriate antibiotics (50 µg/ml kanamycin, 7 µg/ml gentamycin,

10 µg/ml tetracycline). Cultures were grown for 24 h at 37°C with shaking. Cells were collected from 1.5 ml of the overnight culture by centrifugation at 13 000 rpm for 1 min. Pellets were resuspended in 300 µl ice-cold lysis buffer (15 mM Tris-HCl (pH 8.0), 10 mM EDTA, 100 µg/ml Rnase A) to disrupt the cell membranes. To denature proteins and dsDNA, 300 µl of 0.2 N NaOH/1% SDS was added. The contents were mixed gently and tubes were incubated at room temperature for 5 min. 300 µl of a 3 M KAc (pH 5.5) solution was added to decrease the pH in order to precipitate the proteins and genomic DNA. The contents were mixed gently and the tubes were placed on ice for 10 min. Precipitates were collected by centrifugation at 13 000 rpm for 10 min. Supernatants were transferred to clean Eppendorf tubes and 800 µl of Propan-2-ol (isopropanol) was added to precipitate the plasmid DNA. Tubes were incubated on ice for 5 to 10 min after which the DNA was pelleted by centrifugation at 13 000 rpm for 5 min. The resulting pellet was washed with 70% ethanol (EtOH), allowed to air dry and resuspended in 40 µl ddH₂O.

2.2.2.4. Transfection of Sf9 cells with Bacmid DNA

Spodoptera frugiperda (Sf9) cells obtained from American type culture collection (ATCC) were maintained in spinner suspension cultures at 27°C in either Grace's or TC-100 Insect medium supplemented with 10% fetal calf serum, 0.8% pluronic and 1.2% penicillin/streptomycin/fungizone (Highveld Biological).

For transfections, 1×10^6 cells were seeded per 35-mm well (of a 6-well plate) in 2 ml Grace's or TC-100 Insect medium supplemented with 10% fetal calf serum and 1.2% penicillin/streptomycin/fungizone (Highveld Biological). Cells were allowed to attach at 27°C for at least 1 h while the following solutions were prepared: 6 µl of the appropriate miniprep Bacmid DNA isolated in 2.2.2.2. diluted in 100 µl non-supplemented medium and 6 µl CELLFECTIN™ reagent (Invitrogen Life Technologies) diluted in 100 µl non-supplemented medium. The two solutions were combined, mixed gently and incubated at room temperature for 45 min after which an additional 800 µl of non-supplemented medium was added. Cells were washed twice with non-supplemented medium and overlaid with the lipid-DNA complexes. Cells were incubated overnight in a 27°C incubator after which the transfection medium was replaced with 2 ml medium supplemented with 10% fetal calf serum and 1.2% penicillin/streptomycin/fungizone (Highveld Biological). The transfected cells were incubated for a further 72 h at 27°C. After this incubation period, the recombinant baculoviruses in the supernatant were transferred to a sterile tube, clarified by centrifugation at 3000 rpm for 10 min and stored at 4°C for later use.

2.2.2.5. Titration of viruses

Viral titres were determined by means of a viral plaque assay as described in the BAC-to-BAC™ Baculovirus expression system manual (Invitrogen Life Technologies). Sf9 cells were seeded at 1×10^6 cells per 35-mm well (of a 6-well plate) and allowed to attach for 1 h. Ten-fold dilutions of the appropriate baculoviral stock were prepared in TC-100 Insect medium containing 10% fetal calf serum and 1.2% penicillin/streptomycin/fungizone (Highveld Biological). The medium was removed from the cells and replaced with 500 μ l of the appropriate dilution. Infections were carried out for 1 h at room temperature, after which the virus was removed and the monolayer was overlaid with 2 ml 1% BACPLAQ. Cells were incubated for 7 to 10 days at 27°C, after which they were stained with 0.1% 3-[4,5-dimethylthiazol-2-yl]-2,5-diphenyltetrazolium bromide (MTT) for 1 h. The number of plaques in each dilution were counted and used to calculate the viral titre.

Plaque purifications of viral stocks were carried out as described above, but cells were not stained after the 7 to 10 day incubation. At this stage, single plaques were plucked and resuspended in 1 ml TC-100 Insect medium containing 10% fetal calf serum and 1.2% penicillin/streptomycin/fungizone (Highveld Biological). These purifications were used to infect Sf9 cells seeded at 1×10^6 cells per 35-mm well (of a 6-well plate) after which further amplifications were carried out.

2.2.2.6. Amplification of baculovirus recombinants

Recombinant baculoviruses were amplified by infecting monolayers at a multiplicity of infection (MOI) of approximately 0.1 plaque forming unit (pfu)/cell. Amplification was first carried out in 25 cm² flasks containing 3×10^6 cells for 72 h at 27°C and then in 75 cm² flasks containing 1×10^7 cells for 72 h at 27°C. After the second round of amplification the medium containing the amplified recombinant baculoviruses was clarified by centrifugation at 3000 rpm for 10 min. Virus stocks were stored at 4°C for short-term storage and at -70°C for long-term storage.

2.2.2.7. Analysis of protein expression

Sf9 cells, seeded at 1×10^6 cells per 35 mm well of a 6-well plate, were infected with recombinant baculoviruses at a MOI of 5 pfu/cell. The cells were harvested after a 48 h incubation period at 27°C for the analysis of protein expression. Cells were collected by centrifugation at 3000 rpm for 10 min and washed twice with $1 \times$ PBS. The cells were resuspended in $1 \times$ PBS and analysed immediately by SDS-PAGE (2.2.2.7.1.) and/or Western Blot (2.2.2.7.2.).

2.2.2.7.1. SDS-PAGE

Proteins were visualized by Sodium dodecyl sulphate polyacrylamide gel electrophoresis (SDS-PAGE) under denaturing conditions as described by Sambrook and Russell (2001). Cells were treated with an equal volume of 2 x protein solvent buffer (PSB; 0.125 M Tris-HCl pH 6.8, 4% SDS, 20% glycerol, 10% 2-mercaptoethanol), heated at 95°C for 5 min and loaded onto 12% separating (12% polyacrylamide; 0.375 M Tris-HCl, pH 8.8; 0.1% SDS; 0.008% TEMED; 0.08% ammonium persulphate) and 5% stacking (5% polyacrylamide; 0.125 M Tris-HCl, pH 6.8; 0.1% SDS; 0.008% TEMED; 0.08% ammonium persulphate) gels. Gels were run in 1 x TGS buffer (0.3% Tris; 1.44% Glycine, 0.1% SDS) at 120 V in the Hoefer™ II SE 250 mini-vertical gel electrophoresis unit (Amersham Biosciences) for approximately 3 h. Gels were stained in 0.125% Coomassie blue, 50% methanol and 10% acetic acid for 30 min and destained in 5% acetic acid, 5% methanol overnight. The size of proteins was estimated by comparison to the Rainbow Marker (RPN 756, Amersham biosciences).

2.2.2.7.2. Western blots

Protein samples were separated by SDS-PAGE as described in 2.2.2.7.1. Proteins from the unfixed gel were transferred to Hybond-C+ membranes (Amersham Biosciences) in an EC 140 miniblott module (EC-apparatus corporation) submerged in transfer buffer (0.025 M Tris, 0.15 M glycine, 20% methanol pH 8.3) at 12 V for approximately 2 h. At this stage, gels were stained in 0.125% Coomassie blue, 50% methanol and 10% acetic acid for 30 min and destained in 5% acetic acid, 5% methanol to verify transfer. The membrane was rinsed in 1 x PBS and non-specific binding sites were blocked by incubation in blocking solution (1% milk powder in 1 x PBS) for 30 min at room temperature. The membrane was then incubated in the primary antibody; anti-β-gal-NS3 (diluted 1/100) obtained from Dr M. van Niekerk (Department of Genetics, University of Pretoria) or anti-GFP, N-terminal (diluted 1/1000; Sigma-Aldrich) overnight with gentle shaking. The antibody was removed and the membrane was washed three times for 5 min each in wash buffer (0.05% Tween in 1 x PBS). The secondary antibody, a 1/1000 dilution of protein A conjugated to horseradish peroxidase (Cappel) in blocking solution, was then added to the membrane for 1 h with gentle shaking. Unbound antibody was removed by washing three times in washing buffer and once in 1 x PBS for 5 min each. Antibody binding was visualized by incubation of the membrane in enzyme substrate (60 mg 4-chloro-naphthol in 20 ml ice-cold methanol combined with 60 μl hydrogen peroxide in 100 ml 1 x PBS) until bands become visible. Western blots were rinsed with dH₂O and allowed to air dry.

2.2.2.8. [³⁵S]-methionine labelling of proteins

Protein expression can be monitored in baculovirus-infected Sf9 cells by labelling with [³⁵S]-methionine in methionine deficient media (Luckow and Summers, 1988).

Sf9 cells, seeded at 1×10^6 cells per 35 mm well of a 6-well plate, were infected with recombinant baculoviruses at a MOI of 5 pfu/cell. At 27 h.p.i, cells were washed with 1 ml methionine-free Eagles medium (Highveld Biological). This wash media was replaced with 500 μ l fresh media and cells were starved for 1 h at 27°C to deplete intracellular pools of methionine. After this incubation, the wash media was replaced with 500 μ l fresh methionine-free Eagle's medium containing 0.5 μ l EASYTAGTM Methionine, L-[³⁵S] (PerkinElmer Life Sciences, Boston). Labelling was allowed to proceed for 3h. Cells were harvested from wells, collected by centrifugation at 3000 rpm for 10 min and washed twice with $1 \times$ PBS. The cells were resuspended in $1 \times$ PBS and analysed immediately by SDS-PAGE (2.2.2.7.1.). Gels were vacuum dried and exposed to an Imaging (phosphor) screen K (Bio-Rad) overnight. Gels were scanned using the Personal Molecular Imager[®] FX (Bio-Rad) and images were analysed using PDQuestTM 2-D analysis software (Bio-Rad).

2.2.2.9. Isolation of viral DNA from Sf9 cells

Sf9 cells, seeded at 1×10^6 cells per 35 mm well of a 6-well plate, were infected with recombinant baculoviruses at a MOI of 5 pfu/cell. Cells were harvested at 72 h.p.i. and resuspended in 0.5 ml STE-TX buffer (0.01 M NaCl, 0.01 M Tris-HCl pH 7.6, 0.001 M EDTA, 0.5% Triton X-100). The suspension was incubated on ice for 5 min during which it was vortexed every minute. Nuclei were pelleted by centrifugation at 2000 rpm for 5 min, washed once in $1 \times$ PBS and dissolved in 0.5 ml extraction buffer (0.1 M Tris, 0.1 M EDTA, 0.2 M KCl pH 7.5). To this solution, 20 μ g proteinase K was added and the mixture was incubated for 1 h at 50°C, followed by the addition of 50 μ l 10% sarcosyl and a further 2 h incubation at 50°C. An equal volume of phenol/chloroform/isoamylalcohol mixture was added. DNA was separated from the denatured proteins in phenol by centrifugation at 13 000 rpm for 5 min, after which the upper aqueous layer containing the DNA was transferred to a new tube and 100 μ l STE (0.01 M NaCl, 0.01 M Tris-HCl pH 7.6, 0.001 M EDTA) was added. After a 1 min centrifugation at 13 000 rpm for 5 min, the upper aqueous layer containing the DNA was transferred to a new tube. Residual phenol was removed by the addition of one volume chloroform. Phenol/chloroform/isoamylalcohol extraction was repeated, after which DNA was precipitated in the presence of two volumes 96% EtOH and 1/10 volume 3 M NaAc at -20°C for 60 min. DNA was washed with 80% EtOH, air-dried and resuspended in 30 μ l ddH₂O.



2.2.2.10. Glycosylation assay

A glycosylation assay was performed by means of carbohydrate-specific periodic acid Schiff (PAS) staining as described by Carlsson (1993). Samples were separated by SDS-PAGE as described in 2.2.2.7.1. Gels were incubated for 2 h in fixation solution (10% acetic acid, 35% methanol), followed by a 1 h incubation in periodate solution (0.7% periodic acid, 5% acetic acid) with gentle shaking. Gels were then rinsed in dH₂O and incubated for 5 to 10 min in meta-bisulphite solution (0.2% sodium meta-bisulphite, 5% acetic acid) until they turned yellow. They were then incubated in fresh meta-bisulphite solution for 5 to 10 min until they were clear. After this, gels were incubated in Schiffs reagent for 2 h. Because this protocol was previously found to be temperature sensitive, all steps were performed at 30°C. Two positive controls of glycosylated proteins, namely ovalbumin, the 45kDa band of Rainbow marker (RPN 756, Amersham biosciences) and glycosylated blood serum proteins, were included.

2.2.2.11. Cytotoxicity assay

Spinner suspension cultures of 5×10^7 Sf9 cells were infected with recombinant baculoviruses at a MOI of 5 pfu/cell. 100 μ l aliquots of infected cells were removed at 12, 24, 27, 30, 33, 36, 48 and 72 hours post infection. Cells were stained with an equal volume of 0.4% trypan blue in 1 x PBS. The number of stained cells was counted using a haemocytometer and was expressed as a percentage of total cells.

2.2.2.12. Fluorescent microscopy

Sf9 cells, seeded at 1×10^6 cells per 35 mm well of a 6-well plate, were infected with recombinant baculoviruses at a MOI of 5 pfu/cell. Cells were analysed for fluorescence using a Zeiss Axiovert 200 Fluorescent microscope after 24 h, 48 h and 72 h. Magnifications of 5x, 10x, 20x and 40x were used. eGFP was detected at 489nm. Photographs were processed using the standard Axiovert operating software provided with the microscope.

2.2.2.13. Protein release assay

Spinner suspension cultures of 50×10^6 Sf9 cells were infected at a MOI of 5 pfu/cell. A sample of 1 ml of cells was harvested 18 h post-infection as well as every 6 h thereafter up until 72 h post-infection. Cells were collected by centrifugation at 200 g for 5 min, after which the medium in which the cells had been growing was removed and kept. The cells were resuspended in 1ml 1 x STE

(0.01 M NaCl, 0.01 M Tris, 0.05 M EDTA) containing protease inhibitors (1 mg/ml Pepstatin, 0.7 µg/ml Pefabloc). Both the medium and the cells were frozen and kept at -70°C until all samples had been collected. Each sample of cells was lysed by treatment with 0.05% Triton X-100 for 30 min, followed by dounce homogenisation and centrifugation at 13 000 rpm for 10 min to separate soluble and insoluble components. The pellet (insoluble component) was resuspended in 1 ml 1 x STE. A fluorometer (Bio-Rad) was used to take fluorescent measurements of each component for each of the samples collected. To account for any background fluorescence, samples were also taken pre-infection and immediately after infection.

2.2.2.14. Subcellular fractionation

Subcellular fractionations were performed at 24 and 48 hours post infection using a protocol adapted from that used by Brignati *et al.* (2003). Sf9 cells, seeded at 1×10^6 cells per 35mm well of a 6-well plate, were infected with recombinant baculoviruses at a MOI of 5 pfu/cell. Cells were collected by centrifugation at 3000 rpm for 10 min, washed twice with $1 \times$ PBS and resuspended in 300 µl hypotonic buffer (10 mM Tris, 0.2 mM MgCl₂ [pH 7.4]) containing protease inhibitors (1 mg/ml Pepstatin, 0.7 µg/ml Pefabloc). Resuspended cells were incubated on ice for 30 min, after which they were lysed by five passages through a 29G needle. Unbroken cells and nuclei were removed by centrifugation at 1500 rpm for 2 min. Cellular membranes present in the supernatant were pelleted by centrifugation at 13 000 rpm for 1 h. A fluorometer (Fluoroskan Ascent FL Type 374; ThermoLabsystems) was used to take fluorescent measurements of all components of all steps in this procedure. Measurements were captured using Ascent Software Version 2.4.2.

In a separate assay, cells were resuspended in 300 µl hypotonic buffer containing 0.5% Triton X-100 and incubated on ice for 30 min before undergoing subcellular fractionation as described above.

2.2.2.15. Membrane flotation analysis

Membrane flotation analysis was performed using a protocol adapted from that used by Brignati *et al.* (2003). Sf9 cells, seeded at 1×10^6 cells per 35mm well of a 6-well plate, were infected with recombinant baculoviruses at a MOI of 5 pfu/cell. The cells were harvested after a 48 h incubation period at 27°C and collected by centrifugation at 3000 rpm for 10 min. Cells were washed twice with $1 \times$ PBS and were resuspended in 300 µl hypotonic buffer (10 mM Tris, 0.2 mM MgCl₂ [pH 7.4]) containing protease inhibitors (1 mg/ml Pepstatin, 0.7 µg/ml Pefabloc). Resuspended cells were incubated on ice for 30 min, after which they were lysed by five passages through a 29G needle. A 250 µl sample of the lysed cells was combined with 1340 µl 85% sucrose in $1 \times$ NTE

(100 mM NaCl, 10 mM Tris, 1 mM EDTA [pH 7.4]) to give a final sucrose concentration of 72% sucrose. This sample was loaded into a 5 ml polyallomer tube (Beckman) as the bottom fraction of a sucrose gradient. This fraction was overlaid with 2320 μ l 65% sucrose in 1 x NTE and 1090 μ l 10% sucrose in 1 x NTE. Gradients were spun at 38 000 rpm for 18 h at 4°C in the Beckman SW55Ti rotor using a Beckman Coulter Optima™ L-100 XP Ultracentrifuge. Fractions of 200 μ l were collected from the bottom of the tube through a needle and a fluorometer (Fluoroskan Ascent FL Type 374; ThermoLabsystems) was used to take fluorescence readings of each of the fractions. Measurements were captured using Ascent Software Version 2.4.2. The pellet was resuspended in 200 μ l 1 x NTE and was used as the first fraction.

In a separate assay, cells were resuspended in 300 μ l hypotonic buffer containing 0.5% Triton X-100 and incubated on ice for 30 min before undergoing membrane flotation as described above.

2.2.2.16. Brefeldin A treatment

Sf9 cells, seeded at 1×10^6 cells per 35 mm well of a 6-well plate, were infected with recombinant baculoviruses at a MOI of 5 pfu/cell. At 1 h.p.i. the infection medium was replaced with 1 ml medium containing 10 μ g/ml Brefeldin A (MP Biomedicals Inc.). Cells were analysed by fluorescent microscopy (2.2.2.10.) and membrane flotation analysis (2.2.2.15.) at 48 h.p.i.

2.2.2.17. Confocal microscopy

Sf9 cells, seeded at 1×10^6 cells per 35 mm well of a 6-well plate, were infected with recombinant baculoviruses at a MOI of 5 pfu/cell. Cells were analysed for fluorescence using a Zeiss LSM 510 META Laser Scanning Microscope after 24 h, 33 h and 48 h. eGFP was detected at 489nm. For nuclear staining, cells were labelled with 10 μ g/ml DAPI (4'6'-diamidino-2-phenylindole) for 10 minutes at room temperature before being analysed for fluorescence. DAPI was detected at 405 nm. To stain the Golgi complex, cells were incubated in medium containing 5 μ M BODIPY®TR (Molecular Probes Inc., Eugene, OR) for 15 min before examination. BODIPY®TR was detected at 543 nm. To stain the ER, cells were incubated in medium containing 5 μ M VYBRANT™ Dil cell-labelling solution (Molecular Probes Inc., Eugene, OR) for 30 min before examination. VYBRANT™ Dil was detected at 543 nm. Collected images were processed using Zeiss LSM Image Browser Version 4,0,0,157.

2.3. Results

2.3.1. Production of constructs in pFastBac

In order to identify candidate regions of NS3 that may be involved in its subcellular localisation, seven different constructs will be produced and used to generate recombinant baculoviruses for expression as fusion proteins in *Spodoptera frugiperda* (Sf9) insect cells. These constructs involve various truncated or mutated versions of AHSV-3 NS3, linked to the N-terminal of eGFP (Figure 2.1).

The first construct will consist of eGFP on its own and will serve as negative control for membrane association. The second construct will consist of the full-length AHSV-3 NS3 protein fused to the N-terminal of eGFP. This construct will be used to visualize the localisation of wild-type NS3 within a cell. The third construct will consist of the NS3A protein (NS3A is initiated at the second in-frame methionine and so is equivalent to NS3 lacking the 10 amino acids on its N-terminal) fused to the N-terminal of eGFP. This construct will be used to visualize the localisation of NS3A within a cell. The fourth construct will consist of the 11 amino acid region on the N-terminal of NS3 fused to the N-terminal of eGFP. This construct will be used to investigate whether the N-terminal domain of AHSV NS3 can confer specific localisation. The rationale for this was a previous report where BTV NS3 was found to bind to a cellular exocytosis protein via an amphipathic helix formed by the 12 N-terminal amino acids of NS3 (Beaton *et al.*, 2002). The fifth construct will consist of the NS3 protein, with a C-terminal truncation that includes the putative dileucine motif (DTSVLL), fused to the N-terminal of eGFP. This construct will be used to investigate whether this dileucine motif is involved in membrane trafficking as has been described for other proteins containing dileucine motifs (D/EXXXLL; Fernandez-Salas *et al.*, 2004; Greenberg *et al.*, 1998). For constructs six and seven, each of the hydrophobic domains of NS3 has previously been modified by the substitution of four to five amino acids that changes the region from a stretch of nonpolar amino acids to a region of charged residues (Van Niekerk *et al.*, 2001a). Construct six will consist of the NS3 protein, with amino acids 124 to 128 in its first hydrophobic domain mutated from VTMTAT to RTRDK, fused to the N-terminal of eGFP. Construct seven will consist of the NS3 protein, with amino acids 165 to 168 in its second hydrophobic domain mutated from MLLA to KRVD, fused to the N-terminal of eGFP. These constructs will be used to investigate whether mutations in either of the hydrophobic domains result in a change in the localisation patterns of the NS3 protein.

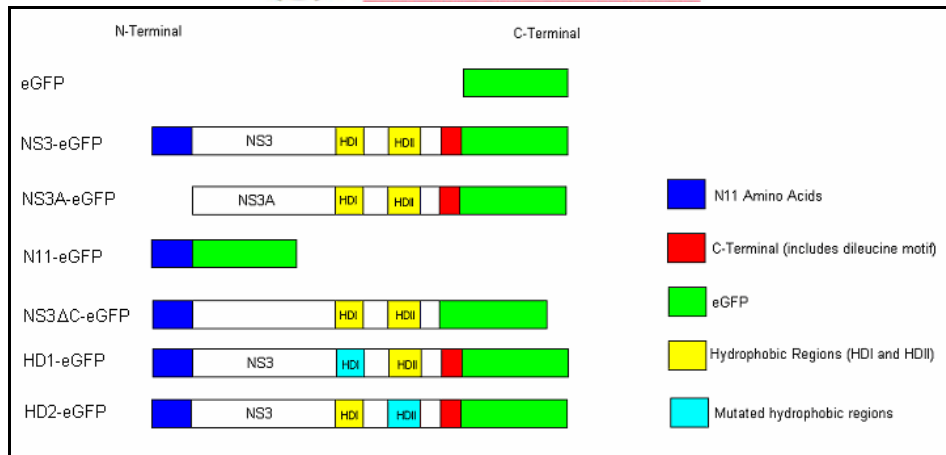


Figure 2.1. Schematic representation of protein constructs that will be produced for baculovirus expression. 1. eGFP: The eGFP protein. 2. NS3-eGFP: The full length AHSV-3 NS3 protein fused to the N-terminal of eGFP. 3. NS3A-eGFP: The NS3A protein (i.e. NS3 minus the 10 amino acids on the N-terminal) fused to the N-terminal of eGFP. 4. N11-eGFP: The 11 amino acid region on the N-terminal of NS3 fused to the N-terminal of eGFP. 5. NS3ΔC-eGFP: The NS3 protein, without the putative dileucine motif on its C-terminal, fused to the N-terminal of eGFP. 6. HD1-eGFP: The NS3 protein, with its first hydrophobic domain mutated, fused to the N-terminal of eGFP. 7. HD2-eGFP: The NS3 protein, with its second hydrophobic domain mutated, fused to the N-terminal of eGFP.

An outline of the cloning strategy to be followed is included in Figure 2.2.

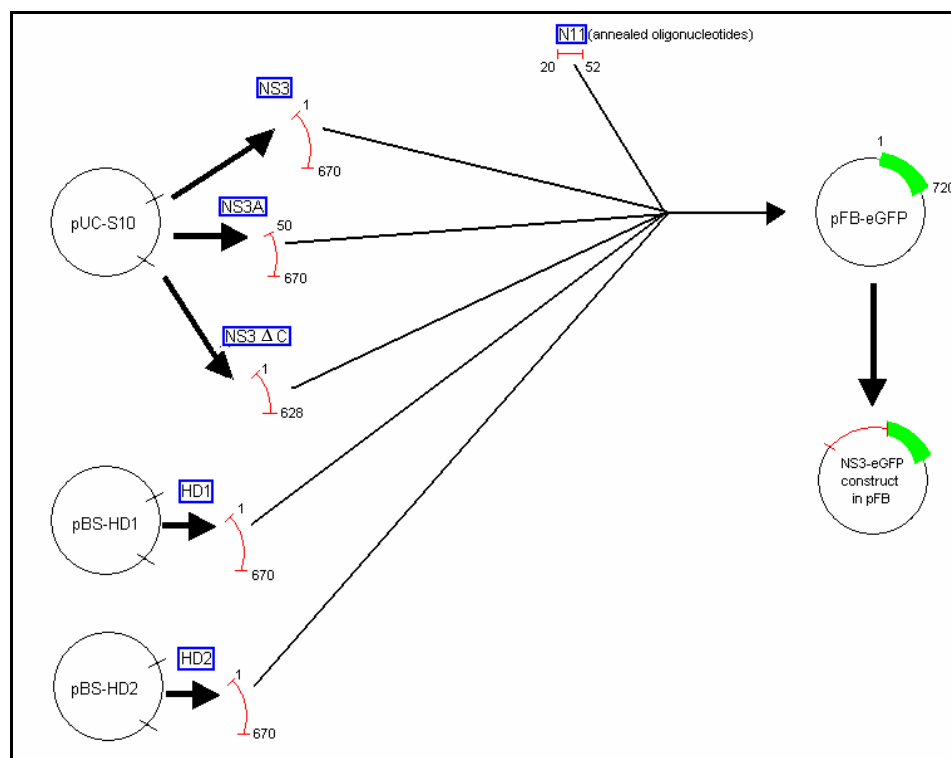


Figure 2.2. Schematic diagram of the cloning process to be used for the production of the seven different constructs in pFastBac. NS3 encoding inserts for NS3-eGFP, NS3A-eGFP and NS3ΔC-eGFP will be amplified from pUC-S10. NS3 encoding inserts for HD1-eGFP and HD2-eGFP will be amplified from pBS-HD1 and pBS-HD2. pFB-eGFP contains the eGFP gene cloned into the *EcoRI* and *HindIII* sites of pFastBac1. The first 11 N-terminal amino acids of NS3 (NS3-N11) to be used for the construction of pFB-N11-eGFP will be ordered as two separate oligonucleotides that are modified by the addition of 5' *Bam*HI and 3' *EcoRI* sites to allow for cloning. These oligonucleotides will be annealed and all NS3 encoding inserts (wild-type and mutant) will be digested and cloned into the *Bam*HI and *EcoRI* sites of pFB-eGFP to produce the seven constructs described above. eGFP is represented by the green bar. NS3 inserts are represented by the red fragments.

2.3.1.1. Generation of different AHSV-3 S10 fragments

The production of the seven constructs depended on four plasmids; pFB-eGFP, pUC-S10, pBS-HD1 and pBS-HD2, that had been constructed previously (2.2.1.1.). pFB-eGFP was to be used as the starting vector for all constructs. pUC-S10, pBS-HD1 and pBS-HD2 were used for PCR amplification of the NS3 inserts used for the construction of NS3-eGFP, NS3A-eGFP, NS3ΔC-eGFP, HD1-eGFP and HD2-eGFP. The starting plasmids were isolated successfully and were visible as bands of between 1500 bp and 5000 bp. Due to the nonlinear natures of these plasmids, the sizes of the bands as seen on this gel do not correlate exactly with the sizes of the plasmids. In addition, a smear of RNA was visible in each of the lanes below the plasmid bands (Figure 2.3).

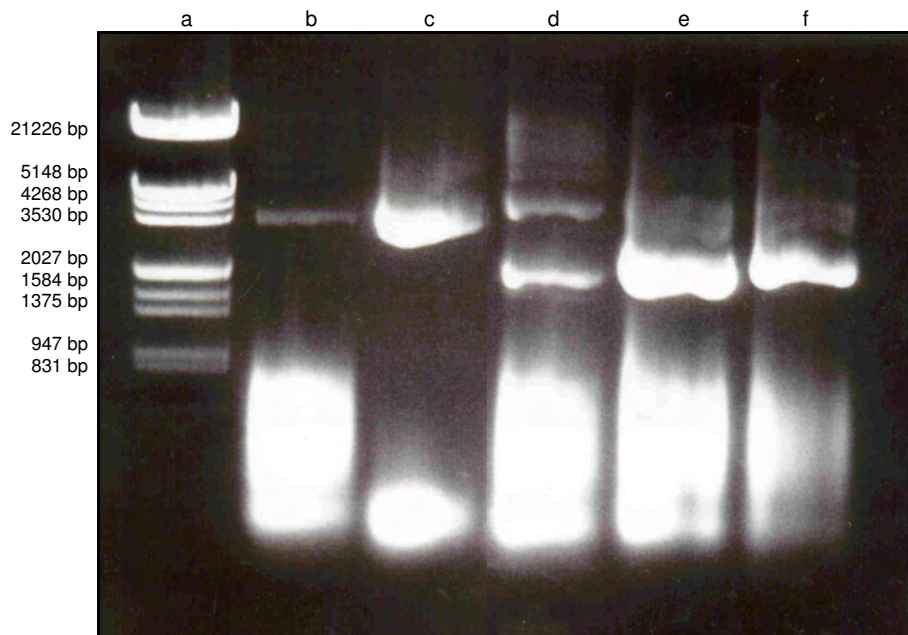


Figure 2.3. Agarose gel (1%) of plasmids pFB (b), pFB-eGFP (c), pUC-S10 (d), pBS-HD1 (e) and pBS-HD2 (f) initially isolated for the production of the seven constructs. Lambda DNA/*EcoRI*+*HindIII* Marker (Fermentas) was included as a molecular weight marker (a), sizes of fragments are as indicated.

NS3 inserts for the construction of pFB-NS3-eGFP, pFB-NS3A-eGFP, pFB-NS3ΔC-eGFP, pFB-HD1-eGFP and pFB-HD2-eGFP were obtained by PCR amplification and were modified by the addition of *Bam*HI sites on their 5' ends and *Eco*RI sites on their 3' ends to facilitate cloning into pFB-eGFP. Details of the PCR amplification reactions can be found in Table 2.3.

Table 2.3. Details of the PCR amplification reactions used for the amplification of the various NS3 inserts. The forward and reverse primers, annealing temperatures and templates used as well as the expected sizes of the fragments obtained are indicated.

Insert	Forward Primer	Reverse Primer	Annealing temperature	Template	Expected Size (bp)
NS3	NS3pBam	NS3StopEcoR	50°C	pUC-S10	670
NS3A	NS3ABamF	NS3StopEcoR	53°C	pUC-S10	620
NS3ΔC	NS3pBam	NS3DileucR	51°C	pUC-S10	625
HD1	NS3pBam	NS3StopEcoR	50°C	pBS-HD1	670
HD2	NS3pBam	NS3StopEcoR	50°C	pBS-HD2	670

PCR reactions were carried out successfully according to the protocol in 2.2.1.4 and fragments of the expected sizes were obtained (Figure 2.4). Fragments were subsequently digested with *Bam*HI and *Eco*RI and purified by column purification.

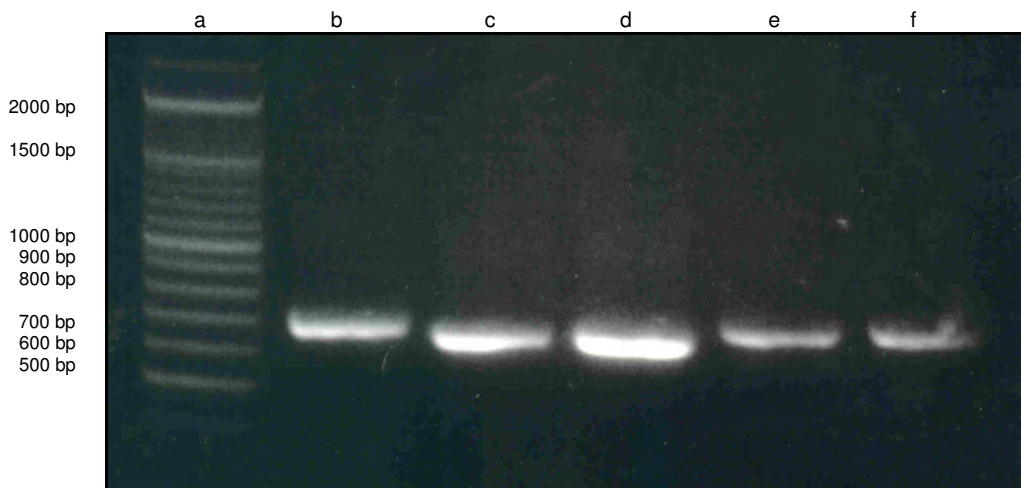


Figure 2.4. Agarose gel (1%) of PCR products generated for the production of the seven constructs. Included in this gel are NS3 (b), NS3A (c), NS3ΔC (d), HD1 (e) and HD2 (f). The O'RangeRuler™ 100 bp + 500 bp DNA ladder (Fermentas) was included as a size marker (a), sizes of fragments are as indicated.

The N11 region used for the construction of pFB-N11-eGFP was formed by the annealing of two oligonucleotides. The oligonucleotides were designed to encode amino acid 1 - 11 (bp 20 - 52) of AHSV-3 NS3 and contain *Bam*HI sites on their 5' ends and *Eco*RI sites on their 3' ends to facilitate cloning into pFB-eGFP. Annealed oligonucleotides were digested with *Bam*HI and *Eco*RI and purified either directly by ethanol precipitation or by phenol/chloroform extraction followed by ethanol precipitation. Following annealing and digestion we expect to be left with a 32 bp fragment. The recovery of the fragment was verified by agarose gel electrophoresis (Figure 2.5).

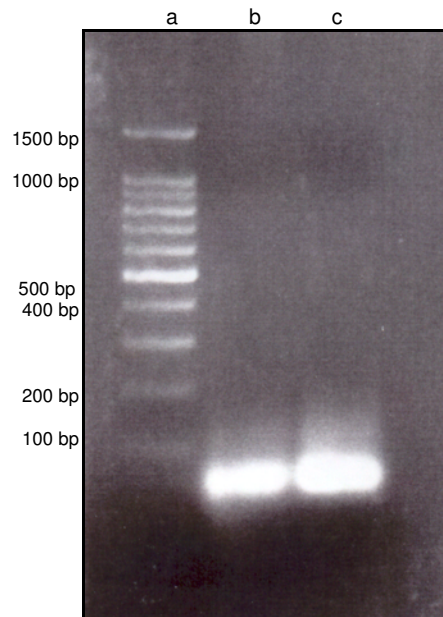


Figure 2.5. Agarose gel (2%) of the annealed oligonucleotides representing the N11 region used for the construction of pFB-N11-eGFP. Following restriction enzyme digestion, the DNA fragment was purified by ethanol precipitation (b) or phenol/chloroform extraction followed by ethanol precipitation (c). The 100 bp ladder (Promega) was included as a size marker (a), sizes of fragments are as indicated.

2.3.1.2. Production of different NS3-eGFP fusions by cloning into the pFB-eGFP vector

pFB-eGFP was digested with *Bam*HI and *Eco*RI and purified by gel purification. eGFP had been cloned into the *Eco*RI/*Hind*III sites of pFB. By cloning the new NS3 encoding DNA fragments into the *Bam*HI/*Eco*RI sites, the NS3 encoding segment is inserted upstream and in-frame with eGFP. NS3 segments to be used as inserts for the production of pFB-NS3-eGFP, pFB-NS3A-eGFP, pFB-NS3 Δ C-eGFP, pFB-HD1-eGFP and pFB-HD2-eGFP were digested with *Bam*HI and *Eco*RI and purified by column purification (Figure 2.6).

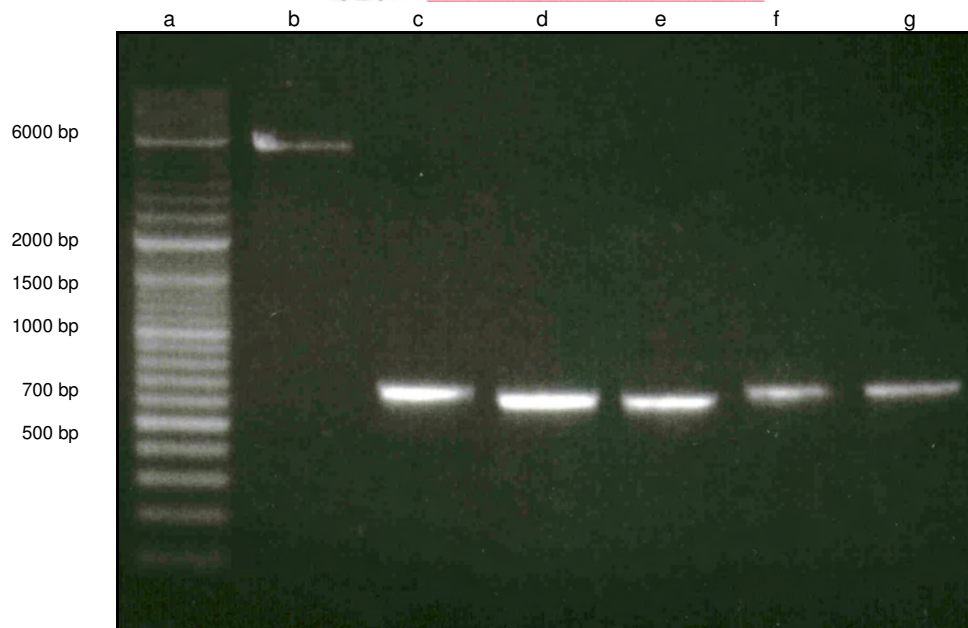


Figure 2.6. Agarose gel (1%) of purified restriction enzyme digestions (*Bam*HI and *Eco*RI) of fragments used for ligation. pFB-eGFP (b) was purified by gel purification. NS3 (c), NS3A (d), NS3ΔC (e), HD1 (f) and HD2 (g) inserts were purified by column purification. The O'RangeRuler™ 100 bp + 500 bp DNA ladder (Fermentas) was included as a size marker (a), sizes of fragments are as indicated.

Concentrations of the vector and inserts were estimated (Figure 2.6) and purified inserts were ligated into pFB-eGFP using an insert: vector ratio of approximately 10:1. Ligations were used to transform competent XL1Blue *E. coli* cells and a number of colonies were obtained for each construct. Colonies were grown up overnight in liquid culture and plasmids were isolated and verified using restriction enzyme digestion (pFB-NS3-eGFP, pFB-NS3A-eGFP, pFB-N11-eGFP and pFB-NS3ΔC-eGFP) or colony PCR (pFB-HD1-eGFP and pFB-HD2-eGFP).

To confirm the presence of the eGFP insert in pFB-NS3-eGFP, pFB-NS3A-eGFP, pFB-N11-eGFP and pFB-NS3ΔC-eGFP, digestions were performed using *Eco*RI and *Hind*III (not shown). To confirm the presence of the NS3 insert in pFB-NS3-eGFP, pFB-NS3A-eGFP and pFB-NS3ΔC-eGFP, digestions were performed using *Bam*HI and *Eco*RI (not shown). These digestions were combined and triple digestions (*Bam*HI/*Eco*RI/*Hind*III) were carried out to verify these constructs. N11-eGFP was verified using *Bam*HI/*Hind*III and *Pvu*I (as the N11 region contains an internal *Pvu*I site) digestions. For *Bam*HI/*Eco*RI/*Hind*III digests of pFB-NS3-eGFP, pFB-NS3A-eGFP and pFB-NS3ΔC-eGFP, we expect to see a large vector fragment of approximately 4775 bp and an eGFP fragment of approximately 720 bp. We expect to see an NS3 fragment of 670 bp for NS3-eGFP, 620 bp for NS3A-eGFP and 625 bp for NS3ΔC-eGFP. For the *Bam*HI/*Hind*III digest of N11-eGFP, we expect to see the large vector fragment as well as a second fragment of approximately 760 bp, corresponding to the size of eGFP and the N11 region together. When pFB-N11-eGFP is digested with *Pvu*I, two fragments should be obtained. One of the fragments should be approximately 2500 bp in size while the other should be approximately 3000 bp in size as there is a *Pvu*I site present in

the plasmid, pFB (at position 1004), as well as in the N11 region of NS3. Digestion products were analysed by 2% agarose gel electrophoresis. Figures 2.7 and 2.8 show the digestion products of verification digestions carried out for plasmids that did seem to contain inserts of the correct size.

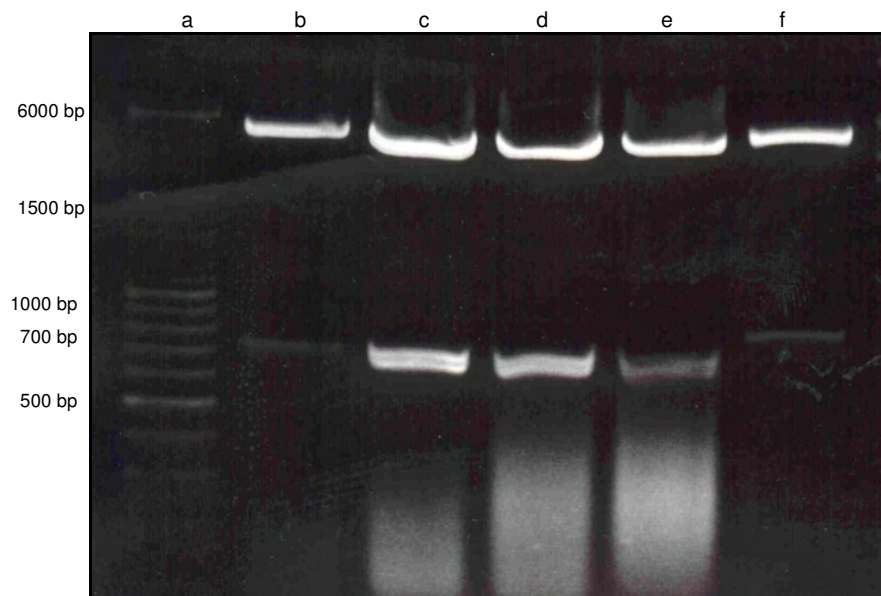


Figure 2.7. Agarose gel (2%) of digestions used to verify pFB-NS3-eGFP, pFB-NS3A-eGFP, pFB-NS3 Δ C-eGFP and pB-N11-eGFP. pFB-NS3-eGFP (c), pFB-NS3A-eGFP (d) and pFB-NS3 Δ C-eGFP (e) were digested with *Bam*HI/*Eco*RI/*Hind*III. pFB-N11-eGFP was digested with *Bam*HI/*Hind*III (f). The O'RangeRuler™ 100 bp + 500 bp DNA ladder (Fermentas) was included as size marker (a), sizes of fragments are as indicated. pFB-eGFP was digested with *Bam*HI/*Eco*RI/*Hind*III and used as a size marker (b).

pFB-eGFP (b) and pFB-N11-eGFP (f) were column purified before digestion, while pFB-NS3-eGFP (c), pFB-NS3A-eGFP (d) and pFB-NS3 Δ C-eGFP (e) were not (Figure 2.7). This explains the high levels of RNA that were present in lanes (c) to (e). The digestions indicated the presence of a large fragment of approximately 4775 bp in (b) to (f). This size is consistent with that of the vector used (pFB). The size of this large band seemed to vary slightly on this gel, especially in lanes (c) to (e) where it appeared to be slightly smaller. This may be due to varying kinetics of the DNA fragments in the gel that may be caused by the large amounts of RNA present in these three samples. A second fragment of approximately 720 bp was present in (b) to (e). This size is consistent with that of the eGFP gene used in the production of these constructs. The size of the second fragment in (f) was approximately 760 bp, which is slightly larger than the size of the eGFP insert on its own. The size of this fragment corresponds to that of eGFP and the N11 region together. The size of the third fragment present in (c), (d) and (e) was 620 - 670 bp, representing the NS3 gene used as the insert for pFB-NS3-eGFP (c), pFB-NS3A-eGFP (d) and pFB-NS3 Δ C-eGFP (e). The third fragment present in lanes (c) to (e) was not always clearly visible. This is due to the small difference in size between these fragments and the eGFP fragment, resulting in an overlap of the two bands.

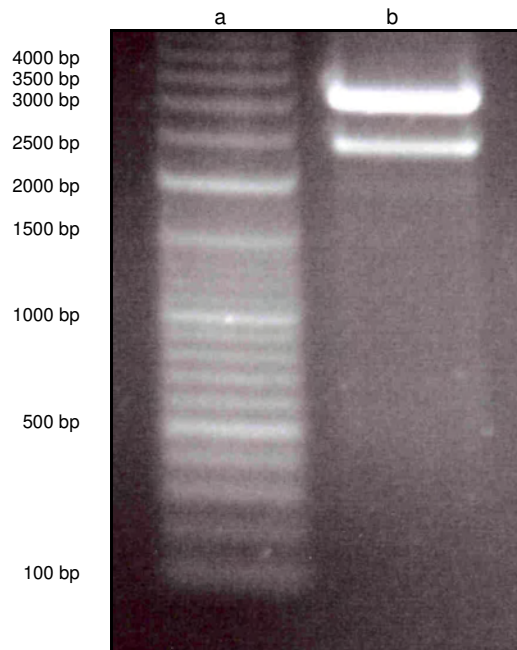


Figure 2.8. Agarose gel (2%) of *PvuI* digestion used to verify pFB-N11-eGFP (b). The O'RangeRuler™ 100 bp + 500 bp DNA ladder (Fermentas) was included as size marker (a), sizes of fragments are as indicated.

When pFB-N11-eGFP was digested with *PvuI*, two fragments were obtained (Figure 2.8). One of the fragments was approximately 2500 bp in size while the other was approximately 3000 bp in size. This is consistent with what was expected as there is a *PvuI* site present in the plasmid, pFB (at position 1004), as well as in the N11 region of NS3.

The presence of the NS3 insert in colonies obtained for pFB-HD1-eGFP and pFB-HD2-eGFP was verified by colony PCR, using the primers NS3pBam and NS3pEco (Table 2.1). PCR products were visualised on 1% agarose gels (Figure 2.9).

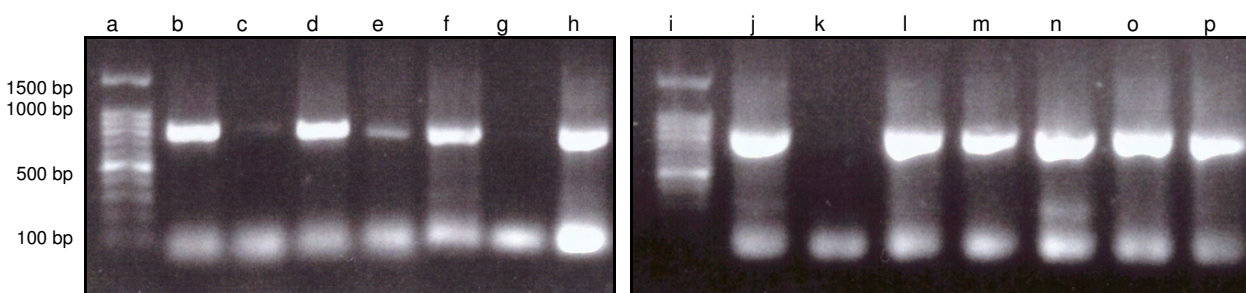


Figure 2.9. Agarose gel (1%) of PCR products obtained from colony PCR for the verification of pFB-HD1-eGFP and pFB-HD2-eGFP. pBS-HD1 was used as the template for the positive control for pFB-HD1-eGFP colony PCR reactions (b). pBS-HD2 was used as the template for the positive control for pFB-HD2-eGFP colony PCR reactions (j). Negative controls lacking any DNA were included (c), (k). Colony PCR products were loaded in lanes (d) - (h) and (l) - (p). The 100 bp ladder (Promega) was included as a size marker (a), (i), sizes of fragments are as indicated.

For pFB-HD1-eGFP, PCR reactions in (d), (e), (f) and (h) were successful and yielded bands of approximately 720 bp. For pFB-HD2-eGFP, PCR reactions in (l), (m), (n), (o) and (p) were successful and yielded bands of approximately 720 bp. The colonies used as templates for these

PCR reactions seemed to contain the NS3 insert, which is approximately 720 bp in size (Figure 2.9).

Once verified by restriction enzyme digestion or colony PCR, one colony for each of the constructs was selected for subsequent analysis.

2.3.1.3. Sequence verification of recombinant pFB constructs

Sequencing reactions were carried out using the flanking primers of the specific construct as well as a primer designed to anneal to the 270 - 249 bp region of the eGFP gene (eGFP_{internal}). This primer was designed specifically for sequencing in a reverse direction to enable verification of the NS3-3' and eGFP-5' junction. Sequencing results confirmed that all constructs had been produced correctly and were in the correct orientation and reading frame for expression (Appendix 1). The stop codon of NS3 had in all cases been removed successfully, yielding a single open reading frame from the NS3 initiation codon to the eGFP stop codon. Inserts had identical sequences to the published sequences of eGFP and AHSV-3 NS3, except for one point mutation (adenine → guanine) at bp 462 of AHSV-3 NS3 in one of the constructs (pFB-NS3-eGFP). The mutation present is a missense mutation that results in a change of amino acid 148 of the NS3 protein from aspartic acid (D), a negatively charged polar amino acid, to glycine (G), a nonpolar amino acid. The amino acid at this position in serotypes 2, 3, 7 and 8 is aspartic acid (D) but is asparagine (N) in serotypes 4, 5, 6 and 9 (Van Niekerk, 2001c). This mutation is present in the variable region of NS3, just before the second hydrophobic domain. Additional clones were sequenced and the PCR reactions and clonings were repeated, but the mutation remained. The PCR product was sequenced and was found to contain the mutation. The original clone was sequenced to confirm that its sequence is correct (D at 148). Analysis of an independent clone, constructed by Michelle Victor (Department of Genetics, University of Pretoria), revealed the same mutation. The reason for the repeated generation of this specific mutation is unknown.

Predictions were carried out using TMMOD (liao.cis.udel.edu/website/servers/TMMOD/) in order to see if this mutation affects the predicted membrane orientation of the NS3 protein (Figure 2.10). TMMOD is a program that uses a hidden markov model to predict transmembrane protein topology (Kahsay *et al.*, 2005).

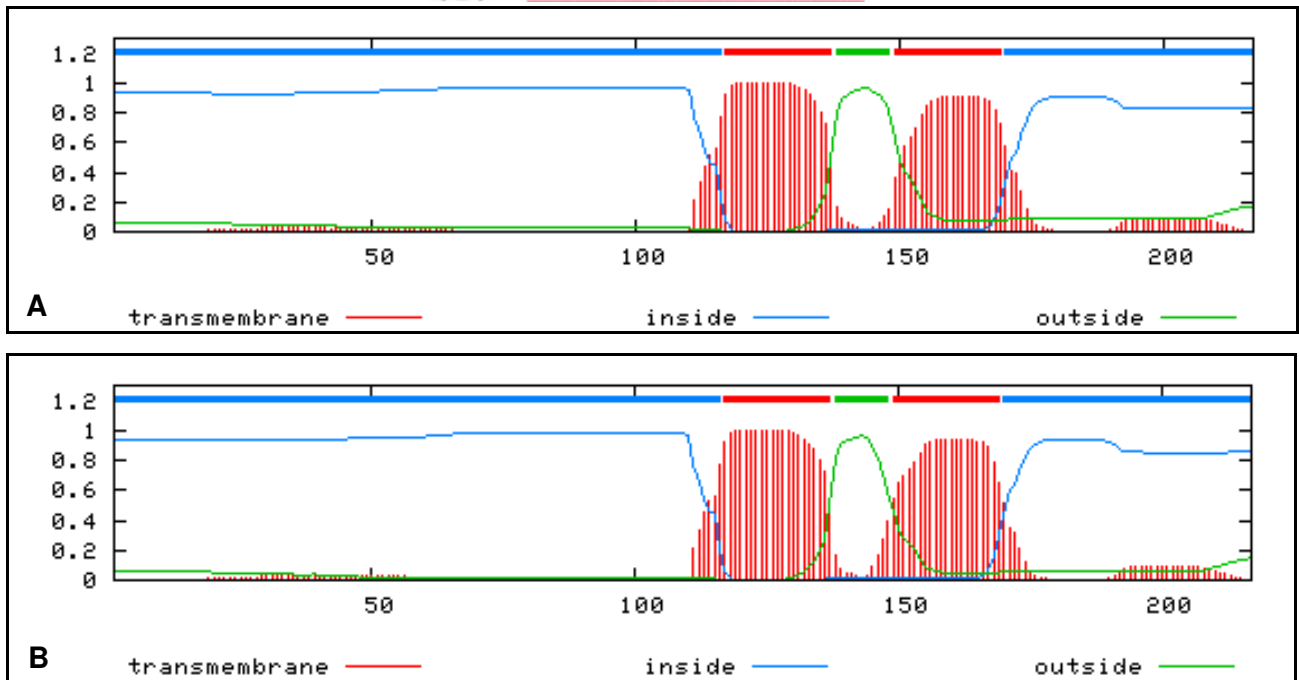


Figure 2.10. A: TMMOD prediction for NS3 (without the mutation). B: TMMOD prediction for NS3 with the mutation. The x-axis indicates the amino acids while the y-axis indicates the probability of a transmembrane region occurring at that position in the protein.

For NS3 without the mutation, TMMOD predicted two transmembrane regions with the N- and C-termini located in the cytoplasm. For NS3 with the mutation, TMMOD also predicted two transmembrane regions with the N- and C-termini located in the cytoplasm.

The prediction outputs show that the mutation does not seem to affect the predicted transmembrane domains or the membrane topology to a great extent, therefore it was decided that all seven constructs produced (Table 2.4) would be used for expression in the Bac-to-Bac[®] baculovirus expression system.

Table 2.4. Summary of the properties of each of the seven constructs produced. Included are the gene fragments and encoding amino acids of both the NS3 insert and the eGFP insert used for the production of each construct. Mutations present in the NS3 inserts of pFB-HD1-eGFP and pFB-HD2-eGFP are as indicated. Plasmid constructs were used to generate recombinant baculoviruses, as indicated, for expression in Sf9 cells.

Construct	NS3 insert (<i>Bam</i> HI/ <i>Eco</i> RI)		eGFP insert (<i>Eco</i> RI/ <i>Hind</i> III)		Recombinant baculovirus
	Gene Fragment (bp)	Encoding AA	Gene Fragment (bp)	Encoding AA	
pFB-eGFP	-	-	1 - 720	1 - 240	Bac-eGFP
pFB-NS3-eGFP	1 - 670	1 - 217	1 - 720	1 - 240	Bac-NS3-eGFP
pFB-NS3A-eGFP	50 - 670	11 - 217	1 - 720	1 - 240	Bac-NS3A-eGFP
pFB-N11-eGFP	20 - 52	1 - 11	1 - 720	1 - 240	Bac-N11-eGFP
pFB-NS3ΔC-eGFP	1 - 628	1 - 203	1 - 720	1 - 240	Bac-NS3ΔC-eGFP
pFB-HD1-eGFP	1 - 670	1 - 217 (124 - 128: VTMAT → RTRDK)	1 - 720	1 - 240	Bac-HD1-eGFP
pFB-HD2-eGFP	1 - 670	1 - 217 (165 - 168: MLLA → KRDV)	1 - 720	1 - 240	Bac-HD2-eGFP

2.3.2. Baculovirus expression of fusion proteins

Once the constructs had been verified in pFB, plasmids were isolated and used to transform DH10BacTM cells. These cells contain a baculovirus vector (bacmid) with a mini-*att*Tn7 target site as well as a helper plasmid. The fusion protein in pFB is flanked by the left and right arms of Tn7 and forms a mini-Tn7 element. When the plasmid is transformed into DH10BacTM cells, transposition occurs between the mini-Tn7 element on the pFB vector and the mini-Tn7 target site on the bacmid to generate a recombinant bacmid. The transposition reaction occurs in the presence of transposition proteins supplied by the helper plasmid present in the DH10BacTM cells (Invitrogen Life Technologies). Transformation reactions were plated in the presence of IPTG and X-gal and blue/white screening was used for the selection of recombinants. A number of white colonies were obtained for each fusion protein. These white colonies were restreaked to verify their phenotype and true white colonies were grown in liquid culture overnight. Bacmid DNA was isolated and verified by PCR and sequencing. PCR reactions were performed as described in 2.2.1.4. using the primers PFB1 POLH FW and PFB1 RV (Figure 2.11).

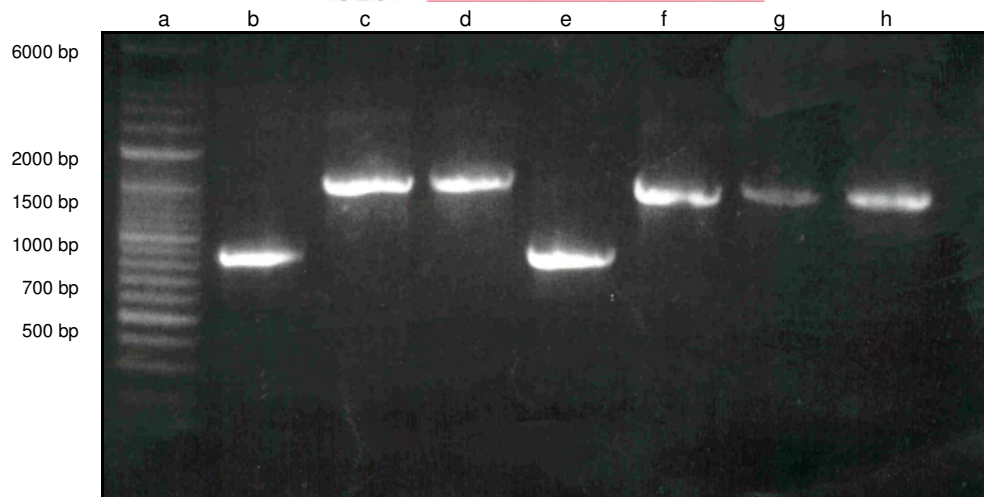


Figure 2.11. Agarose gel (1%) of PCR reactions carried out for the verification of bacmid DNA. Included in this gel are eGFP (b), NS3-eGFP (c), NS3A-eGFP (d), N11-eGFP (e), NS3 Δ C-eGFP (f), HD1-eGFP (g) and HD2-eGFP (h). The O'RangeRuler™ 100 bp + 500 bp DNA ladder (Fermentas) was included as a size marker (a), sizes of fragments are as indicated.

PCR reactions were carried out successfully, and fragments of the expected sizes were obtained. The sizes of the fragments obtained for NS3-eGFP (c) and NS3A-eGFP (d) are very similar as these proteins only differ in size by 11 amino acids. The fragment obtained for NS3 Δ C-eGFP (f) does seem to be slightly smaller than that obtained for NS3-eGFP (c). This is expected as it is 14 amino acids smaller than NS3-eGFP (Figure 2.11). Fragments were purified by column purification and verified by sequencing.

Sequencing reactions were carried out using the primers PFB1 POLH FW, PFB1 RV and eGFP_{internal}. Results confirmed that all constructs had been transposed into the bacmid plasmid correctly and were in the correct orientation and reading frame for expression. Inserts had identical sequences to the published sequences of eGFP and AHSV-3 NS3, except for the point mutation mentioned previously, and the engineered mutations or truncations.

Once verified by PCR and sequencing, bacmid DNA was used to transfect Sf9 cells as described in 2.2.2.4. Viral supernatants were removed after 72 hours, purified by plaque purification as described in 2.2.2.5. and supernatants from single plaques were used to infect Sf9 cells at a low multiplicity of infection (MOI) to amplify the virus. After three rounds of amplification, viral titres were measured. Titres are indicated in Table 2.5.

Table 2.5. Viral titre measurements of each of the virus stocks generated for the expression of the fusion proteins in Sf9 cells using the baculovirus expression system.

Stock	Viral Titre
Bac-eGFP	7×10^7 pfu/ml
Bac 82/61	4.5×10^7 pfu/ml
Bac-NS3	8.5×10^6 pfu/ml
Bac-NS3-eGFP	2.4×10^7 pfu/ml
Bac-NS3A-eGFP	1.6×10^8 pfu/ml
Bac-N11-eGFP	8.4×10^7 pfu/ml
Bac-NS3 Δ C-eGFP	5.7×10^7 pfu/ml
Bac-HD1-eGFP	1.4×10^8 pfu/ml
Bac-HD2-eGFP	1.1×10^8 pfu/ml

To verify expression of the fusion proteins, Sf9 cells seeded at 1×10^6 cells per well of a 6-well plate were infected at a MOI of 5 pfu/cell. Cells were harvested after 48 h and washed twice with 1 x PBS. Cells were resuspended in 50 μ l 1 x PBS and mixed with an equal volume of 2 x PSB. Fusion proteins were analysed by sodium dodecyl sulphate polyacrylamide gel electrophoresis (SDS-PAGE) under denaturing conditions (2.2.2.7.1.) followed by Coomassie blue staining.

A 12% PAGE gel was run to verify expression of the fusion proteins (Figure 2.12).

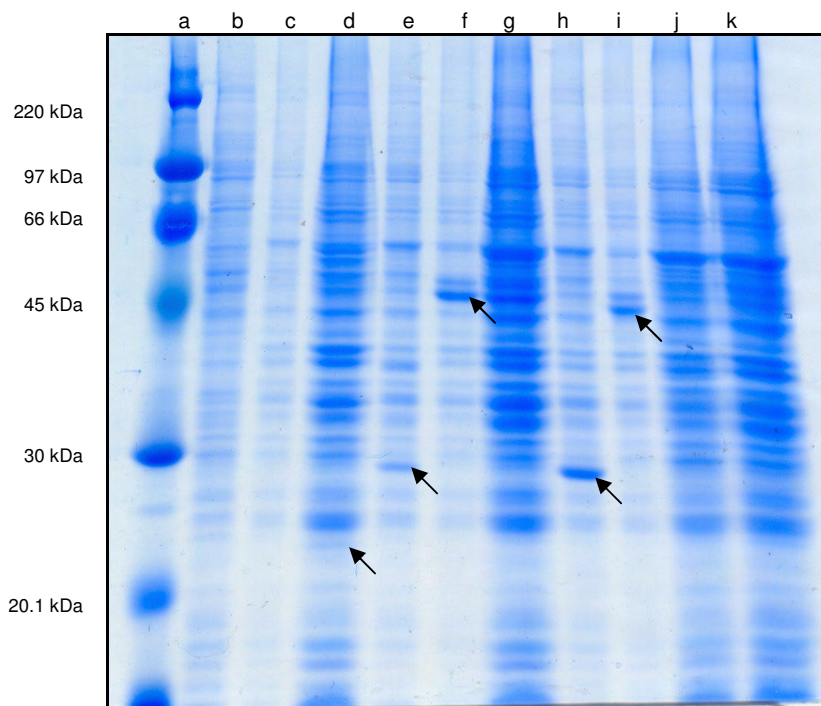


Figure 2.12. Analysis of expression of the seven fusion proteins. Proteins were separated by 12% SDS-PAGE. Included in this gel are mock infected (b), wild-type bac infected (c), Bac-NS3 infected (d), Bac-eGFP infected (e), Bac-NS3-eGFP infected (f), Bac-NS3A-eGFP infected (g), Bac-N11-eGFP infected (h), Bac-NS3 Δ C-eGFP infected (i), Bac-HD1-eGFP infected (j) and Bac-HD2-eGFP infected (k) Sf9 cells. Rainbow marker was included as a size marker (a), sizes of proteins are as indicated.

Four of the seven proteins showed good levels of expression that could be detected by Coomassie staining (Figure 2.12). For eGFP (e) and N11-eGFP (h), a band of approximately 27 kDa was present. For NS3-eGFP (f) and NS3 Δ C-eGFP (i), a band of approximately 51 kDa was present. In addition, a very faint protein band of approximately 23 kDa was present in the lane containing cells infected with NS3 (d). The sizes of these bands are consistent with what was expected as eGFP is 27 kDa in size and NS3 is 24 kDa in size. NS3A-eGFP (g), HD1-eGFP (j) and HD2-eGFP (k) were not visible on this gel. This may be due to low levels of expression of these proteins.

Western blots (2.2.2.7.2.) were performed with anti-GFP antibodies to confirm the expression of the eGFP protein (Figure 2.13) and with rabbit anti- β -Gal-NS3 antiserum to confirm the expression of the NS3 protein (Figure 2.14).

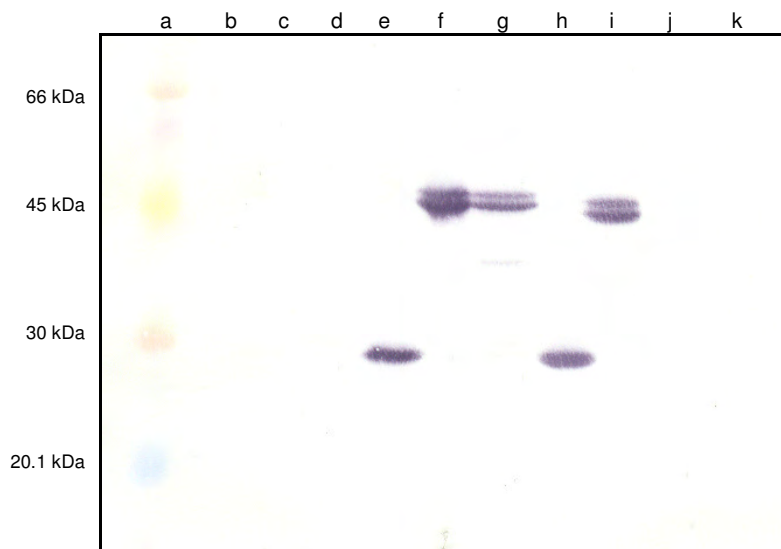


Figure 2.13. Anti-GFP Western blot of mock infected (b), Wild-type bac infected (c), Bac-NS3 infected (d), Bac-eGFP infected (e), Bac-NS3-eGFP infected (f), Bac-NS3A-eGFP infected (g), Bac-N11-eGFP infected (h), Bac-NS3 Δ C-eGFP infected (i), Bac-HD1-eGFP infected (j) and Bac-HD2-eGFP infected (k) Sf9 cells. Rainbow marker was included as a size marker (a), sizes of proteins are as indicated.

The expression of the eGFP insert in eGFP, NS3-eGFP, NS3A-eGFP, N11-eGFP and NS3 Δ C-eGFP, was confirmed by Western blot with anti-eGFP antibodies. For eGFP (e) and N11-eGFP (h), a band of approximately 27 kDa was present. For NS3-eGFP (f), NS3A-eGFP (g), and NS3 Δ C-eGFP (i), a band of approximately 51 kDa was present. In this Western blot, an additional band was observed along with the protein bands of NS3-eGFP, NS3A-eGFP and NS3 Δ C-eGFP. One explanation for the presence of an extra band is that it may represent a glycosylated form of the protein. This was investigated further by means of a glycosylation assay by PAS staining. Other possibilities are that this extra band may represent a larger modified form of the protein or breakdown products resulting from the overexpression of the protein. This band was also visible in Coomassie stained gels when large quantities of protein were loaded and at later stages of infection. NS3 (d), HD1-eGFP (j) and HD2-eGFP (k) did not react with the sera.

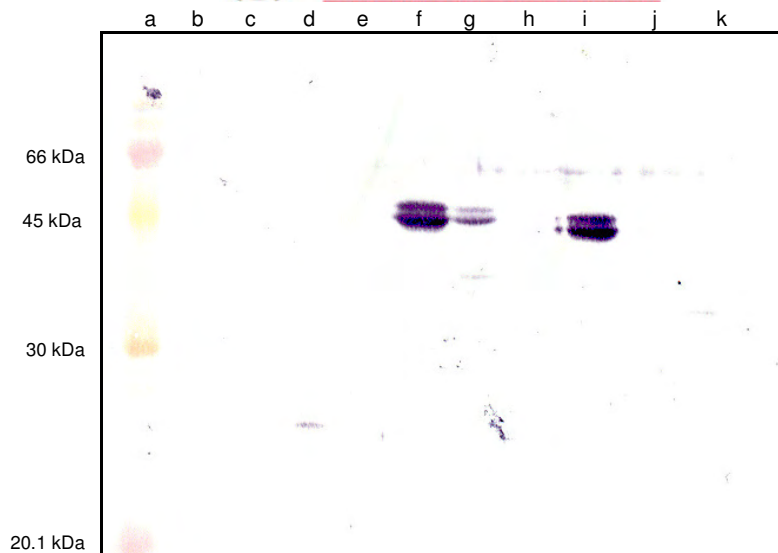


Figure 2.14. Anti- β -gal-NS3 Western blot of mock infected (b), Wild-type bac infected (c), Bac-NS3 infected (d), Bac-eGFP infected (e), Bac-NS3-eGFP infected (f), Bac-NS3A-eGFP infected (g), Bac-N11-eGFP infected (h), Bac-NS3 Δ C-eGFP infected (i), Bac-HD1-eGFP infected (j) and Bac-HD2-eGFP infected (k) Sf9 cells. Rainbow marker was included as a size marker (a), sizes of proteins are as indicated.

The expression of the NS3 insert in NS3, NS3-eGFP, NS3A-eGFP and NS3 Δ C-eGFP was confirmed by Western blot with anti- β -gal-NS3 antibodies. A faint protein band of approximately 23 kDa was present in the lane containing cells infected with NS3 (d). A protein band of approximately 51 kDa was present in the lanes containing cells infected with NS3-eGFP (f), NS3A-eGFP (g) and NS3 Δ C-eGFP (i). Once again, an additional band was observed just above the protein bands of NS3-eGFP, NS3A-eGFP and NS3 Δ C-eGFP. The proteins eGFP (e), N11-eGFP (h), HD1-eGFP (j) and HD2-eGFP (k) did not react with the sera. It is possible that the 11 amino acid domain specific to NS3 in N11-eGFP does not contain epitopes recognised by the serum, however it is not clear why HD1-eGFP and HD2-eGFP were not detected.

For more sensitive detection of poorly expressing fusion proteins and to investigate the additional bands present for some of the fusion proteins, Sf9 cells seeded at 1×10^6 cells per well of a 6-well plate were infected at a MOI of 5 pfu/cell. At 27 hours post infection, proteins were labelled with [35 S]-methionine before being analysed by sodium dodecyl sulphate polyacrylamide gel electrophoresis (SDS-PAGE) under denaturing conditions (2.2.2.7.1.). The gel was stained with Coomassie blue so that the sizes of the bands could be verified by comparing the exposed image to the original gel (not shown). The gel was vacuum dried and exposed to a phosphor screen overnight before being scanned with the Personal Molecular Imager[®] FX (Bio-Rad). Images were analysed using PDQuest[™] 2-D analysis software (Bio-Rad, Figure 2.15).

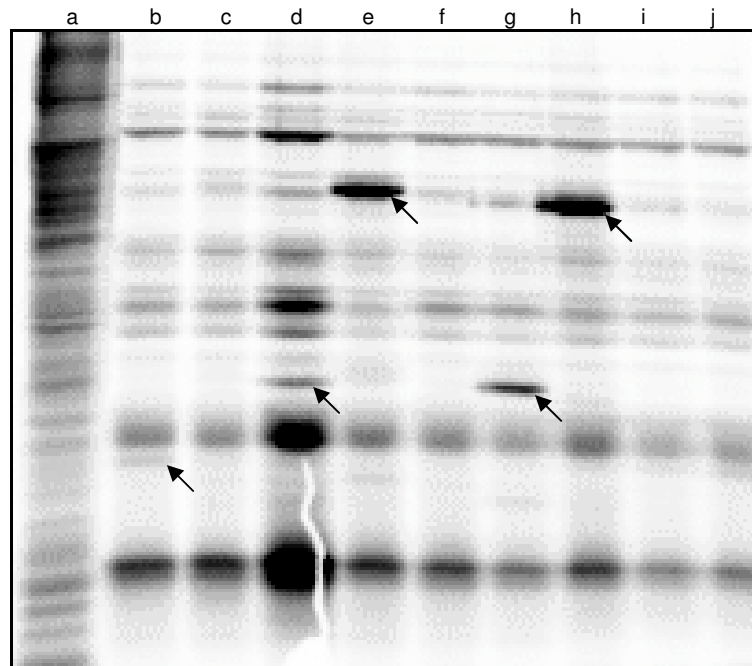


Figure 2.15. 12% PAGE gel of [³⁵S]-methionine labelled mock infected (a), Bac-NS3 infected (b), Wild-type bac infected (c), Bac-eGFP infected (d), Bac-NS3-eGFP infected (e), Bac-NS3A-eGFP infected (f), Bac-N11-eGFP infected (g), Bac-NS3ΔC-eGFP infected (h), Bac-HD1-eGFP infected (i) and Bac-HD2-eGFP infected (j) Sf9 cells.

Four of the seven proteins were clearly labelled, enabling distinction from the background (Figure 2.15). For eGFP (d) and N11-eGFP (g), a band of approximately 27 kDa was present. For NS3-eGFP (e) and NS3ΔC-eGFP (h), a band of approximately 51 kDa was present. In addition, a faint protein band of approximately 23 kDa was present in the lane containing cells infected with NS3 (b). The sizes of these bands are consistent with what was expected. No extra bands were observed for NS3-eGFP or NS3ΔC-eGFP. Comparisons between the original Coomassie stained gel and the exposed image showed that the extra band lies just above the native protein bands of NS3-eGFP and NS3ΔC-eGFP (not shown), indicating that these bands may represent larger, modified forms of the proteins. NS3A-eGFP (f), HD1-eGFP (i) and HD2-eGFP (j) were not visible on this gel. This may be due to low levels of expression of these fusion proteins at the specific time point (27 h.p.i) when labelling took place.

As protein expression could not be detected for two of the constructs, it was decided to verify the sequences of the viral DNA. DNA was isolated from Sf9 cells that had been infected with recombinant baculoviruses expressing each of the fusion proteins at a MOI of 5. This DNA was used as a template in a PCR reaction performed as described in 2.2.1.4. using the primers PFB1 POLH FW and PFB1 RV (Figure 2.16).

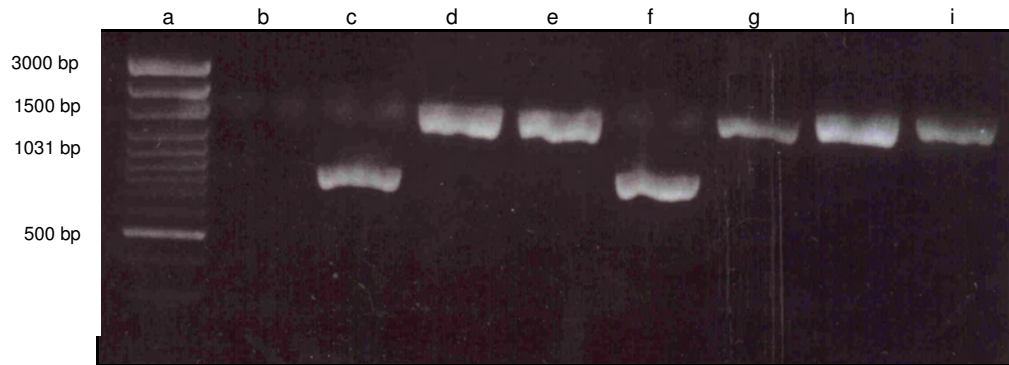


Figure 2.16. Agarose gel (2%) of PCR reactions carried out for the verification of viral DNA. Included in this gel are a mock sample as the negative control (b), eGFP (c), NS3-eGFP (d), NS3A-eGFP (e), N11-eGFP (f), NS3 Δ C-eGFP (g), HD1-eGFP (h) and HD2-eGFP (i). The 100 bp plus DNA ladder (Fermentas) was included as a size marker (a), sizes of fragments are as indicated.

PCR reactions were carried out successfully, and fragments of the expected sizes were obtained (Figure 2.16). Fragments were purified by column purification and verified by sequencing.

Sequencing reactions were carried out using the primers PFB1 POLH FW, PFB1 RV and eGFP_{internal}. Sequencing results confirmed that all bacmids had been transfected into Sf9 cells correctly and all inserts had sequences identical to what was expected.

2.3.3. Glycosylation assay

The presence of additional bands in the PAGE gels and Western blots of NS3-eGFP, NS3A-eGFP and NS3 Δ C-eGFP raised a number of questions. It was thought that perhaps one of the bands may represent a glycosylated form of the NS3 protein as glycosylation is one of the main post-translational modification steps in the synthesis of viral membrane proteins (Doms *et al.*, 1993) and BTV NS3 is glycosylated in both mammalian and insect cells (Bansal *et al.*, 1998). Glycosylation has never been observed for AHSV NS3, but this may be due to the fact that the protein, when expressed by itself, is expressed to very low levels in Sf9 cells. To investigate whether AHSV-3 NS3 is glycosylated, a glycosylation assay by PAS staining was performed. For this assay, a 12% PAGE gel was run and stained according to the protocol of Carlsson (1993) (Figure 2.17). Following the staining procedure, glycosylated proteins stain pink while non-glycosylated proteins remain clear.

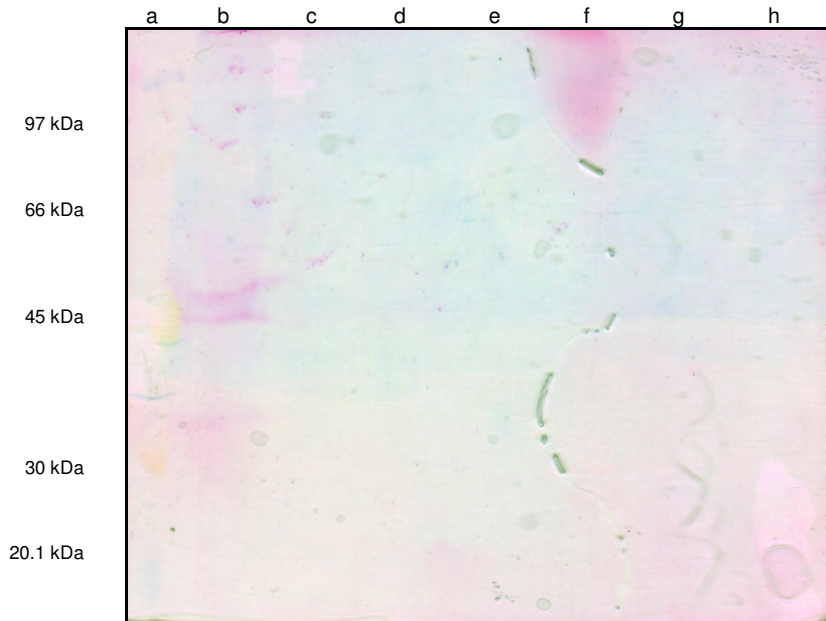


Figure 2.17. 12% PAGE gel of Wild-type bac infected (c), Bac-eGFP infected (d), Bac-NS3-eGFP infected (e, f and h) and Bac-N11-eGFP infected (g) Sf9 cells. This gel was stained by PAS staining. Blood serum proteins were included as a glycosylated control (b). Rainbow marker was included as a size marker (a), sizes of proteins are as indicated.

From this gel, it could be seen that only the blood serum proteins, which are known to be glycosylated, stained pink. The fusion proteins did not seem to be glycosylated (Figure 2.17). A duplicate gel was stained with Coomassie blue to verify the presence of the proteins (not shown). The presence of the extra bands in the gels of these proteins cannot be explained at this stage, but it seems likely that they represent larger, modified forms of the proteins.

2.3.4. Cytotoxicity assay

An interesting feature of baculovirus expressed AHSV NS3 is that it is cytotoxic when expressed in insect cells as a result of its interaction with the cell membrane (Van Staden *et al.*, 1995). In order to investigate whether NS3 retains this cytotoxicity when fused to eGFP, a cytotoxicity assay was carried out using the vital exclusion dye, trypan blue. AHSV-2 NS3 (Bac 82/61), which has previously been shown to be cytotoxic when expressed in Sf9 cells, was used as a positive control for cytotoxicity. eGFP was used as a negative control for cytotoxicity. Cells were monitored at 12, 24, 27, 30, 33, 36 and 48 hours post infection (Figure 2.18).

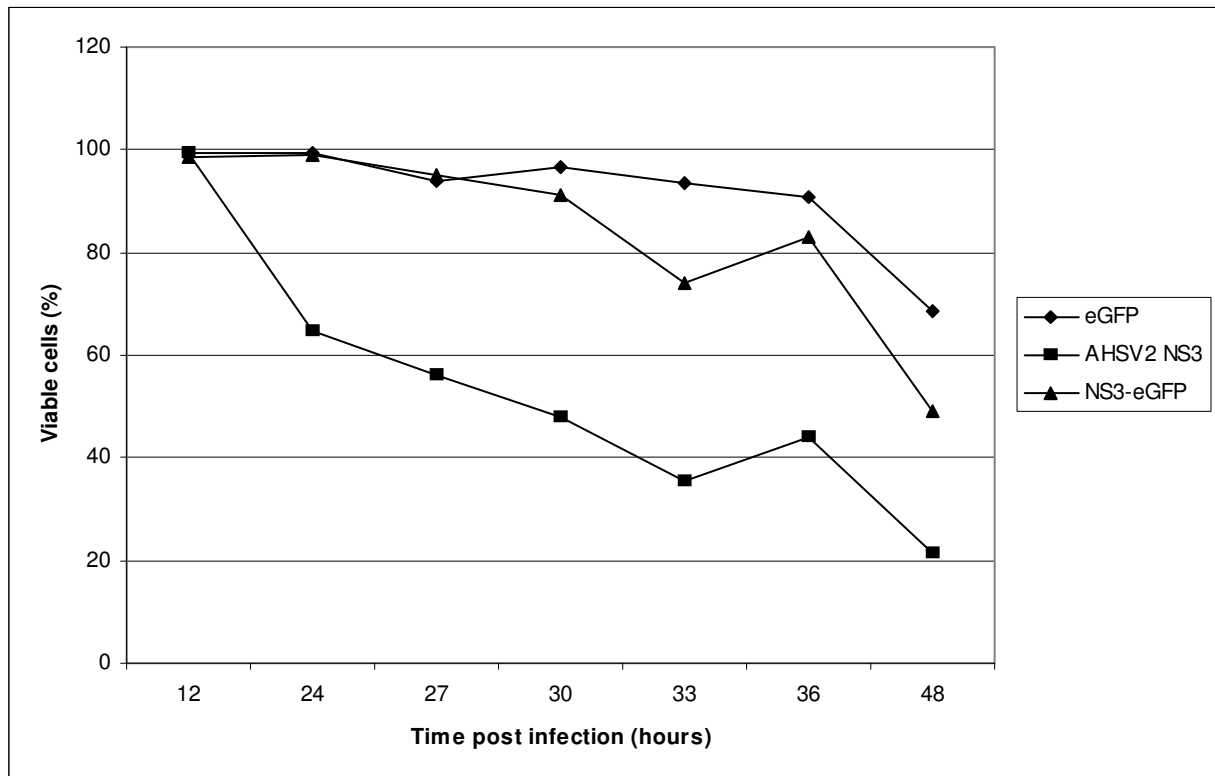


Figure 2.18. Percent viable (unstained) cells present at various time points post infection. Cells were infected with recombinant baculoviruses expressing eGFP, AHSV-2 NS3 or NS3-eGFP.

In Sf9 cells infected with AHSV-2 NS3, the number of unstained cells decreased rapidly from 12 hours post infection and only 21% of the cells were unstained or viable after 48 hours. A decreased cytotoxic effect was observed in cells infected with NS3-eGFP, with approximately 50% viable cells after 48 hours. In Sf9 cells infected with eGFP, there were approximately 70% viable cells after 48 hours. The viability of cells expressing AHSV-2 NS3 did not conform to previously published results where only 5% of Sf9 cells harbouring NS3 were found to be viable at 48 h.p.i. (Van Staden *et al.*, 1995). Despite this, these results do still indicate that NS3-eGFP is not as cytotoxic as pure AHSV-2 NS3 when expressed in Sf9 cells.

2.3.5. Fluorescent microscopy

Fluorescent microscopy was carried out in order to visualise the localisation of the various fusion proteins within the cells. Sf9 cells were infected with recombinant baculoviruses at a MOI of 5 pfu/cell. Cells were analysed for fluorescence after 24 h, 48 h and 72 h under magnifications of 5x, 10x, 20x and 40x. The following figures are representative of what was seen for each of the fusion proteins (Figure 2.19 a - h).

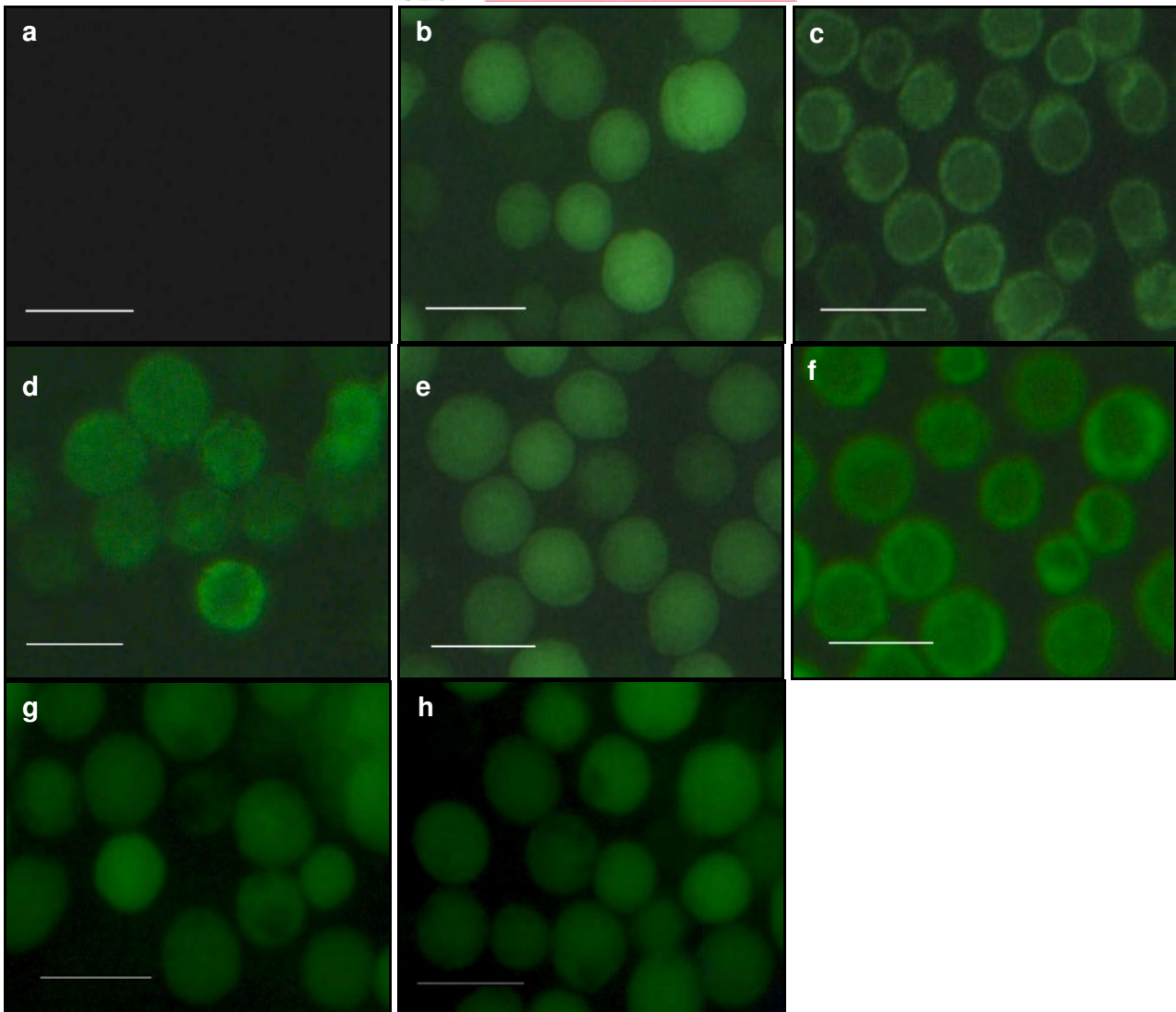


Figure 2.19. Fluorescent microscopy of mock infected (a), Bac-eGFP infected (b), Bac-NS3-eGFP infected (c), Bac-NS3A-eGFP infected (d), Bac-N11-eGFP infected (e), Bac-NS3 Δ C-eGFP infected (f), Bac-HD1-eGFP infected (g) and Bac-HD2-eGFP infected (h) Sf9 cells at 48 h.p.i. The scale bar represents 20 μ m.

From fluorescent microscopy it could be seen that eGFP (b), N11-eGFP (e), HD1-eGFP (g) and HD2-eGFP (h) showed no membrane localisation and seemed to be dispersed throughout the cells, while NS3-eGFP (c) and NS3 Δ C-eGFP (f) showed membrane localisation and were clearly visible at the membrane regions of the cells. NS3A-eGFP (d) was interesting in that it showed membrane localisation in some cells, but seemed to be distributed throughout the cytoplasm of others (Figure 2.19d). Microscopy was performed a number of times using different time intervals post infection and different magnifications. The abovementioned results were constant throughout these experiments and the figures (Figure 2.19) represent results that were seen throughout. Another noticeable difference between the various fusion proteins was that eGFP and N11-eGFP showed extremely high levels of fluorescence, while NS3-eGFP, NS3A-eGFP and NS3 Δ C-eGFP showed intermediate levels of fluorescence. The levels of fluorescence for HD1-eGFP and HD2-eGFP were very low in comparison. Different times post infection also revealed differences in the levels of fluorescence and in the percentage of cells that showed signs of fluorescence. At 24

hours post infection fluorescence levels were still reasonably low and a number of cells did not show any signs of fluorescence. Despite this, the localisation of the various fusion proteins was clearly visible. At 48 hours post infection fluorescence levels were high, most cells showed fluorescence and the localisations of the various fusion proteins were clearly visible. This proved to be the best time post infection for fluorescent microscopy to be carried out. At 72 hours post infection, a number of cells had broken open and there were high levels of fluorescence in the surrounding medium. Despite this background fluorescence, the localisation of the various fusion proteins was still clearly visible. All proteins in essence showed the same localisation profile at 24 h, 48 h and 72 h post infection. NS3 was found to be membrane targeted even when fused to eGFP. NS3 requires the presence of two intact hydrophobic domains for this targeting. This was confirmed by the localisation of HD1 and HD2, where abolishing the hydrophobic nature of either of the hydrophobic domains prevented membrane targeting and/or anchoring of the proteins. The truncation of the C-terminal does not seem to have any effect whatsoever, while the truncation of the N-terminal seems to have quite a large effect on the targeting of NS3.

2.3.6. Protein release assay

NS3 has previously been found to be membrane associated and is thought to play a key role in viral release. However, the exact mechanism for this remains unclear. One way in which NS3 may be doing this is by damaging or breaking the cell membrane, resulting in the release of the virus. An initial assay was carried out to determine whether NS3-eGFP is released into the surrounding medium and whether it occurs in the soluble or particulate fractions of a cell at various time periods post infection. Spinner cultures were infected with eGFP (as a control) and NS3-eGFP and samples were taken every three hours over a 72-hour period. Samples were first separated into cells and medium after which the cells were separated into soluble and particulate components. Fluorescence readings of all representative fractions were taken (Figure 2.20).

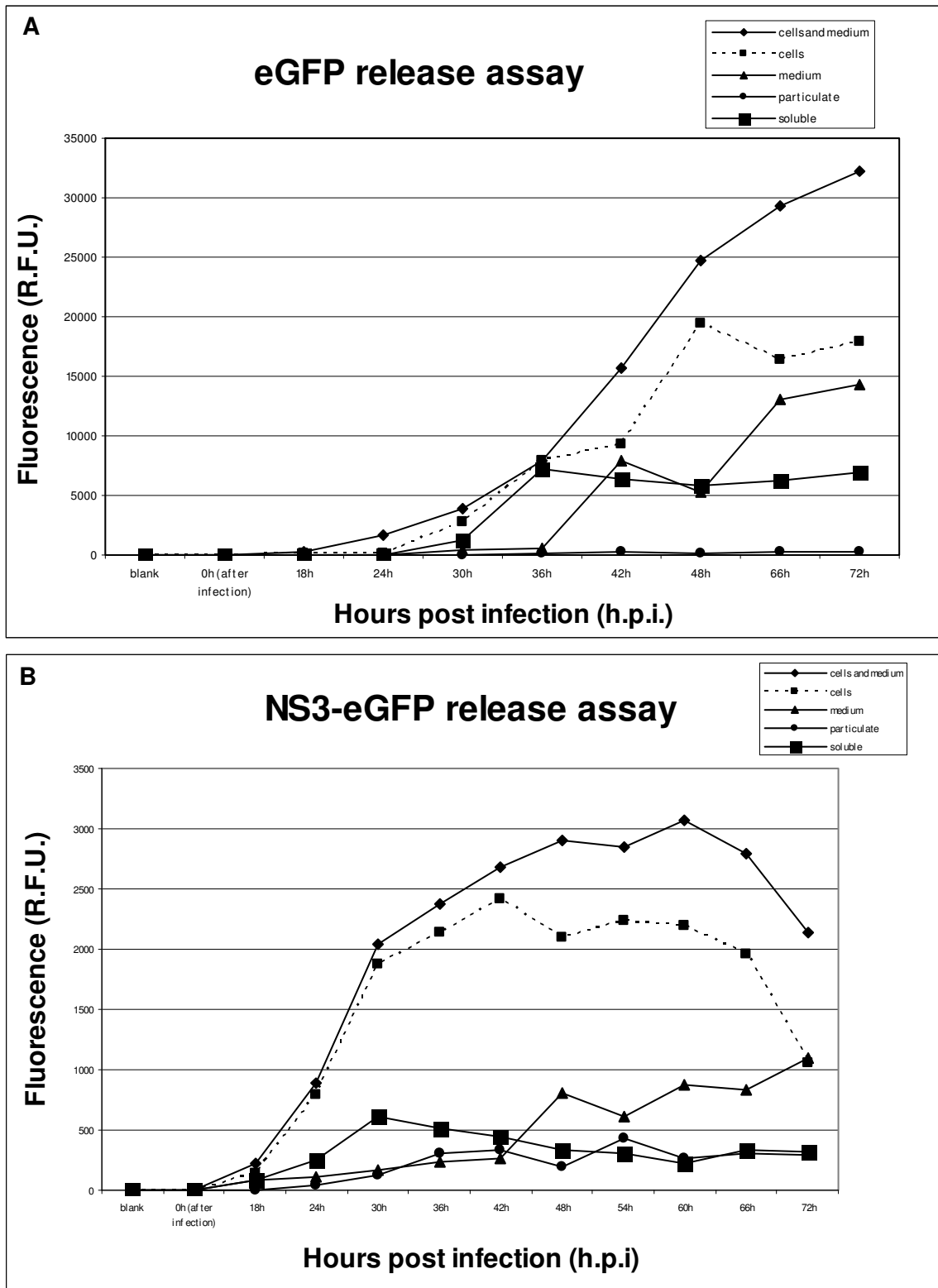


Figure 2.20. Fluorometer readings of the representative fractions of samples taken every 3 hours from spinner cultures infected with Bac-eGFP (A) or Bac-NS3-eGFP (B). Separate curves are included for the total sample (cells and medium), the cells in the sample, the medium in the sample, the particulate components of the cells and the soluble components of the cells.

In the eGFP spinner culture (Figure 2.20A), the total fluorescence (cells and medium) peaked at 72 h.p.i. The fluorescence in the cells peaked at 48 h.p.i. The fluorescence in the medium showed a peak at 72 h.p.i. The particulate component of the cells did not show detectable fluorescence,

while the fluorescence in the soluble component of the cells increased up to 36 h.p.i and remained reasonably constant thereafter.

In the NS3-eGFP spinner culture (Figure 2.20B), the total fluorescence (cells and medium) peaked at 60 h.p.i and decreased slightly after that. The fluorescence in the cells peaked at 42 h.p.i, and remained fairly constant thereafter before decreasing until 72 h.p.i. The fluorescence in the medium gradually increased throughout, peaking at 72 h.p.i. The particulate component of the cells showed a gradual increase in fluorescence throughout the experiment, while the fluorescence in the soluble component of the cells peaked at 30 h.p.i and decreased slightly thereafter.

A noticeable difference between the graphs obtained from the eGFP spinner culture and those obtained from the NS3-eGFP spinner culture is the vast difference in the absolute fluorescent values. The values indicate that either eGFP is expressed at much higher levels than NS3-eGFP in Sf9 cells or that eGFP fluoresces better when not fused to another protein. A lower fluorescence was also observed for NS3-eGFP in comparison to that observed for eGFP during fluorescent microscopy.

At first observation the values for the particulate component of the cells in the NS3-eGFP spinner culture seemed to be extremely low in comparison to what was expected for a membrane associated protein. However, another member of our laboratory recently found that soluble VP7-eGFP fluoresces approximately 7 times better per unit of VP7 protein than insoluble VP7-eGFP particles (E. Mizrachi, personal communication). These results indicate that fluorescence values obtained from particulate samples may be underrepresented in comparison to those obtained from soluble samples. This may be the case in the NS3-eGFP spinner culture, where the fluorescence present in the particulate fraction may actually be higher than the values that were obtained.

Of interest in the graphs for the NS3-eGFP spinner culture was the peak in fluorescence in the soluble component of the cells at 30h and the gradual increase in soluble protein released into the medium throughout. This indicates the presence of a soluble version of the AHSV NS3 protein that is released into the medium as has recently been identified for rotavirus NSP4. Bugarcic and Taylor (2006) recently identified a soluble form of NSP4 that is secreted into the surrounding medium from the apical surface of the cells. This secreted soluble form of NSP4 has been proposed to be responsible for the protein's enterotoxic properties.

2.3.7. Subcellular fractionation

Initial results from the protein release assay indicate that NS3-eGFP has a small soluble component, but that the bulk is probably particulate. These results lead us to expect that the bulk of NS3 exists in a membrane associated form. This hypothesis was further tested by means of a subcellular fractionation experiment performed at both 24 and 48 hours post infection.

Because of their association with insoluble membrane fractions, membrane proteins are expected to be highly insoluble. This insolubility enables us to pellet membrane fractions, and therefore membrane proteins, by high-speed centrifugation. A simple subcellular fractionation experiment was carried out according to a protocol adapted from that of Brignati *et al.* (2003) as a preliminary study of the membrane association of NS3-eGFP in comparison to that of eGFP. In this protocol, cells were first broken open mechanically by dounce homogenisation and the unbroken cells and nuclei were removed by low-speed centrifugation. The post-nuclear supernatant was then separated into membrane (particulate) and cytoplasmic (soluble) components by high-speed centrifugation. One would expect proteins targeted to membrane components of a cell (e.g. ER, Golgi) to be in the particulate fraction. Fluorescent readings were taken of all representative fractions.

Because the levels of fluorescence were so much lower for cells infected with Bac-NS3-eGFP than for those infected with Bac-eGFP, it was difficult to compare the two sets of values. Values were converted to percentages of the total fluorescence so that the graphs obtained for Bac-eGFP infected cells could be compared to those obtained for Bac-NS3-eGFP infected cells (Figure 2.21).

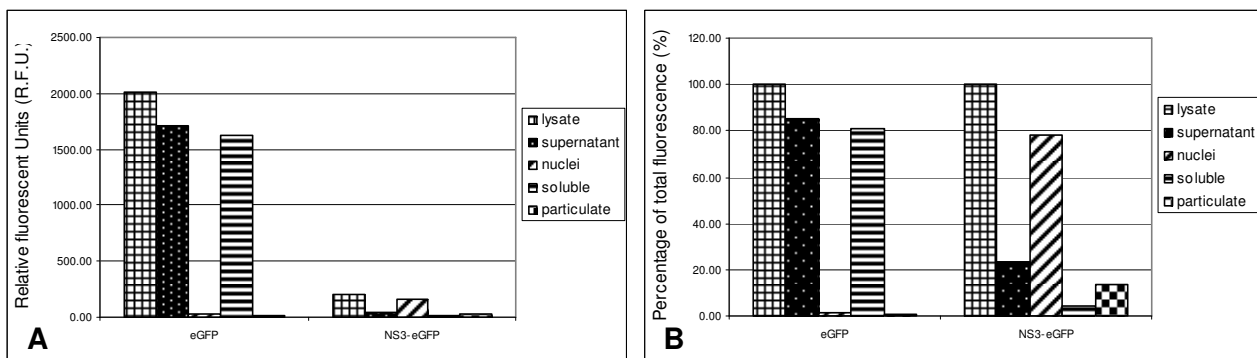


Figure 2.21. Fluorescence values (A) and percentages of total fluorescence (B) obtained for subcellular fractionations carried out for cells infected with Bac-eGFP and Bac-NS3-eGFP at 48 h.p.i. Included are values for the lysate (total), the post-nuclear supernatant, the nuclei, the soluble component of the post-nuclear supernatant and the particulate component of the post-nuclear supernatant.

From these graphs (Figure 2.21), it can be seen that for Bac-eGFP infected cells, most of the fluorescence (almost 85%) remained in the post-nuclear supernatant and very little (approximately 1%) was pelleted with the nuclear fraction. Most of the fluorescence (approximately 81%) ended up in the soluble fraction with less than 1% ending up in the particulate fraction. For Bac-NS3-eGFP

infected cells, most of the fluorescence was pelleted with the nuclear fraction (approximately 78%) with very little remaining in the post-nuclear supernatant (just over 23%). Of this, most ended up in the particulate fraction (approximately 13%), with very little remaining in the soluble fraction (just over 4%). This experiment was repeated approximately ten times with similar results.

From these results, it seems as if one of two things is occurring; NS3-eGFP is either being targeted to the nucleus or nuclear membrane where it is pelleted with the nuclear fraction, or NS3-eGFP is targeted to the cell membrane and may be forming aggregations that are pelleted with the nuclei at low-speed centrifugation because of the high levels of insolubility of these aggregations. Because of this, we are left with very little protein and very low fluorescent readings in the final fractions for the NS3-eGFP fractionations. The above subcellular fractionations were carried out with all seven fusion proteins in order to get a general idea of the localisation of each of the proteins.

Subcellular fractionations were carried out at both 24 h.p.i and 48 h.p.i. Cell lysates were passed through a 29G needle five times or treated with Triton X-100 to break open the cells. Triton X-100 is a non-ionic detergent that solubilises lipid membranes leaving behind detergent-resistant membrane fractions that may contain lipid rafts. Fractionations were repeated at least three times for each of the fusion proteins. Percentages of fluorescence present in each of the fractions are indicated in Tables 2.6 and 2.7. These values are then also represented in the following graphs (Figure 2.22 and 2.23). The average values of three of the repeats for each fusion protein were used to generate the tables and graphs.

The following was obtained at 24 h.p.i:

Table 2.6. Percentages of total fluorescence obtained for subcellular fractionations carried out for cells infected with Bac-eGFP, Bac-NS3-eGFP, Bac-NS3A-eGFP, Bac-N11-eGFP, Bac-NS3ΔC-eGFP, Bac-HD1-eGFP and Bac-HD2-eGFP at 24 h.p.i. Cells were lysed by 5 passages through a 29G needle. Included are values for the lysate (total), the nuclei, the soluble component of the post-nuclear supernatant and the particulate component of the post-nuclear supernatant.

Fusion Protein	Lysate	Nuclei	Soluble	Particulate
eGFP	100%	7%	72%	1%
NS3-eGFP	100%	14%	3%	19%
NS3A-eGFP	100%	12%	28%	6%
N11-eGFP	100%	2%	60%	1%
NS3ΔC-eGFP	100%	18%	4%	13%
HD1-eGFP	100%	5%	59%	5%
HD2-eGFP	100%	4%	64%	4%

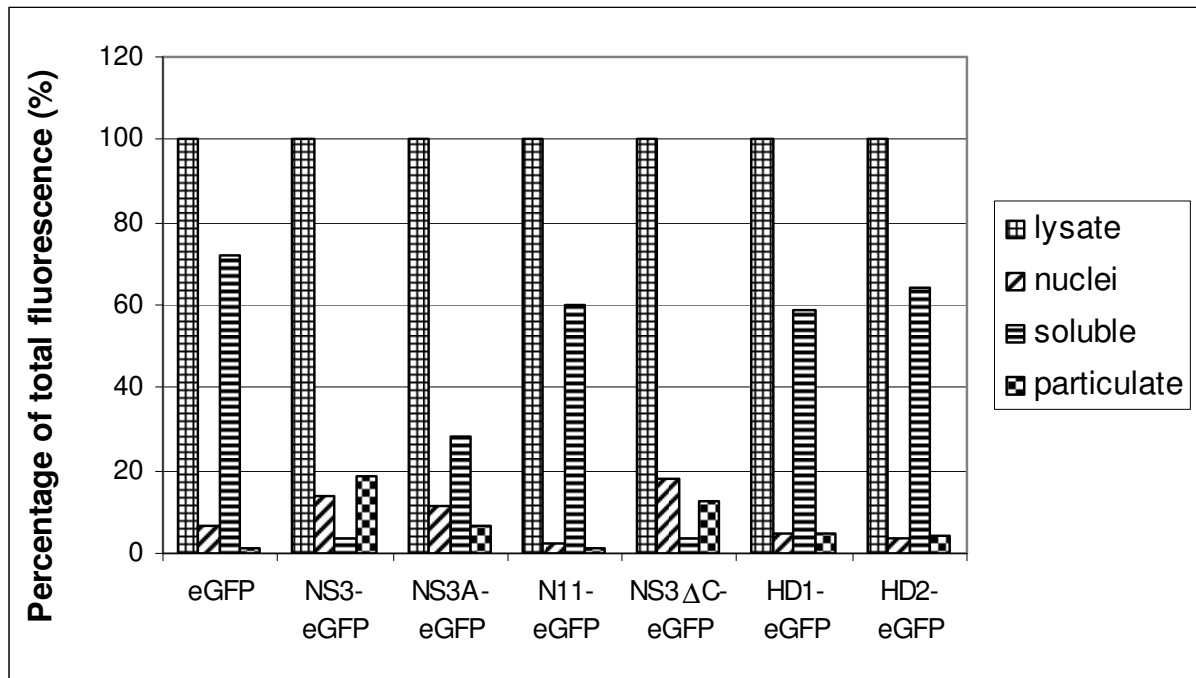


Figure 2.22. Percentages of total fluorescence obtained for subcellular fractionations carried out for cells infected with Bac-eGFP, Bac-NS3-eGFP, Bac-NS3A-eGFP, Bac-N11-eGFP, Bac-NS3ΔC-eGFP, Bac-HD1-eGFP and Bac-HD2-eGFP at 24 h.p.i. Cells were lysed by 5 passages through a 29G needle. Included are values for the lysate (total), the nuclei, the soluble component of the post-nuclear supernatant and the particulate component of the post-nuclear supernatant.

At 24 hours post infection, eGFP, N11-eGFP, HD1-eGFP and HD2-eGFP had large soluble components (59% - 72%) and 2% - 7% of the fluorescence was pelleted with the nuclear fraction. On the other hand, for NS3-eGFP and NS3ΔC-eGFP, 14% - 18% of the fluorescence was pelleted with the nuclear fraction. For these fusion proteins, 3% - 4% of the remaining fluorescence was located in the soluble component of the postnuclear supernatant and 13% - 19% of the remaining fluorescence was located in the particulate component of the post-nuclear supernatant. This is probably an under representation of the actual amount of fluorescence due to quenching caused by the particulate nature of the fraction. This would explain the apparent loss of fluorescence in the NS3-eGFP and NS3ΔC-eGFP fractionations. For NS3A-eGFP, 12% of the fluorescence was pelleted with the nuclear fraction, 28% of the remaining fluorescence was located in the soluble component of the post-nuclear supernatant and 6% of the remaining fluorescence was located in the particulate component of the postnuclear supernatant.



The following was obtained at 48 h.p.i:

Table 2.7. Percentages of total fluorescence obtained for subcellular fractionations carried out for cells infected with Bac-eGFP, Bac-NS3-eGFP, Bac-NS3A-eGFP, Bac-N11-eGFP, Bac-NS3ΔC-eGFP, Bac-HD1-eGFP and Bac-HD2-eGFP at 48 h.p.i. Cells were lysed by 5 passages through a 29G needle or by treatment with Triton X-100. Included are values for the lysate (total), the nuclei, the soluble component of the post-nuclear supernatant and the particulate component of the post-nuclear supernatant.

Fusion Protein	Lysate	Nuclei	Soluble	Particulate
eGFP	100%	2%	76%	1%
eGFP (Triton X-100)	100%	2%	90%	1%
NS3-eGFP	100%	62%	0%	2%
NS3-eGFP (Triton X-100)	100%	57%	3%	2%
NS3A-eGFP	100%	58%	6%	2%
NS3A-eGFP (Triton X-100)	100%	60%	8%	7%
N11-eGFP	100%	2%	71%	1%
N11-eGFP (Triton X-100)	100%	3%	81%	1%
NS3ΔC-eGFP	100%	70%	5%	1%
NS3ΔC-eGFP (Triton X-100)	100%	65%	7%	3%
HD1-eGFP	100%	14%	68%	3%
HD1-eGFP (Triton X-100)	100%	17%	70%	1%
HD2-eGFP	100%	13%	71%	1%
HD2-eGFP (Triton X-100)	100%	4%	56%	1%

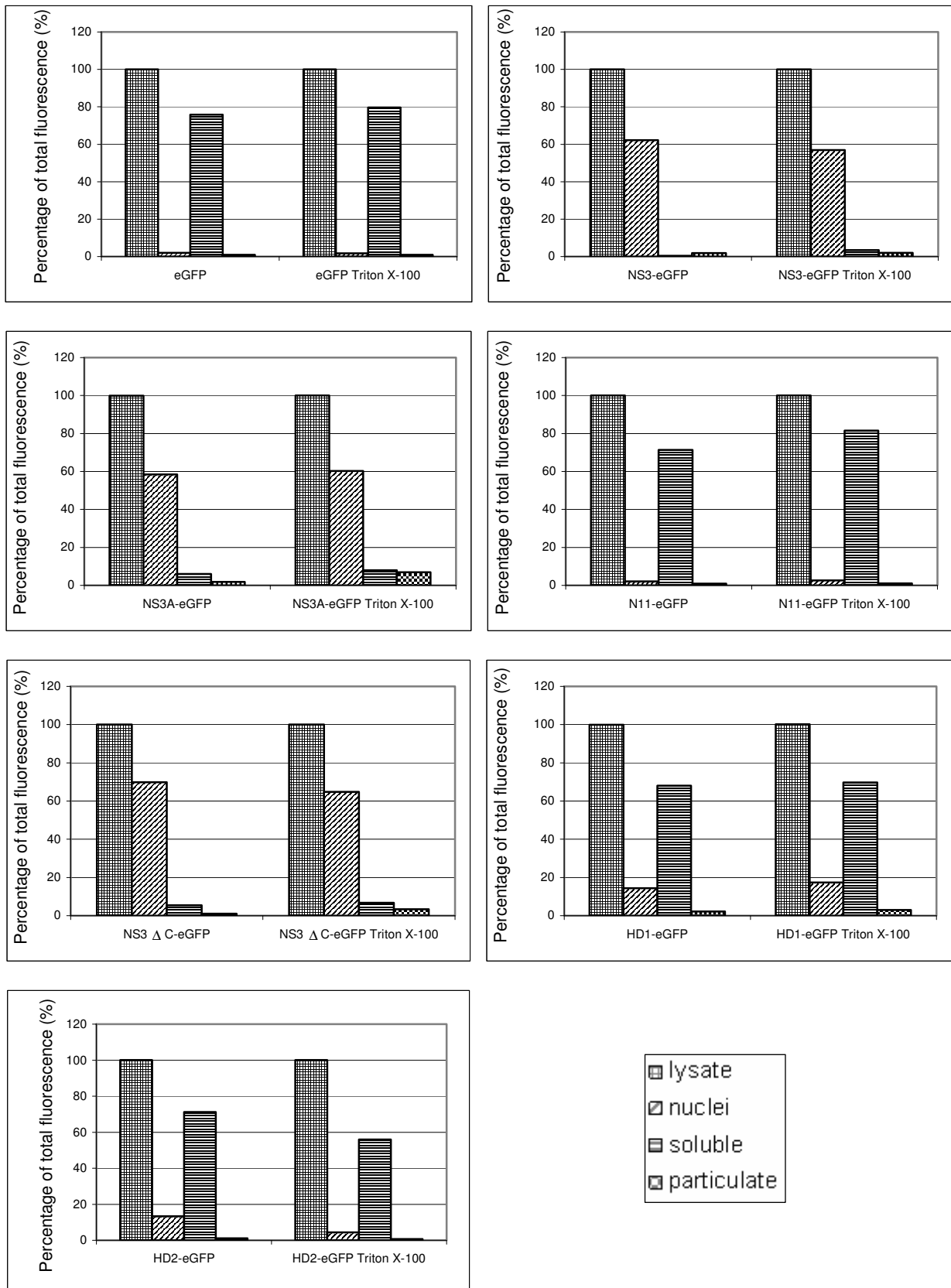


Figure 2.23. Percentages of total fluorescence obtained for subcellular fractionations carried out for cells infected with Bac-eGFP, Bac-NS3-eGFP, Bac-NS3A-eGFP, Bac-N11-eGFP, Bac-NS3 Δ C-eGFP, Bac-HD1-eGFP and Bac-HD2-eGFP at 48 h.p.i. Cells were lysed by 5 passages through a 29G needle or by treatment with Triton X-100. Included are values for the lysate (total), the nuclei, the soluble component of the post-nuclear supernatant and the particulate component of the post-nuclear supernatant.

At 48 hours post infection, results were similar to what was observed at 24 hours post infection for eGFP, N11-eGFP, HD1-eGFP and HD2-eGFP, however results varied slightly for NS3-eGFP, NS3A-eGFP and NS3 Δ C-eGFP. eGFP and N11-eGFP had large soluble components (76% - 81%) and 2% - 3% of the fluorescence was pelleted with the nuclear fraction. HD1-eGFP and HD2-eGFP also had large soluble components (56% - 71%) but 4% - 17% of the fluorescence was pelleted with the nuclear fraction. On the other hand, for NS3-eGFP, NS3A-eGFP and NS3 Δ C-eGFP, 58% - 70% of the fluorescence was pelleted with the nuclear fraction. For these fusion proteins, 0% - 6% of the remaining fluorescence was located in the soluble component of the postnuclear supernatant and 1% - 2% of the remaining fluorescence was located in the particulate component of the post-nuclear supernatant. Once again, these values are probably an under representation of the actual amount of fluorescence due to quenching caused by the particulate nature of the fraction. This would explain the apparent loss of fluorescence in the NS3-eGFP, NS3A-eGFP and NS3 Δ C-eGFP fractionations.

It is interesting to note that at 24 h.p.i only 12% - 18% of the fluorescence was pelleted with the nuclear fraction for NS3-eGFP, NS3A-eGFP and NS3 Δ C-eGFP. At 48 h.p.i, 58% - 70% of the fluorescence was pelleted with the nuclear fraction for these three fusion proteins. In addition, at 24 h.p.i, the particulate component of the postnuclear supernatant had a fluorescence of between 6% and 19% for these three fusion proteins. After 48 hours, this value had decreased to between 1% and 2%. These results indicate that these three fusion proteins may initially be targeted to the cell membrane, but may later accumulate in the nuclei or nuclear membrane due to the overexpression of these proteins.

Following Triton X-100 treatment, results remained the same for most fusion proteins. For NS3-eGFP however, the amount of fluorescence located in the soluble fraction of the post-nuclear supernatant increased from 0% to 3%. For NS3A-eGFP, this value increased from 6% to 8% and for NS3 Δ C-eGFP, this value increased from 5% to 7%. This indicates that some protein is released from membrane fractions following treatment with Triton X-100. However, some protein (2% - 7%) remained membrane associated, indicating a possible association of NS3-eGFP with detergent resistant membrane fractions (DRMs) that may contain lipid rafts. For eGFP and N11-eGFP, values for the soluble component of the cells increased by 10 to 15% following treatment with Triton X-100. This results in the combined values of the soluble and particulate components being more “additive” to the total of 100% (the cell lysate). These results indicate better lysis of the cells, resulting in the complete solubilization of all components.

2.3.8. Membrane flotation analysis

In order to verify the results obtained from fluorescent microscopy and subcellular fractionation experiments, membrane flotation analysis was carried out as described in 2.2.2.15. For membrane flotation, the cells were broken open by dounce homogenisation and the unbroken cells and nuclei were removed by low-speed centrifugation. The cell lysate was loaded onto the bottom of a discontinuous gradient made up of 85%, 65% and 10% sucrose. These gradients underwent centrifugation at 38 000 rpm for 18 hours at 4°C after which they become continuous. During centrifugation, membranes and their associated proteins will float to the 10% - 65% sucrose interface due to the buoyant density of the lipids. We, therefore, expect to find membrane associated proteins in the upper fractions of the gradient. Proteins that are not membrane associated will remain trapped at the bottom of the gradient. Because all seven fusion proteins are labelled with eGFP, they are fluorescent. Fluorescent readings of the various fractions were taken. For membrane associated proteins fluorescence will be found in the upper fractions of the gradient, while for proteins that are not membrane associated fluorescence will be located in the bottom fractions of the gradient.

The membrane flotation analysis protocol was first optimised for use with our protein expression system. Initially, the effect of two different methods that can be used to break open the cells was investigated. Gradients were compared where cells were broken open by dounce homogenisation and by passing them through a needle (29G). For these initial gradients, 6 to 10 fractions of approximately 800 µl were taken.

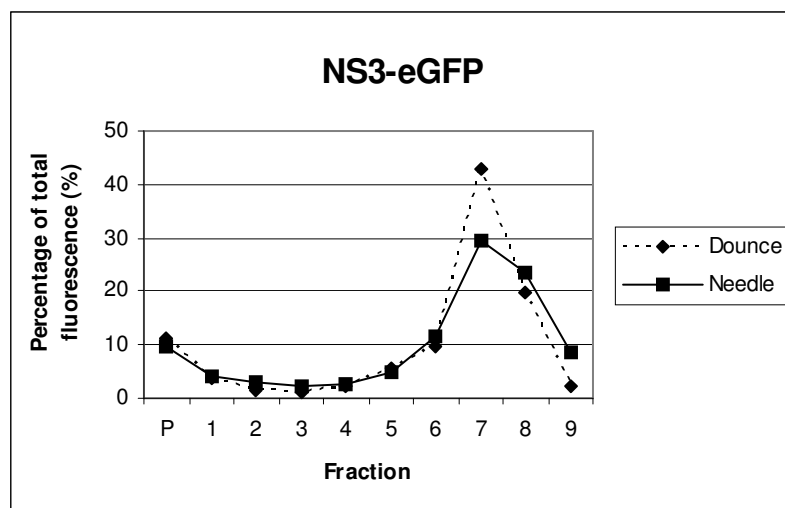


Figure 2.24. Percentage of total fluorescence from membrane flotation gradients carried out to compare two methods that may be used to break open the cells. Included are gradients of cells that had been broken open by dounce homogenisation and by being passed through a 29G needle. Bac-NS3-eGFP infected cells were used. Fractions were taken from the top of the gradient with a pipette. Fraction 9 represents the fraction at the top of the gradient, while fraction 1 represents the fraction at the bottom of the gradient. P is the pellet.

Both methods seemed to work well and yielded similar results (Figure 2.24). The membrane flotation graph of the cells that were broken open by dounce homogenisation did, however, give a slightly stronger peak at the top of the gradient (fraction 7).

Further investigations were carried out to determine the best method for the tapping of fractions from the gradients. Two methods were compared: removal of fractions from the top of a gradient with a pipette and tapping of fractions from the bottom of a gradient through a needle. These methods were compared using membrane flotation gradients carried out with Bac-eGFP infected cells and Bac-NS3-eGFP infected cells (Figure 2.25).

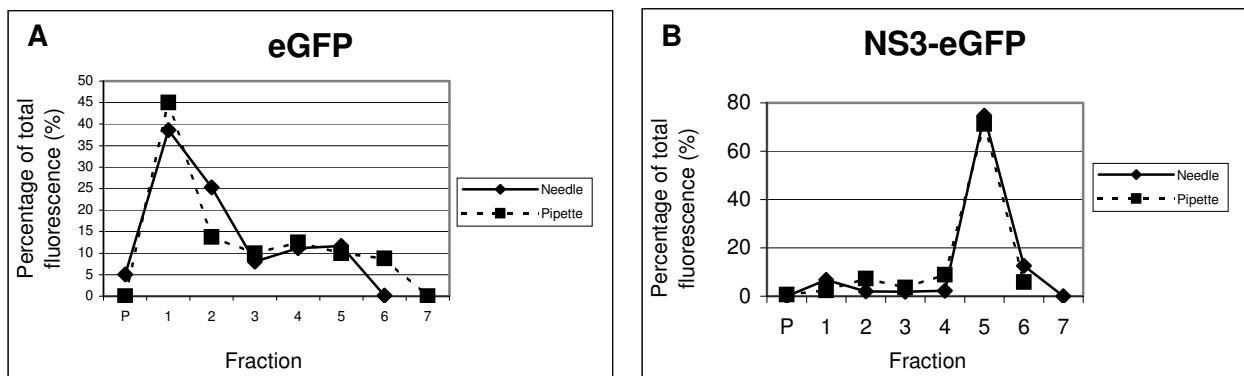


Figure 2.25. Percentage of total fluorescence from membrane flotation gradients carried out to compare two methods that can be used to tap fractions from a gradient. Bac-eGFP (A) or Bac-NS3-eGFP (B) infected cells were used and were broken open by dounce homogenisation. Fractions were taken from the top of the gradient with a pipette or from the bottom of the gradient through a needle. Fraction 6/7 represents the fraction at the top of the gradient, while fraction 1 represents the fraction at the bottom of the gradient. P is the pellet.

Both methods seemed to work well and similar results were obtained. As it was technically easier and more reproducible, it was decided that fractions would be tapped from the bottom of gradients through a needle. In order to get a clearer representation of the curve, it was decided that 200 µl fractions would be taken; therefore approximately 20 fractions would be tapped from each gradient.

Once again, we were faced with the problem that a lot of NS3-eGFP was aggregating and being removed with the nuclear fraction. Because of this, the fluorescent readings for membrane flotation gradients carried out with cells infected with Bac-NS3-eGFP were extremely low and differences in the fluorescent readings of the various fractions were not always clearly visible. We decided to investigate whether the breaking of the cells and the removal of the nuclei does in fact make any difference to the general trends observed in the curves. Membrane flotation analyses were carried out with untreated cells (Cells) as well as cells that had been broken by five passages through a 29G needle (With Nuclei), and cells that had been broken open by five passages through a 29G needle and had their nuclei removed (Without Nuclei). These membrane flotation gradients were

compared using Bac-eGFP infected cells and Bac-NS3-eGFP infected cells (Figure 2.26).

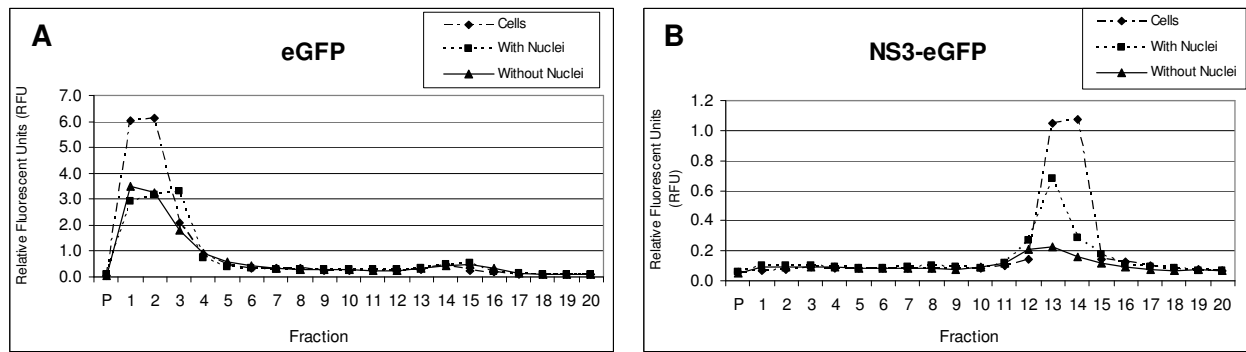


Figure 2.26. Fluorometer readings of the various fractions taken from the bottom of membrane flotation gradients containing cells infected with Bac-eGFP (A) and Bac-NS3-eGFP (B). Flotations were performed with whole cells, with cells that had been passed through a 29G needle and with cells that had been passed through a 29G needle and had their nuclei removed. Sample 20 is the sample that was at the top of the gradient following centrifugation while sample 1 is the sample that was at the bottom of the gradient following centrifugation. P is the pellet.

For flotations with both Bac-eGFP and Bac-NS3-eGFP infected cells, approximately 23% of the total fluorescence was lost when the cells were passed through a needle. The lower counts could be attributed to the loss of some of the sample as the void volume in the syringe. For Bac-eGFP infected cells, a further 2% of the fluorescence was lost when the nuclei were removed. For Bac-NS3-eGFP infected cells, a further 27% was lost when the nuclei were removed. Because of this, the fluorescence levels that we were left to work with were very low.

The general trends remain the same when comparing the three curves, with almost all of the fluorescence remaining at the bottom fractions (fractions 1 to 3) of the eGFP gradients. For NS3-eGFP, all three curves show a similar trend with most of the fluorescence “floating” up to the top of the gradient (fractions 12 to 14). The presence of the nuclei and untreated cells in two of the curves does not seem to interfere with this result. These results indicate that treatment with hypotonic buffer followed by the addition of a high percentage of sucrose is sufficient to lyse the cells. It was decided that cells would be broken open by five passages through a 29G needle and that the entire cell lysate would be used for flotation.

To verify the presence of eGFP in the fractions containing increased levels of fluorescence, some of the fractions were combined and a 12% PAGE gel was run (Figure 2.27A). A Western blot with anti-GFP as the primary antibody was performed to verify that the bands present were in fact eGFP (Figure 2.27B).

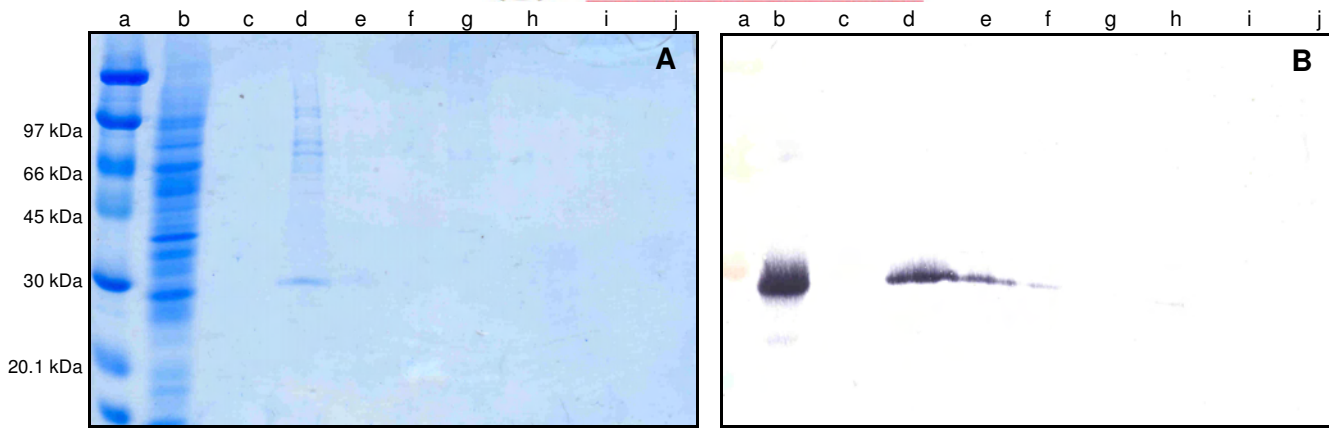


Figure 2.27. Coomassie stained 12% PAGE gel (A) and anti-GFP Western blot (B) of an eGFP membrane flotation gradient. Included are the pellet (c), fractions 1 and 2 (d), fractions 3 and 4 (e), fractions 5 and 6 (f), fractions 11 and 12 (g), fractions 13 and 14 (h), fractions 17 and 18 (i) and fractions 19 and 20 (j). Bac-eGFP infected cells were included as a control (b). Rainbow marker was included as a size marker (a), sizes of proteins are as indicated.

In the PAGE gel (Figure 2.27A), a protein band of approximately 27 kDa was present in lane d. This size corresponded to that of eGFP, which can be seen as a control in lane b. The presence of eGFP in these fractions was confirmed by Western blotting with anti-GFP antibodies (Figure 2.27B). A band of approximately 27 kDa was present in lanes b (containing eGFP as a control), d and e. This result confirmed the presence of the eGFP protein in fractions 1, 2, 3 and 4, at the bottom of the membrane flotation gradient.

To verify the presence of NS3-eGFP in the fractions containing increased levels of fluorescence, some of the fractions were combined and a 12% PAGE gel was run (Figure 2.28A). An anti- β -gal-NS3 Western blot was performed to verify that the bands present were in fact NS3 (Figure 2.28B).

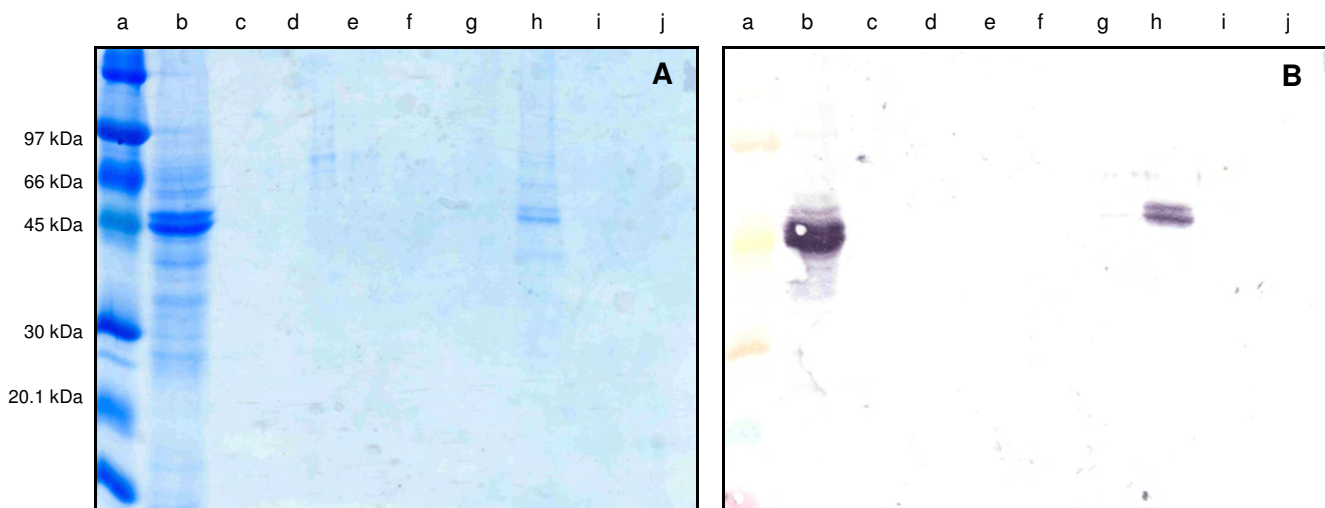


Figure 2.28. Coomassie stained 12% PAGE gel (A) and anti- β -gal-NS3 Western blot (B) of an NS3-eGFP membrane flotation gradient. Included are the pellet (c), fractions 1 and 2 (d), fractions 3 and 4 (e), fractions 5 and 6 (f), fractions 12 and 13 (g), fractions 14 and 15 (h), fractions 16 and 17 (i) and fractions 18 and 19 (j). Bac-NS3-eGFP infected cells were included as a control (b). Rainbow marker was included as a size marker (a), sizes of proteins are as indicated.

In the PAGE gel (Figure 2.278), a protein band of approximately 51 kDa was present in lane h. This size corresponded to that of NS3-eGFP, which can be seen as a control in lane b. The presence of NS3-eGFP in these fractions was confirmed by Western blotting with anti- β -gal-NS3 antibodies (Figure 2.28B). A band of approximately 51 kDa was present in lanes b (containing NS3-eGFP as a control) and h. This result confirms the presence of the NS3-eGFP fusion protein in fractions 14 and 15, at the top of the membrane flotation gradient. No NS3 was detected in any other fractions.

Much evidence exists to suggest that lipid rafts are sorting centres that also play an important role in the targeting of proteins to the plasma membrane (Brown and Breton, 2000). Lipid rafts are microdomains that are enriched in cholesterol and sphingolipids. Because of this, they are resistant to extraction with non-ionic detergents, like Triton X-100, at low temperatures. To investigate a possible association of NS3 with lipid rafts, cells were treated with Triton X-100 before being subjected to membrane flotation analysis. If cells are treated with Triton X-100 at 4°C, any proteins that are associated with membrane fractions should be released and will remain at the bottom of a membrane flotation gradient. On the other hand, proteins that are associated with detergent resistant membrane fractions will remain associated and will still “float” up in a membrane flotation gradient (Briggs *et al.*, 2003). Preliminary evidence from subcellular fractionations (Figure 2.23) indicated that Triton X-100 has some effect, but does not totally solubilise all of the particulate protein present.

Membrane flotation analysis was carried out at 48 hours post infection with all seven fusion proteins. Cell lysates were passed through a 29G needle five times or treated with Triton X-100 before undergoing density gradient centrifugation. Each of the flotations was repeated at least three times with similar results (Figure 2.29). Fluorescent readings from fractions are also summarised in Table 2.8.

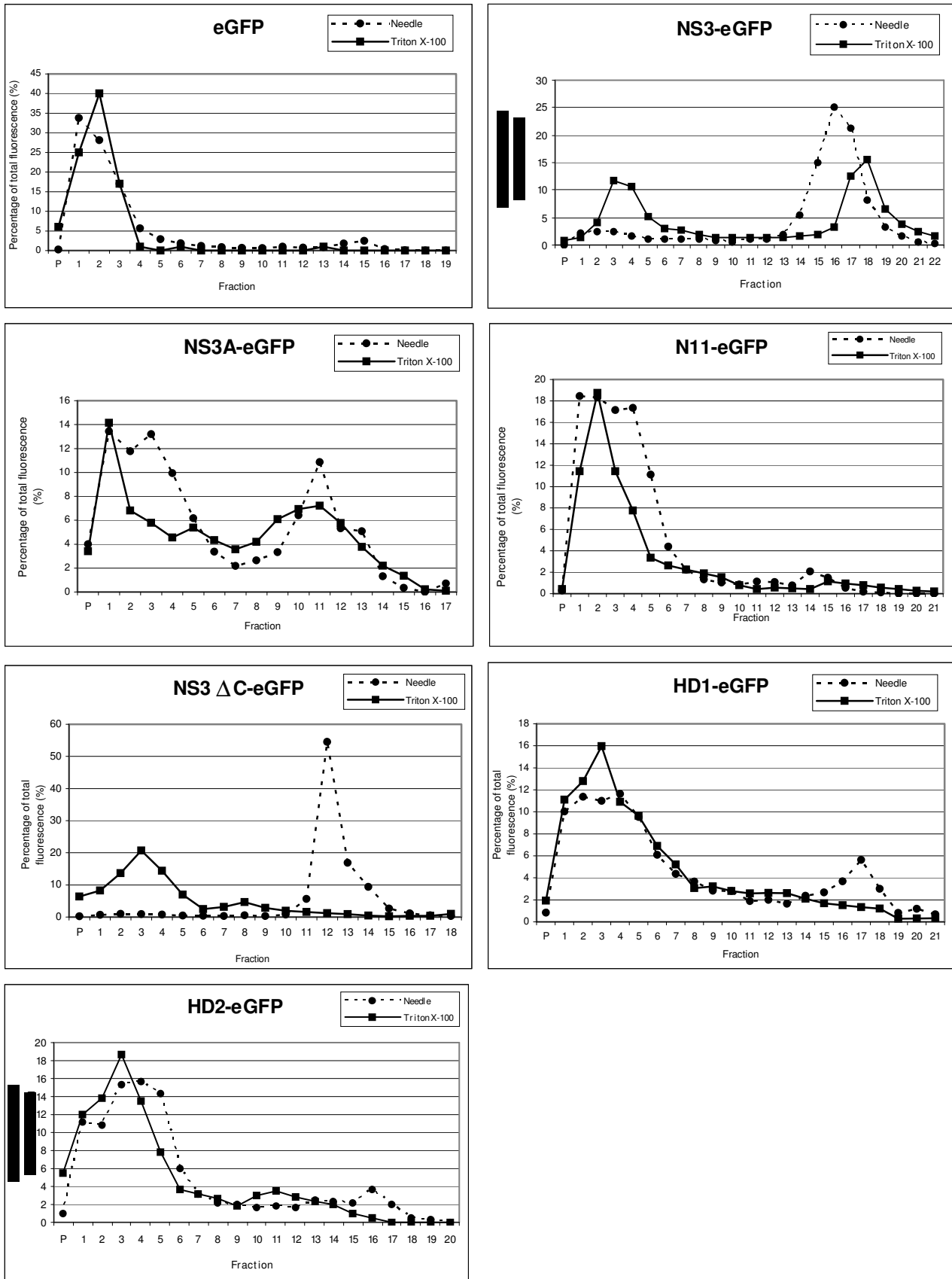


Figure 2.29. Fluorometer readings of the fractions taken from the bottom of sucrose gradients containing cells infected with Bac-eGFP, Bac-NS3-eGFP, Bac-NS3A-eGFP, Bac-N11-eGFP, Bac-NS3ΔC-eGFP, Bac-HD1-eGFP or Bac-HD2-eGFP. The sample was passed through a 29G needle five times (dotted line) or treated with Triton X-100 (solid line) before undergoing density gradient centrifugation. Sample 17 - 22 is the sample that was at the top of the gradient while sample 1 is the sample that was at the bottom of the gradient. P is the pellet.

Table 2.8. Location of the bulk of the fluorescence and the percentage fluorescence present in these fractions. Membrane flotations were carried out with cells infected with Bac-eGFP, Bac-NS3-eGFP, Bac-NS3A-eGFP, Bac-N11-eGFP, Bac-NS3ΔC-eGFP, Bac-HD1-eGFP and Bac-HD2-eGFP at 48 h.p.i. Samples were passed through a 29G needle five times or treated with Triton X-100 before undergoing density gradient centrifugation.

Fusion Protein	Location of bulk of fluorescence	Percent fluorescence present in these fractions
eGFP	Fractions 1 - 4	84%
eGFP (Triton X-100)	Fractions 1 - 3	82%
NS3-eGFP	Fractions 14 - 19	79%
NS3-eGFP (Triton X-100)	Fractions 1 - 8	40%
	Fractions 16 - 22	46%
NS3A-eGFP	Fractions 1 - 5	54%
	Fractions 10 - 13	28%
NS3A-eGFP (Triton X-100)	Fractions 1 - 4	32%
	Fractions 11 - 14	26%
N11-eGFP	Fractions 1 - 6	87%
N11-eGFP (Triton X-100)	Fractions 1 - 5	53%
NS3ΔC-eGFP	Fractions 15 - 19	89%
NS3ΔC-eGFP (Triton X-100)	Fractions P - 5	70%
HD1-eGFP	Fractions 1 - 7	64%
	Fractions 15 - 18	15%
HD1-eGFP (Triton X-100)	Fractions 1 - 7	73%
HD2-eGFP	Fractions 1 - 7	76%
	Fractions 13 - 17	13%
HD2-eGFP (Triton X-100)	Fractions 1 - 5	66%

For eGFP and N11-eGFP, the bulk of the fluorescence was located in the lower fractions of the gradient, indicating no membrane association. For HD1-eGFP and HD2-eGFP, the bulk of the fluorescence was located in the lower fractions of the gradient, but there were small peaks present in the upper portions of the gradient, indicating that there may be some membrane association. This may indicate that these fusion proteins are targeted to the membrane, but are not anchored into the membrane and remain loosely bound as was previously found by van Niekerk *et al.* (2001a). For NS3-eGFP and NS3ΔC-eGFP, the bulk of the fluorescence was located in the upper fractions of the gradient, indicating membrane association. For NS3A-eGFP, there were peaks in both the upper and the lower fractions of the gradient, indicating some membrane association.

Following Triton X-100 treatment, little change was observed for eGFP and N11-eGFP. For HD1-eGFP and HD2-eGFP, the peak in the upper portions was no longer present. For NS3-eGFP, some of the fluorescence shifted to the lower fractions of the gradient and two fluorescent peaks were observed. For NS3A-eGFP, there was also a shift and the amount of fluorescence present in the upper portions of the gradient did not form a clear peak, as was the case prior to Triton X-100 treatment. For NS3ΔC-eGFP, all of the fluorescence was observed to be in the lower fractions of

the gradient following treatment with Triton X-100. These results indicate that the Triton X-100 had an effect and disrupted the association of these proteins with the membrane fractions. However, the disruption was not always complete, indicating a possible association of NS3-eGFP with detergent resistant membrane fractions (DRMs) that may contain lipid rafts. This association may be mediated by the C-terminal amino acids, as when these amino acids are not present as in NS3 Δ C-eGFP, Triton X-100 is able to completely abolish the association of the protein with the membrane fractions.

2.3.9. Use of a drug treatment to block ER to Golgi transport in cellular trafficking pathways

One way in which NS3 may be targeted to the plasma membrane is that it may be “hijacking” one or more of the host cells general trafficking pathways to carry out its functions in the viral life cycle. To test this, cells infected with Bac-NS3-eGFP were treated with Brefeldin A, a drug that blocks ER to Golgi trafficking in the normal cellular secretory pathway (Klausner *et al.*, 1992). By treating infected cells with Brefeldin A, we can investigate whether NS3 is using the cells secretory pathway to get to the membrane. If, following treatment with Brefeldin A, NS3 no longer reaches the cell membrane; we will know that it is using this cellular pathway. If NS3 is still able to get to the plasma membrane, we will know that it is using an alternate pathway to reach the plasma membrane. Cells were treated with 10 μ g/ml Brefeldin A and analysed by conventional fluorescent microscopy (Figure 2.30) and membrane flotation analysis (Figure 2.31) at 48 h.p.i. Bac-eGFP infected cells were used as a control.

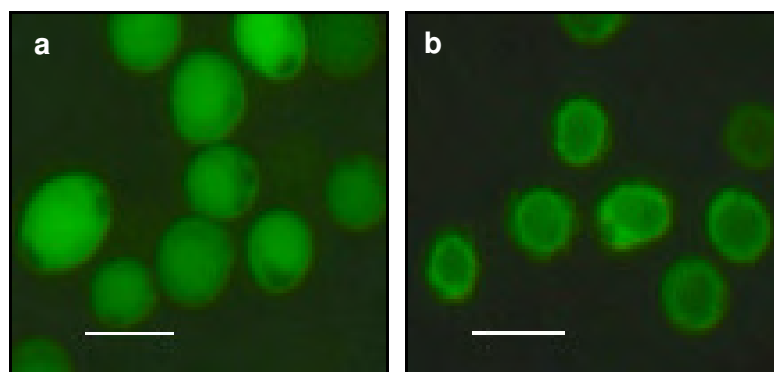


Figure 2.30. Fluorescent microscopy of Bac-eGFP infected (a) and Bac-NS3-eGFP infected (b) Sf9 cells treated with Brefeldin A. Photos were taken 48 h.p.i. The scale bar represents 20 μ m.

Following Brefeldin A treatment it can be seen that eGFP (a) had no membrane localisation and seemed to be dispersed throughout the cell, while NS3-eGFP (b) showed membrane localisation and was clearly visible at the membrane regions of the cells.

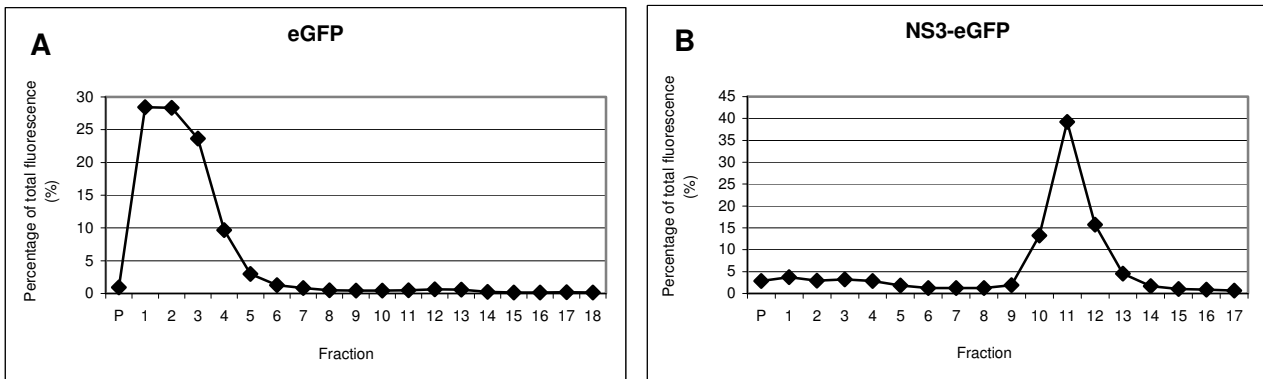


Figure 2.31. Fluorometer readings of the various fractions taken from the bottom of a sucrose gradient containing cells infected with Bac-eGFP (A) or Bac-NS3-eGFP (B) and treated with Brefeldin A. The sample was passed through a 29G needle five times before undergoing density gradient centrifugation. Sample 17/18 is the sample that was at the top of the gradient while sample 1 is the sample that was at the bottom of the gradient. P is the pellet.

For eGFP, it can be seen that the bulk of the fluorescence (approximately 90%) remained at the bottom of the gradient (fractions 1 to 4). For NS3-eGFP, it can be seen that the bulk of the fluorescence (approximately 68%) was found in the upper portions of the gradient (fractions 10 to 12) with the greatest peak (approximately 39%) occurring in fraction 11. This is the first time that we have used Brefeldin A in our laboratory and the treatment protocol may need to be optimised. In order to do this, one would need a proper positive control to ensure the Brefeldin A treatment is actually working. We would need to use a protein that is known to use the conventional secretory pathway to reach the cell membrane. If such a control is still able to reach the cell membrane following treatment with Brefeldin A, we will know that there is a problem with either the Brefeldin A or with the treatment protocol.

2.3.10. Confocal Microscopy

The recent acquisition of a Zeiss LSM 510 META Laser Scanning Microscope at the University of Pretoria enabled us to carry out a few additional microscopic analyses and some initial colocalisation studies. Confocal laser microscopy was carried out with all fusion proteins in order to get a clearer picture of the localisation of each of the proteins within the cells. The main difference between normal fluorescent microscopy and confocal microscopy is that the confocal microscope focuses on a specific level within the sample thus eliminating background fluorescence above and below this level, resulting in much better definition of the fluorescent signal. The software also enables adjustments to be made to contrast and brightness, thus enhancing the final image obtained. Another feature of confocal microscopy is the ability to perform colocalisation studies using dyes for specific compartments within the cells. For example, one could express NS3-eGFP in cells labelled with a Golgi or ER specific dye to investigate whether NS3 is specifically localised to the membranes of either of these organelles. In this way, one could pinpoint the exact locations of the various fusion proteins within the cells.

Sf9 cells were infected with recombinant baculoviruses at a MOI of 5 pfu/cell. Cells were analysed for fluorescence after 24 h.p.i, 33 h.p.i and 48 h.p.i. The following figures are representative of what was seen for each of the fusion proteins (Figure 2.32 and 2.33).

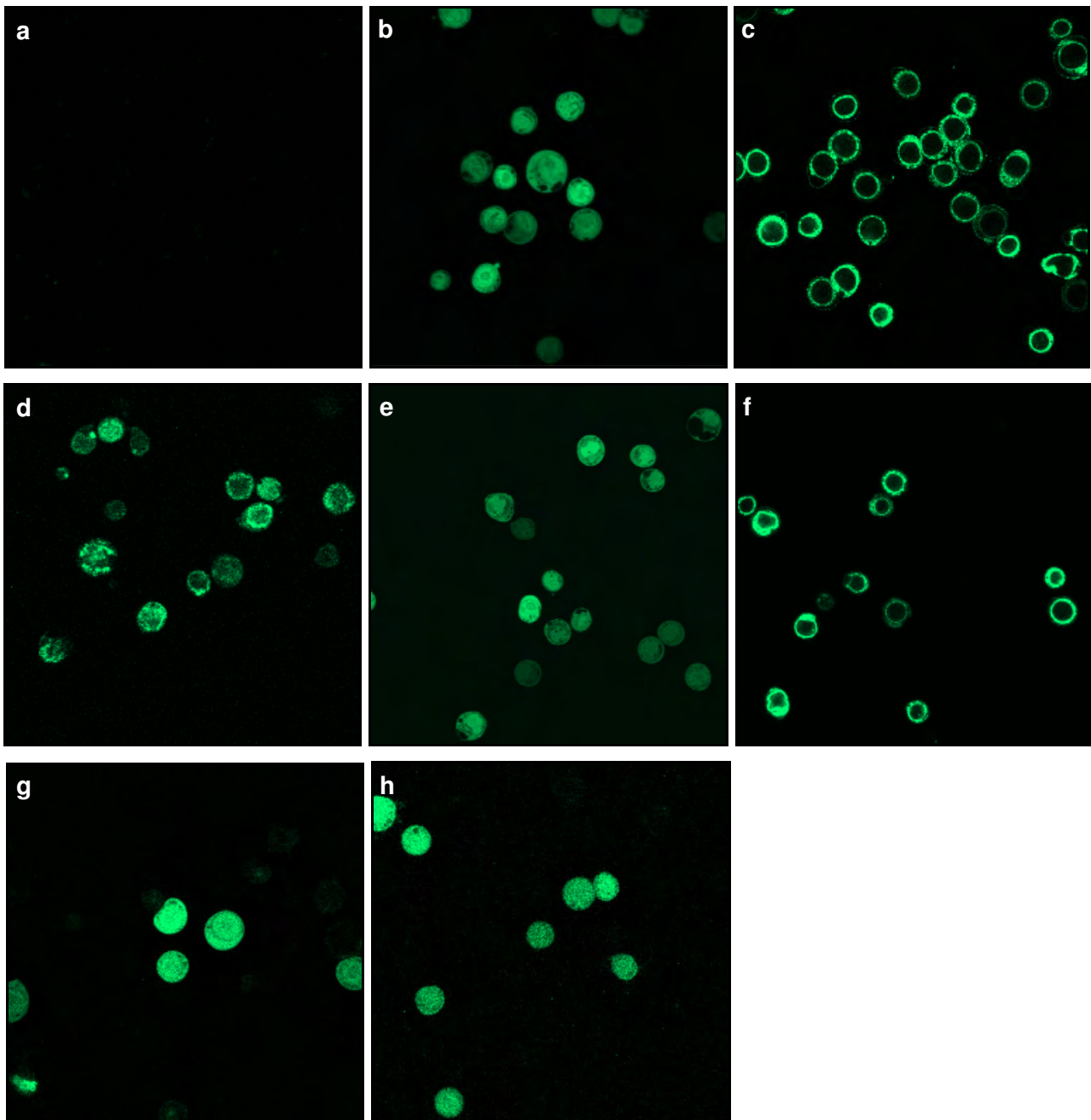


Figure 2.32. Confocal microscopy of mock infected (a), Bac-eGFP infected (b), Bac-NS3-eGFP infected (c), Bac-NS3A-eGFP infected (d), Bac-N11-eGFP infected (e), Bac-NS3 Δ C-eGFP infected (f), Bac-HD1-eGFP infected (g) and Bac-HD2-eGFP infected (h) Sf9 cells at 48 h.p.i.

Figure 2.33 shows enlargements of single cells expressing Bac-eGFP, Bac-NS3-eGFP and Bac-NS3A-eGFP to allow a clearer view of the localisation of these fusion proteins within a cell.

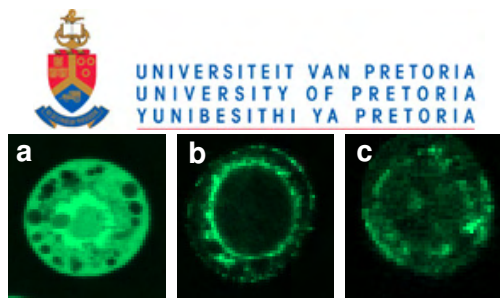


Figure 2.33. Enlargements of single cells from confocal microscopy images of Bac-eGFP infected (a), Bac-NS3-eGFP infected (b) and Bac-NS3A-eGFP infected (c) Sf9 cells at 48 h.p.i.

At first glance, images looked similar to those obtained from fluorescent microscopy (Figure 2.19). eGFP (b), N11-eGFP (e), HD1-eGFP (g) and HD2-eGFP (h) showed no membrane localisation and were observed to be dispersed throughout the cells (nucleus and cytoplasm), while NS3-eGFP (c) and NS3 Δ C-eGFP (f) showed membrane localisation and were clearly visible at the membrane regions of the cells. NS3A-eGFP (d) was localised in patches on the surface in the plasma membrane of some cells, but was distributed throughout the cytoplasm of others (Figure 2.32d and 2.33c). Upon closer inspection, it appeared as if the bulk of NS3-eGFP showed localisation to the nuclear membrane. A small amount of fluorescence was visible at the outer membrane of the cell, but the bulk of the fluorescence was present within this membrane, localised to what may be the nuclear membrane (Figure 2.33b). This was further investigated using the nuclear dye, DAPI, to stain the nuclei of cells that had been infected with either eGFP or with NS3-eGFP. Mock infected cells were used as a control for the staining procedure (Figure 2.34).

The staining procedure worked well. Nuclei were visible as fairly large blue circles within the cytoplasm of the cells. eGFP had a cytoplasmic and nuclear distribution, as indicated by overlap with the nuclear dye. This same distribution was previously observed for eGFP in Sf9 cells by Matsumoto *et al.* (2004). NS3-eGFP was observed to have a perinuclear distribution and was visible in the cell membrane. The proximity of the protein to the nuclear stain indicated localisation of NS3 at the nuclear membrane (Figure 2.34 and 2.35).

In addition to the nuclear labelling, we optimised Golgi labelling with BODIPY[®]TR ceramide as well as ER labelling with VYBRANT[™] DiI cell-labelling solution in mock infected cells (Figure 2.36). According to Kawar and Jarvis (2001), Golgi elements in Sf9 cells appear as punctate structures located throughout the cytoplasm. We managed to achieve a staining pattern similar to this in mock infected cells (Figure 2.36).

The optimisation of these staining procedures in cells expressing our fusion proteins proved to be more challenging and we were unable to complete these experiments in the time course of this project. We found that cells infected with baculoviruses expressing eGFP or NS3-eGFP fusion proteins did not stain with the ER/Golgi dyes (Figure 2.37). This may be due to changes in the physiology of the cell caused by the expression of our fusion proteins. Fixing protocols need to be

investigated further and further training on the confocal microscope and its software is required in order to complete this work.

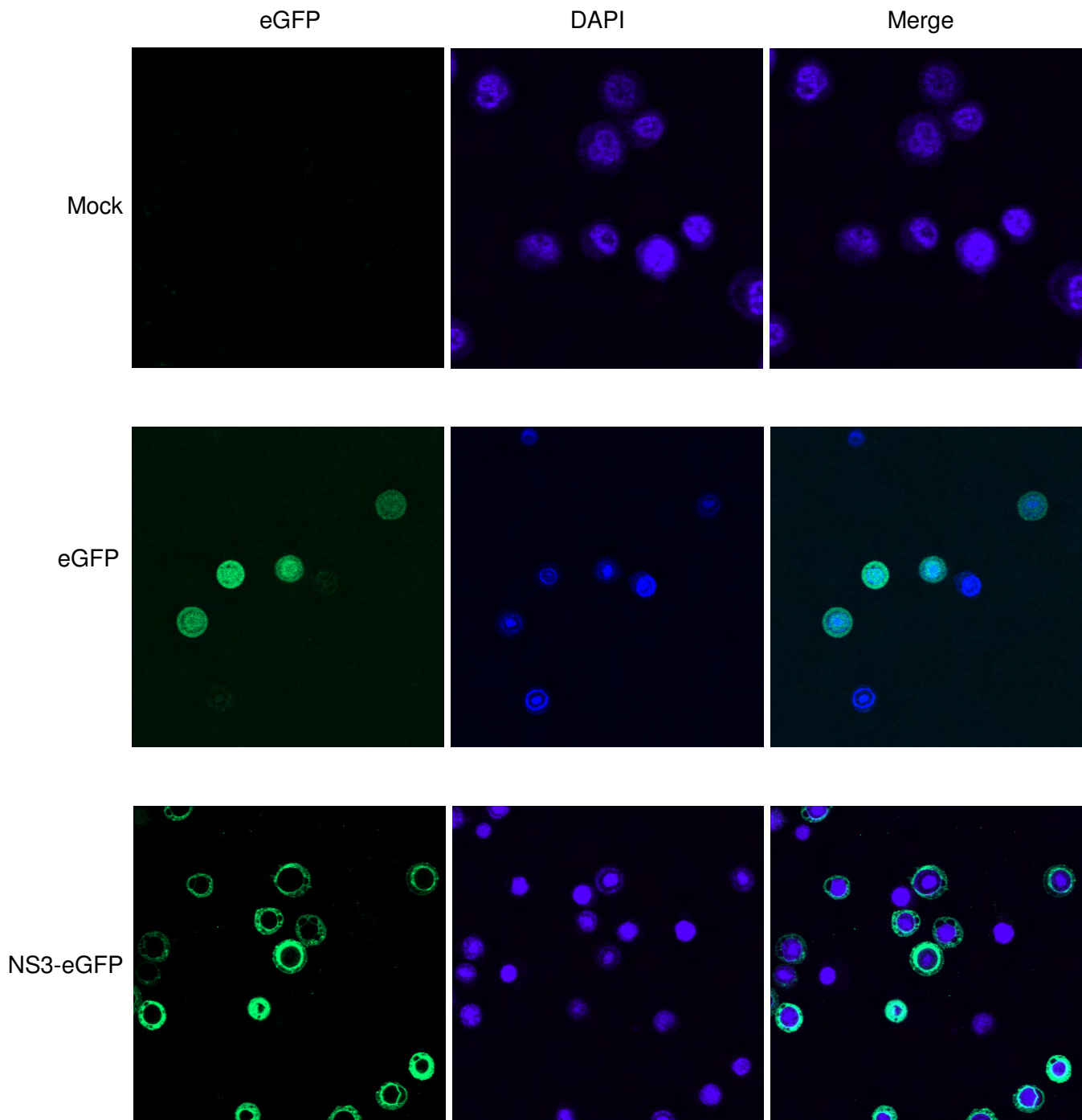


Figure 2.34. Confocal microscopy of baculovirus infected Sf9 cells labelled with a nuclear dye (DAPI). Sf9 cells were infected with baculoviruses expressing eGFP or NS3-eGFP. At 48 h post infection, cells were labelled with 4'6'-diamidino-2-phenylindole (DAPI) and examined by confocal microscopy. Mock infected cells were used as an uninfected control for the labelling process. The panels on the left represent the fluorescence pattern of the GFP fusion proteins (green). The panels in the middle represent the fluorescence pattern of the dye (blue). The panels on the right represent an overlay of the two panels.

Figure 2.35 shows enlargements of single DAPI-labelled cells expressing Bac-eGFP and Bac-NS3-eGFP to allow a clearer view of the colocalisation of these fusion proteins with the nuclear dye.

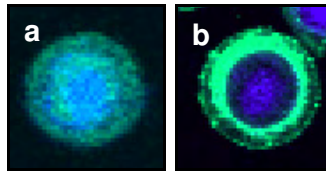


Figure 2.35. Enlargements of single cells from confocal microscopy images of DAPI-labelled Bac-eGFP infected (a) and Bac-NS3-eGFP infected (b) Sf9 cells at 48 h.p.i.

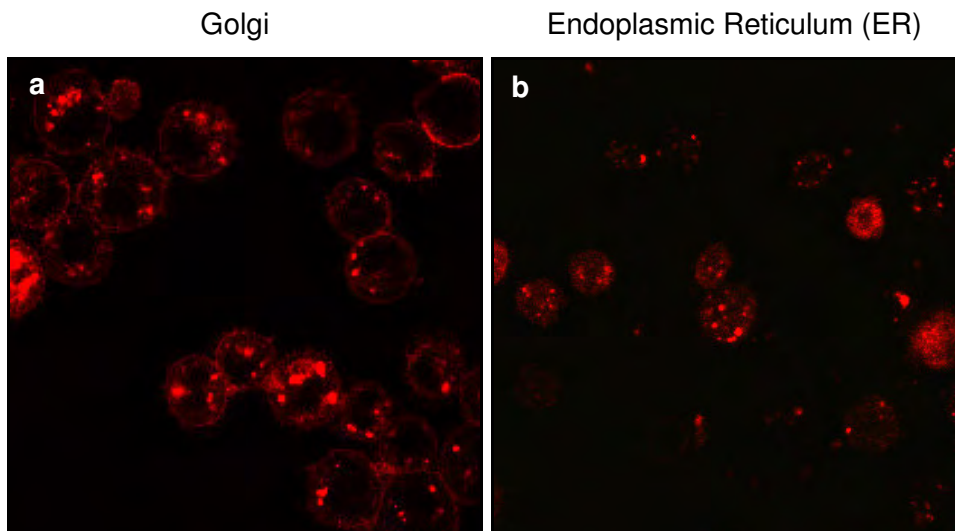


Figure 2.36. Confocal microscopy of mock infected Sf9 cells labelled with a Golgi/ER specific dye (red). Cells were labelled with BODIPY[®]TR ceramide (left) or VYBRANT[™] DiI cell-labelling solution (right) and examined by confocal microscopy.

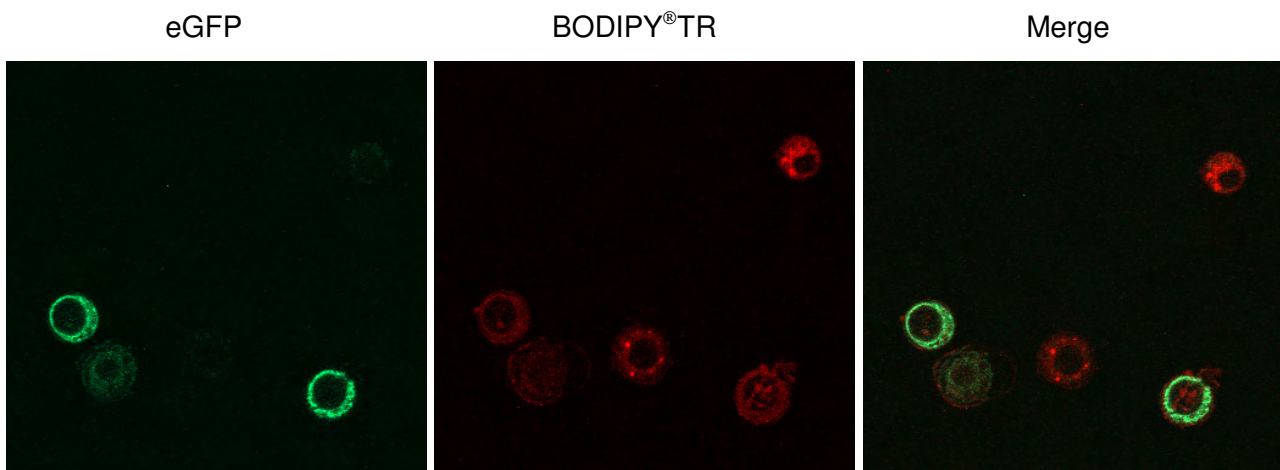


Figure 2.37. Confocal microscopy of Bac-NS3 Δ C-eGFP infected Sf9 cells labelled with a Golgi specific dye (red). The panels on the left represent the fluorescence pattern of the GFP fusion proteins (green). The panels in the middle represent the fluorescence pattern of the BODIPY[®]TR ceramide (red). The panels on the right represent an overlay of the two panels.

It was important to establish if NS3-eGFP had a different localisation pattern to native NS3 (without the eGFP tag). It is possible that the eGFP tag could affect the folding of NS3 and thereby influence its localisation within cells. We tried to eliminate the effect, if any, of the eGFP tag by investigating the localisation of an immunolabelled version of native NS3 in Sf9 cells. Sf9 cells

expressing Bac-NS3 were fixed and labelled with α - β -gal-NS3 as the primary antibody and α -rabbit-fluorescein isothiocyanate (FITC) as the secondary antibody. Unfortunately results from this experiment were inconclusive as high levels of background labelling were observed in mock-infected cells (not shown). Immunolabelling should be optimized and repeated to ensure the eGFP tag is not affecting the localisation of NS3.

In summary, results obtained from confocal microscopy once again indicated that NS3 requires the presence of two intact hydrophobic domains for membrane targeting. The truncation of the C-terminal did not seem to have any effect whatsoever, while the truncation of the N-terminal seemed to have quite a large effect on the targeting of NS3.

2.4. Discussion

Many aspects of the functioning and roles of NS3 and NS3A in the life cycle of African horsesickness virus, as well as the reasons for the conservation of both of these proteins, remain unclear. In addition, the exact roles of the two proteins in the cytotoxicity, virulence, pathogenesis, trafficking and release of the virus remain to be determined.

The main aim of this project was to investigate whether eGFP could be used as a molecular reporter molecule to monitor the localisation of AHSV NS3 within a cell. If so, further aims were to identify the different domains of AHSV NS3 that may affect its subcellular localisation and/or trafficking to specific compartments within a cell. Such findings could eventually help to identify functional domains of AHSV NS3 that may play a role in the viral life cycle and could, for example, affect viral pathogenesis, cytotoxicity, virulence, trafficking or release.

In order to assay the effect of specific candidate regions of NS3 that may be involved in its subcellular localisation, seven different constructs were produced and used to generate recombinant baculoviruses for the expression of fusion proteins in *Spodoptera frugiperda* (Sf9) insect cells. Constructs involved full-length, truncated or mutant versions of AHSV-3 NS3 that were produced as C-terminal eGFP (enhanced green fluorescent protein) fusion proteins. Fusion proteins were compared in terms of their subcellular localisation by conventional fluorescence microscopy and confocal laser microscopy. Subcellular fractionations and membrane flotation analyses were used to confirm membrane interactions and to identify detergent-resistant membrane fractions.

Enhanced Green Fluorescent Protein (eGFP) was shown to be a good tool with which to answer the questions proposed for this project. Not only were the proteins clearly visible under the fluorescent microscope and the confocal laser microscope, fluorescent readings also enabled us to pinpoint the location of the various fusion proteins in subcellular fractionations and membrane flotation analyses.

eGFP did, however, have some effect on the cytotoxicity of NS3. NS3-eGFP seemed to have a decreased cytotoxic effect when compared to pure NS3 (Figure 2.18). This may be attributed to the mutation present at amino acid 148 of NS3-eGFP, but this is unlikely as the mutation occurs in a highly variable region of the gene and does not affect the transmembrane domain prediction (Figure 2.10). It is more likely that this decrease in cytotoxicity is a result of incorrect folding due to the presence of the eGFP extension at the C-terminus of the protein. In addition to decreased cytotoxicity levels, NS3-eGFP showed elevated levels of expression when compared to native NS3

in PAGE gels and Western blots (Figure 2.12 and 2.14). This is probably in part due to the decrease in cytotoxicity caused by the eGFP tag. However, NS3-eGFP is still cytotoxic when compared to native eGFP. The levels of expression for this fusion protein (NS3-eGFP) are much greater than would be expected for a cytotoxic protein. This observation indicates that the eGFP tag's influence on the folding of the NS3 insert results in a conformation that enables the protein to be expressed at much higher levels.

These observations lead us to question whether the eGFP tag also affects the subcellular localisation of NS3 by affecting the folding of the protein. From our observations in microscopy and membrane flotation analysis, it seems as if the eGFP tag does not have an effect on the subcellular localisation of NS3. As an additional precaution, we tried to eliminate any effect that may be caused by the presence of the eGFP tag by using immunofluorescence to visualize an immunolabelled version of native NS3 (without the eGFP tag). This did not work well as high levels of background labeling were observed in mock-infected cells. Therefore, no answer was obtained from this experiment (not shown).

Immunofluorescence has previously been used successfully in our laboratory with Sf9 cells infected with AHSV-3 NS3 (Van Staden, 1993). In fixed cells NS3 was observed to have a perinuclear cytoplasmic distribution, while in unfixed cells NS3 was shown to be present on the surface of infected cells. These results indicate that AHSV NS3 interacts with smooth-surfaced intracellular membranes and is transported to the cell membrane (Van Staden, 1993). In addition, immunofluorescence was used by van Niekerk *et al.* (2001a) to visualize Bac-NS3, Bac-HD1 and Bac-HD2 in Sf9 cells. Fixed cells displayed a bright perinuclear cytoplasmic staining for all three recombinants while unfixed cells expressing NS3 clearly showed a homogenous fluorescence of the entire cell surface. Unfixed cells expressing HD1 and HD2 gave a low background signal, indicating the absence of accessible epitopes on the cell surface (Van Niekerk *et al.* 2001a).

The presence of two protein bands for NS3-eGFP, NS3A-eGFP and NS3 Δ C-eGFP in PAGE gels and Western blots raised a number of questions. At first it was thought that these bands could represent a glycosylated form of the NS3 protein. This was unlikely as the only N-linked glycosylation sites present in the AHSV NS3 sequence are present in non-conserved regions of the gene and none of these sites are present in the sequence of AHSV-3 NS3. Despite this, a simple glycosylation assay was carried out to investigate the possibility of a glycosylated form of AHSV-3 NS3 (Figure 2.17). This assay verified that AHSV-3 NS3 is not N-glycosylated. When labelled with [³⁵S]-methionine, the additional bands were not visible (Figure 2.15). Closer inspection of the [³⁵S]-labelled image and comparison to the Coomassie stained gel revealed that the extra bands seem to be present just above the native protein bands of these constructs. This

indicates that these bands must represent larger, modified forms of the proteins that accumulate later on during infection.

A novel, soluble form of rotavirus NSP4 was recently identified. This soluble form is secreted from virus-infected cells and has the potential to carry out the enterotoxic effects of the protein. The protein band corresponding to the secreted form exhibited a slightly higher molecular mass than the cell-associated form of the protein, most likely due to a posttranslational modification that occurs within the secretory pathway. The precise nature of the modification is unclear, but results indicate that modification of glycan residues during transit through the Golgi apparatus may be responsible (Bugarcic and Taylor, 2006). The protein release assay carried out with NS3-eGFP infected cells showed a peak in the soluble component of the cells at 30 h.p.i. The amount of soluble protein in the cells then decreased as the amount of soluble protein in the medium increased (Figure 2.20B). Together, these results indicate that there may be a soluble form of AHSV NS3 that is slightly larger than the native protein. This form of the protein may be released when dead cells break open or may be actively secreted from virus-infected cells. A number of ways exist to investigate the possibility and nature of such a form of the AHSV NS3 protein. Initially, one should run gels comparing the form of NS3 present in the medium to the form of NS3 present in the cells at different times post infection. This would enable us to see if there are any clear differences between these two forms. The next step would be to perform a pulse-chase experiment to investigate exactly when in the infection cycle the second form arises. Such an experiment would enable us to investigate whether the second form arises as a result of a modification to the first form or whether the second form is produced separately at later stages in the infection cycle. To investigate multimer formation, one could run unboiled samples of the proteins on non-denaturing gels.

Another concern in this project was the fact that the expression of HD1-eGFP and HD2-eGFP could not be confirmed. The bacmid DNA encoding HD1-eGFP and HD2-eGFP was retransfected and the post-transfection virus stock was plaque purified before undergoing three rounds of amplification. Single plaques could easily be identified by the green fluorescent phenotype. Despite high viral titres (Table 2.5), these two fusion proteins were not visible on PAGE gels, Western blots or when radioactively labelled with [³⁵S]-methionine. A possible reason for their low levels of expression may be that these two proteins are cytotoxic. This is highly unlikely though, as these same mutations in the two hydrophobic domains of NS3 have previously been shown to greatly decrease the cytotoxic effect of the protein (Van Staden *et al.*, 1998). Therefore, no explanation can be given at this stage for the low levels of expression of these two proteins. Although not visible on PAGE gels or Western blots, HD1-eGFP and HD2-eGFP were clearly visible under the fluorescent microscope and the confocal laser microscope. Fluorescent readings obtained were

high enough to be used for subcellular fractionations and subsequent membrane flotation analyses. DNA was extracted from Sf9 cells expressing these proteins and was sequenced to verify that they were produced correctly and that no mutations had occurred during their production or expression.

HD1-eGFP and HD2-eGFP showed a general cytoplasmic distribution in infected cells, compared to the perinuclear localisation observed for untagged proteins (i.e. not fused to eGFP). This result, combined with the fact that these proteins could never be detected by any methods other than fluorescence, raised the question of whether they were authentically expressed or if the fluorescence may be the result of low levels of downstream initiation of eGFP only? This does, however, seem unlikely based on results of sequencing directly from the viral genome that showed an intact initiation sequence.

In fluorescent microscopy, eGFP, N11-eGFP, HD1-eGFP and HD2-eGFP showed a cytoplasmic distribution where fluorescence was dispersed throughout the cells. NS3-eGFP and NS3 Δ C-eGFP showed membrane localisation where fluorescence was clearly visible at the membrane regions of the cells. NS3A-eGFP showed mixed results, displaying membrane localisation in some cells and a cytoplasmic distribution in others (Figure 2.19). These results indicate that both of the hydrophobic domains are crucial for the membrane targeting of AHSV NS3 to take place. In addition, the N11 region seems to play a large role in this membrane targeting. While NS3A is sometimes able to reach the membrane without the N11 region, this is not always the case. Also, the N11 region alone is not sufficient to enable membrane targeting to take place. Rather, it seems as if all three of these domains must be present and some kind of interaction between the three results in the membrane localisation of NS3. To further investigate this hypothesis, additional fusion proteins should be constructed and expressed. For example, it would be interesting to produce a protein consisting of just the N11 region and the two hydrophobic domains. This would enable us to investigate whether these domains alone are sufficient for membrane targeting of NS3 to occur.

Subcellular fractionations verified the results obtained in fluorescent microscopy. At 48 h.p.i, for eGFP, N11-eGFP, HD1-eGFP and HD2-eGFP, most of the fluorescence was found to be in the soluble component of the cells, verifying a cytoplasmic distribution of these proteins. For NS3-eGFP and NS3 Δ C-eGFP, most of the fluorescence was lost with the nuclear fraction. The remaining fluorescence was mainly particulate for NS3-eGFP, indicating membrane association and mainly soluble for NS3 Δ C-eGFP, indicating a cytoplasmic component. For NS3A-eGFP, a fair amount of fluorescence was lost with the nuclear fraction. Of the remaining fluorescence, most ended up in the soluble component, indicating a cytoplasmic distribution (Figure 2.23). Subcellular fractionations performed at 24 hours post infection yielded similar results. The main differences

here were observed in the fractionations performed for NS3-eGFP, NS3A-eGFP and NS3ΔC-eGFP. For all three of these fusion proteins, the amount of fluorescent protein pelleted with the nuclei was lower at 24 h.p.i than at 48 h.p.i. For NS3-eGFP and NS3ΔC-eGFP, the amount of particulate protein present in the final fraction was greater at 24 h.p.i than at 48 h.p.i. For NS3A-eGFP, the amount of soluble protein present in the final fraction was greater at 24 h.p.i than at 48 h.p.i (Figure 2.22). From these results, it seems as if NS3 may be targeted initially to the plasma membrane and later on to the nuclear membrane. This may be caused by the overexpression of the protein, resulting in an accumulation of excess protein at the nuclear membrane.

A number of general trafficking pathways exist within a cell. Although many ordinary cellular processes rely on these trafficking events, pathogens often gain entry by “hijacking” and utilizing these pathways (Altschuler *et al.*, 2003). In this way, NS3 may be utilizing one or more of the host cell’s general trafficking pathways to carry out its functions in the viral life cycle. General trafficking pathways within a cell include secretory pathways, endocytic pathways, nuclear pathways and mitochondrial pathways (Lodish *et al.*, 2004). Generally, proteins are synthesized from mRNA, which is translated on cytosolic ribosomes. For proteins containing an ER signal sequence, ribosomes are directed to the rough Endoplasmic Reticulum. After translation on the ER, these proteins move via transport vesicles to the Golgi apparatus where further sorting to the plasma membrane or lysosomes takes place. For proteins lacking an ER signal sequence, synthesis is completed on free ribosomes in the cytosol. Proteins that do not harbour targeting sequences are released into cytosol and remain there. Proteins containing signal sequences are released into cytosol and then imported into mitochondria, chloroplasts, peroxisomes or the nucleus (Lodish *et al.*, 2004).

Many of the steps in the abovementioned trafficking pathways require specific signal sequences that carry the necessary information to target a protein to a specific destination within the cell (Lodish *et al.*, 2004). Signal peptides are generally between 20 and 50 amino acids in length and usually contain a short basic region at the amino-terminus as well as a hydrophobic “core” region that helps anchor the protein in the membrane (Lodish *et al.*, 2004). Examples of known sorting signals are KDEL in ER-resident luminal proteins, a dilysine motif (KKXX) in ER-resident membrane proteins, a di-acidic (Asp-X-Glu) signal in cargo membrane proteins in the ER, the Mannose 6-phosphate motif in soluble lysosomal enzymes after processing in the *cis* Golgi, NPXY in the low density lipoprotein (LDL) receptor in the plasma membrane, YXXΦ in membrane proteins in the *trans* Golgi and in plasma membrane proteins and the dileucine motif (D/EXXXLL) in plasma membrane proteins (Brown and Breton, 2000; Fernandez-Salas *et al.*, 2004; Lodish *et al.*, 2004). In addition to these, a three-residue motif, RxR, has been described as a signal sequence for targeting of transmembrane proteins to the nuclear membrane (Meyer and Radsak,

2000; Meyer *et al.*, 2002).

Membrane flotation analysis is a technique that relies on the buoyancy of lipid membranes and their associated proteins to separate them from the other cellular components. For membrane flotation analysis, the cell lysate is loaded onto the bottom of a discontinuous gradient. During high-speed centrifugation, membranes and their associated proteins “float” up due to the buoyant density of the lipids. We, therefore, expect to find membrane associated proteins in the upper fractions of the gradient.

Membrane flotation has been attempted once before in our laboratory (Smit, 1999). A protocol described by Sanderson *et al.* (1993) and modified by Matsumoto *et al.* (1996) was used. Results were inconclusive as proteins were dispersed throughout the fractions and were not restricted to the upper fractions as would be expected for membrane associated proteins. The same protocol was attempted in this project, but once again proved to be unsuccessful as proteins were again dispersed throughout the fractions. A number of protocols were investigated before attempting one used by Brignati *et al.* (2003), who had used membrane flotation to look at the membrane association of VP22, a herpes simplex virus type 1 tegument protein. Their experiments were similar to ours in that they also used GFP fusion proteins and took fluorescent readings to estimate the amount of protein present in the various fractions. The main difference between this protocol and the protocol of Matsumoto *et al.* (1996) was in the composition of the buffers used. The protocol of Brignati *et al.* (2003) worked well and membrane associated proteins “floated” to the upper fractions of the gradient as expected. We further optimised this protocol to be used with our protein expression system. Examples of modifications are that we chose to disrupt the cells by passage through a needle rather than dounce homogenisation and we chose not to remove the nuclear fraction before loading the sample onto the gradient. This method leads us to question the behaviour of the nuclei in the membrane flotation gradients i.e. are whole nuclei “floating” up in the gradients or are the nuclei breaking open, releasing their membranes to “float” up and leaving their contents at the bottom of the gradients? In order to answer this question one should investigate further by investigating where (in which fractions) the nuclei are actually located following centrifugation.

Membrane flotation analyses further verified results obtained from fluorescent microscopy and subcellular fractionation experiments. For eGFP, N11-eGFP, HD1-eGFP and HD2-eGFP, the bulk of the fluorescence remained at the bottom of the gradients indicating an absence of membrane association. This result verifies the cytoplasmic distribution of these proteins observed during fluorescent microscopy. For NS3-eGFP and NS3 Δ C-eGFP, a large amount of fluorescence was present in the upper fractions of the gradient, indicating membrane association of these proteins.

This result verifies the membrane distribution observed during fluorescent microscopy. For NS3A-eGFP, two peaks occurred. One of the peaks was at the bottom of the gradient, while the other was in the upper fractions of the gradient. This indicates both membrane association and cytoplasmic distribution, once again verifying what was observed in fluorescent microscopy (Figure 2.29). To further investigate the locations of the various fusion proteins within the cells, flotations should be carried out using markers for specific compartments within the cell. The use of such markers would enable us to identify the exact location of the various fusion proteins within a cell. Examples of such markers include Calnexin, a marker for the Endoplasmic Reticulum (ER) that has been used to investigate the subcellular localisation of rotavirus NSP4 (Mirazimi *et al.*, 1998; Berkova *et al.*, 2006) and β -COP, a marker for the Golgi apparatus that has been used to investigate the subcellular localisation of rotavirus NSP4 (Berkova *et al.*, 2006) and Hepatitis C NS5A (Shi *et al.*, 2002).

Over the past years, increasing evidence has accumulated to support the idea that many pathogens, such as viruses, use lipid rafts for their own benefit. Due to their role in membrane sorting and intracellular trafficking, raft domains provide sites for the assembly or budding of a number of viruses (Briggs *et al.*, 2003). In the *Reoviridae* family, Sapin *et al.* (2002) found high proportions of rotavirus VP4, the outermost protein of the triple-layered structure, to be associated with rafts within the cell as early as 3 hours post infection. At 6 hours post infection, high proportions of NSP4 were found to be associated with rafts within the cell. These findings support the conclusion that infectious rotavirus virions use rafts as assembly platforms and are transported to the cell surface using a raft-dependent pathway i.e. a non-conventional vesicular transport mechanism. Cuadras *et al.* (2006) recently found that silencing of VP4 and NSP4 reduced the association of rotavirus particles with rafts, confirming a possible role for NSP4 as a “raft receptor”. In addition, Parr *et al.* (2006) recently showed colocalisation between NSP4 and caveolin-1, a marker for detergent resistant membrane fractions, in NSP4-transfected and rotavirus infected mammalian cells. Amino acids 114 to 135 were found to be directly involved in this association, which most likely contributes to the intracellular trafficking of NSP4 from the ER to the cell surface (Parr *et al.*, 2006).

It is not known whether AHSV NS3 may also be using lipid rafts as platforms to enable the transport and release of the virus from infected cells. To investigate this, detergent-resistant membrane fractions, which may contain lipid rafts, were isolated by treatment with the non-ionic detergent Triton X-100. Preliminary evidence from the subcellular fractionation experiments indicates that Triton X-100 has some effect, but does not totally solubilise all of the particulate protein present. In the initial subcellular fractionation assays, the only fusion proteins that showed differences following Triton X-100 treatment were NS3-eGFP, NS3A-eGFP and NS3 Δ C-eGFP. For

these proteins, the amount of soluble protein in the cells showed a slight increase following Triton X-100 treatment (Figure 2.23).

In membrane flotation analyses, little change was observed for eGFP and N11-eGFP following Triton X-100 treatment. For HD1-eGFP and HD2-eGFP, the peak in the upper portions is no longer present. For NS3-eGFP, some of the fluorescence shifted to the lower fractions of the gradient and two fluorescent peaks were observed. For NS3A-eGFP, there was also a shift and more fluorescence was located in the lower fractions of the gradient than prior to Triton X-100 treatment. For NS3 Δ C-eGFP, all of the fluorescence was observed to be in the lower fractions of the gradient following treatment with Triton X-100 (Figure 2.29). These results indicate that the Triton X-100 had an effect and disrupted the association of these proteins with the membrane fractions. However, the disruption was not always complete, indicating a possible association of NS3-eGFP with detergent resistant membrane fractions (DRMs) that may contain lipid rafts. This association may be mediated by the C-terminal amino acids as, when these amino acids are not present as in NS3 Δ C-eGFP, Triton X-100 is able to completely abolish the association of the protein with the membrane fractions. To be sure of this, however, further experiments need to be carried out. Examples of such experiments include the use of density markers or raft markers in membrane flotation experiments. The use of such markers would enable us to identify the exact location of raft domains in membrane flotation gradients. We would then be able to compare the location of the raft domains to the location of our fusion proteins in the gradients. One example of a marker that can be used for lipid rafts is Caveolin-1. This marker has been used previously by Gosselin-Grenet *et al.* (2006) to study the association of Sendai virus with lipid rafts and by Parr *et al.* (2006) who used Caveolin-1 to show a direct association of rotavirus NSP4 with lipid rafts. Another possibility for further experimentation would be to use drug treatments such as Methyl- β -cyclodextrin (M β CD). M β CD removes membrane embedded cholesterol, thereby disrupting DRM insolubility. This drug was also used successfully by Gosselin-Grenet *et al.* (2006) to show an association of Sendai virus with lipid rafts. This study should also be expanded to include non-eGFP tagged NS3, transiently expressed NS3 in mammalian cells and eventually AHSV infected mammalian/insect cells.

The values for the particulate components of the cells for membrane associated proteins in all assays seem to be lower than would be expected for these proteins. Another member of our laboratory recently found that soluble VP7-eGFP fluoresces approximately 7 times better per unit of VP7 protein than insoluble VP7-eGFP particles (E. Mizrachi, personal communication). These results indicate that fluorescence values obtained from particulate samples may be underrepresented by up to 7 times in comparison to those obtained from soluble samples. To get an idea of the actual amount of particulate protein present, assays should be repeated and protein

samples should be quantified from PAGE gels.

The recent acquisition of a Confocal Microscope at the University of Pretoria enabled us to get a better picture of the localisation of the seven fusion proteins within Sf9 cells. At first glance, images looked similar to those obtained from fluorescent microscopy (Figure 2.19). eGFP (b), N11-eGFP (e), HD1-eGFP (g) and HD2-eGFP (h) show no membrane localisation and are observed to be dispersed throughout the cells (nucleus and cytoplasm), while NS3-eGFP (c) and NS3 Δ C-eGFP (f) show membrane localisation and are clearly visible at the membrane regions of the cells. NS3A-eGFP (d) is localised in patches on the surface in the plasma membrane of some cells, but is distributed throughout the cytoplasm of others (Figure 2.32d and 2.33c). However, upon closer inspection of NS3-eGFP infected cells, it appears as if a small amount of fluorescence is visible at the outer membrane of the cell, but the bulk of the fluorescence is present within this membrane, localised to what may be the nuclear membrane (Figure 2.33b).

We chose to further investigate the nuclear membrane localisation of NS3-eGFP using a nuclear dye (DAPI) to stain cells that had been infected with eGFP or NS3-eGFP. Mock-infected cells were used as a control for the staining procedure. DAPI has been used successfully in Sf9 cells by a number of groups including Caballero *et al.* (2004) and Matsumoto *et al.* (2004). The staining procedure worked well. eGFP had a cytoplasmic distribution and nuclear distribution, as indicated by overlap with the nuclear dye. This same distribution was observed previously for eGFP in Sf9 cells by Matsumoto *et al.* (2004). NS3-eGFP was visible as a circle around the nuclear stain. The proximity of the protein to the stain may indicate targeting of NS3 to the nuclear membrane (Figure 2.34).

Another feature of confocal microscopy is the ability to perform colocalisation studies using dyes for specific compartments within the cells. By using the right dyes one could pinpoint the exact locations of the various fusion proteins within the cells. A problem that we came across is that most dyes have only been used in mammalian cell systems and there is no guarantee that they will be transferrable to insect cell systems. We, therefore, tried to look for dyes that had previously been used successfully in Sf9 cells.

In addition to the nuclear labeling, we optimized Golgi labeling with BODIPY[®]TR ceramide as well as ER labeling with VYBRANT[™] Dil cell-labeling solution in mock-infected cells (Figure 2.35). Kwar and Jarvis (2001) successfully used BODIPY[®]TR ceramide to stain the Golgi and Dil to stain the ER in Sf9 cells while studying the subcellular localisation of the insect α 1,2-mannosidase, SfManI. According to Kwar and Jarvis (2001), Golgi elements in Sf9 cells appear as punctate structures located throughout the cytoplasm. We managed to achieve a staining

pattern similar to this in mock infected cells (Figure 2.35). The optimisation of these staining procedures in cells expressing the seven fusion proteins proved to be more challenging and we were unable to complete these experiments in the time course of this project. We found that cells infected with baculoviruses expressing our fusion proteins (green fluorescing) did not stain with the ER/Golgi dyes (red stain), however directly adjacent uninfected cells (no fluorescence) were able to take up the membrane dyes efficiently (Figure 2.36). This may be due to changes in the physiology of the cell caused by the expression of our fusion proteins. Fixing protocols need to be investigated further and further training on the confocal microscope and its software is required in order to complete this work.

Viral membrane proteins often “hijack” and utilize general trafficking pathways within a cell for their own purposes (Altschuler *et al.*, 2003). Unless the protein contains additional sorting signals, post-translational targeting occurs via the default pathway used by cellular membrane proteins. This pathway is from the ER through the Golgi apparatus and on to the cell surface. Further modifications such as glycosylation and oligomerisation may occur in the Golgi apparatus (Bassel-Duby *et al.*, 1985; Hegde and Lingappa, 1997). In this way, NS3 may be utilizing one or more of the host cells general trafficking pathways to carry out its functions in the viral life cycle. One way to test this would be to use the drug Brefeldin A, which blocks ER to Golgi trafficking in the general secretory pathway (Klausner *et al.*, 1992). When used in this project, Brefeldin A did not affect the subcellular localisation of NS3-eGFP (Figure 2.30). This could mean that NS3 does not use the conventional secretory pathway but uses some kind of alternate pathway to reach the cell membrane. However, it is the first time that we have used Brefeldin A in our laboratory and the treatment protocol may need to be optimized. In order to do this, one would need a proper positive control to ensure the Brefeldin A treatment is actually working. We would need to use a protein that is known to use the conventional secretory pathway to reach the cell membrane. If such a control is still able to reach the cell membrane following treatment with Brefeldin A, we will know that there is a problem with either the Brefeldin A or with the treatment protocol. In conclusion, this experiment needs to be repeated with a proper positive control in order to investigate whether NS3 is using the default trafficking pathway of the cell or some kind of alternate pathway to reach the cell membrane.

Another way to test whether viruses are “hijacking” the host cells pathways and using them to their own benefit is to investigate possible interactions that may occur between viral proteins and cellular proteins. For example, Beaton *et al.* (2002) have shown that BTV NS3 interacts with a cellular protein p11, which is part of the annexin II complex that is involved in exocytosis. They also showed interaction between the C-terminal domain of BTV NS3 and VP2. These results suggest that BTV NS3 acts as a bridging molecule that draws the assembled virus into contact with the

cellular export machinery. In addition, Wirblich *et al.* (2006) recently found that BTV and AHSV NS3 bind to a cellular protein Tsg101, which is a component of the ESCRT-I (endosomal sorting complex required for transport) complex. The ESCRT proteins form three distinct complexes. ESCRT-I, II and III, that act sequentially to form the budding multivesicular body (MVB) vesicle (Katzmann *et al.*, 2001; Babst *et al.*, 2002a; Babst *et al.*, 2002b). The interaction between NS3 and Tsg101 is mediated by a conserved PSAP motif, part of the proline rich region of NS3. AHSV NS3 also harbours a PSAP motif, but the consensus sequence is replaced by ANAP. The depletion of Tsg101 was found to inhibit the release of both BTV and AHSV. These results indicate that NS3 interacts with Tsg101, thereby facilitating virus release (Wirblich *et al.*, 2006).

We have also begun to look for evidence of NS3 “hijacking” the host cells pathways and using them for its own benefit in the viral life cycle. We are doing this by investigating interactions that may occur between NS3 and proteins in the host cells. A member of our laboratory recently used yeast two-hybrid analysis with the NS3 N-terminal (amino acids 1 – 118) as bait to screen a *Drosophila* cDNA library for protein interactions. Results indicate an interaction of AHSV NS3 with ubiquitin and Hsp70 (M. Beyleveld, personal communication). Ubiquitin is a small, highly conserved protein that is well known for its role in protein degradation by the proteasome (Vogt, 2000). It also acts as a sorting signal in both the secretory pathway and in endosomes where it targets proteins to multivesicular bodies. It has been reported that viral budding is dependent on the presence of a late domain (PPXY), which recruits ubiquitin. This motif is present in AHSV NS3 as PPPY/PSPY (Wirblich *et al.*, 2006). Ubiquitin and ubiquitin ligase have been shown to play a role in the budding of retroviruses e.g. HIV (Vogt, 2000). In the *Reoviridae* family, rotavirus NSP1 has recently been found to act as an ubiquitin ligase. NSP1 recruits ubiquitin to target itself to the proteasome, where it is degraded. In addition, NSP1 binds to viral mRNAs and to IRF3 (Interferon regulatory factor 3), inducing IRF3 degradation through a proteasome dependent pathway. IRF3 is a key transcription factor involved in the induction of interferon (IFN) response to viral infection (Graff *et al.*, 2007; Pina-Vazquez *et al.*, 2007). Heat shock/stress protein 70 (HSP 70) was recently shown play a role in the control of the bioavailability of viral proteins in cells infected by rotavirus. Whether Hsp70-dependent ubiquitination of rotaviral structural proteins is involved only in this degradation pathway or may also play an additional role in the targeting or assembly of progeny virions remains to be determined (Broquet *et al.*, 2007).

Both Hsp70 and ubiquitination have been shown to play a role in the regulation of certain viral proteins. Hsp70 and ubiquitin may both bind to NS3 to regulate its availability i.e. high levels of expression in insect cells where there is non-lytic release via budding and low levels of expression in mammalian cells where lytic release takes place. These studies highlight the fact that virus-host interactions are extremely important in regulating the viral life cycle and levels of protein

expression. These interactions play a large role in the release of mature virions in reoviruses.

Results from microscopy, subcellular fractionations and membrane flotation analyses confirm that eGFP does not display any membrane association and is distributed throughout the cytoplasm of the cells. The 11 amino acid region unique to NS3 and absent from NS3A, which has been shown to bind to cellular exocytosis proteins in bluetongue virus (BTV), did not display any membrane interaction. Site-specific mutations to either of the hydrophobic domains abolished membrane association and resulted in a cytoplasmic localisation. NS3A showed mixed results, displaying membrane localisation in some cells and a cytoplasmic distribution in others. NS3 and a C-terminal deletion of NS3 targeting a putative dileucine motif on the C-terminal of the protein both localised to cellular membrane components. NS3 was shown to be present in detergent-resistant membrane fractions, indicative of a possible localisation within lipid rafts. In addition, NS3 was pelleted with the nuclear fraction in subcellular fractionation experiments and was shown to localise to the region bordering the nuclei in confocal microscopy. These results indicate the possible targeting of a large proportion of the baculovirus expressed NS3 to the nuclear membrane and not the plasma membrane as had been expected.

These results indicate that both the hydrophobic domains as well as the N11 region are required to be present for NS3 to be properly targeted to the plasma/nuclear membrane. As soon as one of the hydrophobic domains has been modified to disrupt its function, NS3 is no longer only membrane associated. In addition, the N11 region on its own is not enough to ensure the membrane association of NS3. While NS3 is sometimes able to reach the membrane without N11, this is not always the case. It seems as if all three of these domains must be present and some kind of interaction between the three results in the membrane localisation of NS3.

In summary, we have shown that certain regions of the NS3 protein contain specific signals involved in membrane targeting, confirming a potential role for NS3 in viral localisation and release in the AHSV replication cycle. This is also the first time that any clear difference has been observed between NS3 and NS3A. This difference in localisation suggests that there may be a difference in function, which may explain the conservation of these two proteins. A more in-depth structural and functional analysis of AHSV NS3 is needed to further understand the exact roles of these two proteins in the life cycle of African horsesickness virus. Results from further studies will provide us with a better understanding of the precise role of AHSV NS3 in virus release and pathogenesis.

Chapter 3: Concluding Remarks

In summary, we have shown that certain regions of AHSV NS3 contain specific signals involved in its localisation. Results obtained in this project indicate that both hydrophobic domains as well as the N11 region are required to be present for NS3 to be properly targeted to the plasma and/or nuclear membrane. While NS3A is sometimes able to reach the membrane without the N11 region, this is not always the case. It seems as if all three of these domains must be present and some kind of interaction between the three results in the membrane localisation of NS3.

From results obtained, it seems as if NS3 may be targeted initially to the plasma membrane and later on to the nuclear membrane. This may be caused by the overexpression of the protein, resulting in an accumulation of excess protein at the nuclear membrane. Results also indicate that there may be association with detergent resistant membrane fractions (DRMs), which may contain lipid rafts. This association may be mediated by the C-terminal amino acids of NS3.

In addition, results indicate that there may be a soluble form of AHSV NS3 that is slightly larger than the native protein and is secreted from virus-infected cells. This is also the first time that any clear difference has been observed between NS3 and NS3A. This difference in localisation suggests that there may be a difference in function, which may explain the conservation of both of these proteins.

A more in-depth structural and functional analysis of AHSV NS3/NS3A is needed to further understand the exact roles of these proteins in the life cycle of African horsesickness virus. The next logical step would be to investigate the colocalisation of the seven fusion proteins with dyes specific for certain organelles within the cell using confocal laser microscopy. We were hoping to be able to carry out such experiments during the course of this project but, unfortunately the confocal microscope was only obtained by the University of Pretoria during the final stages of this project. Due to inexperience and a lack of technical knowledge relating to the microscope and its software, we were unable to optimize these colocalisation experiments during the time course of this project. Once further training has been obtained, we will be able to use this microscope to investigate the possible colocalisation of our seven fusion proteins with the Golgi and the ER. One could even purchase dyes for lipid rafts to investigate a possible colocalisation of the fusion proteins with these microdomains. By doing this we will be able to narrow down the locations of these fusion proteins within the cells and we may be able to better understand the trafficking mechanisms used.

Further investigations into the subcellular localisation of these fusion proteins using membrane

flotation analysis could also be carried out by using known markers for specific compartments in the cell e.g. markers for the ER/Golgi. Markers for lipid rafts could also be purchased and included in the experiments. This would enable us to narrow down the location of the various fusion proteins in the cell and to investigate which membranes they are associated with within the cell.

The association of NS3 with cellular proteins of the host cell should also be investigated further. Knowledge of the interactions that occur between NS3 and host cell proteins would allow us to understand how African horsesickness virus may be using the host cells trafficking pathways to its own benefit. Results from further studies such as these will provide us with a better understanding of the precise role of AHSV NS3/NS3A in virus release and pathogenesis.

Parts of this work have been presented at the following scientific meetings:

Van Staden, V., Meiring, T., Hatherell, T.L., Fick, W. and Huismans, H. 2005. Cytotoxicity and membrane permeabilising activity of non-structural protein NS3 of different orbiviruses. Virology Africa conference. November 8 – 11. Cape Town.

Hatherell, T.L., Van Staden, V. and Huismans, H. 2006. Subcellular localisation of nonstructural protein NS3 of African Horsesickness virus. 19th conference of the South African Genetics Society. April 3 – April 5. Bloemfontein.

Van Staden, V., Hatherell, T.L. and Huismans, H. 2006. Subcellular localisation of African Horsesickness virus non-structural protein NS3. 9th International Symposium on Double-Stranded RNA Viruses. October 21 – 26. Cape Town.

References

- Agirre, A., Barco, A., Carrasco, L. and Nieva, J.L. 2002. Viroporin-mediated membrane permeabilization. *J. Biol. Chem.* 277: 40434 – 40441.
- Altschuler, Y., Hodson, C. and Milgram, S.L. 2003. The apical compartment: trafficking pathways, regulators and scaffolding proteins. *Current Opinion in Cell Biology.* 15: 423 – 429.
- Andrew, M., Whiteley, P., Janardhana, V., Lobato, Z., Gould, A. and Coupar, B. 1995. Antigen specificity of the ovine cytotoxic T lymphocyte response to bluetongue virus. *Vet Immunol Immunopath.* 47: 311 – 322.
- Ashby, M.C., Ibaraki, K. and Henley, J.M. 2004. It's green outside: tracking cell surface proteins with pH-sensitive GFP. *Trends in Neurosciences.* 27: 257 – 261.
- Au, K.S., Chan, W.K., Burns, J.W. and Estes, M.K. 1989. Receptor activity of rotavirus non-structural glycoprotein NS28. *J. Virol.* 63: 4553 – 4562.
- Awad, F.I., Amin, M.M., Salama, S.A. and Aly, M.M. 1981. The incidence of African horse sickness in animals of various species in Egypt. *Bull. Anim. Health. Prod. Afr.* 29: 285 – 287.
- Babst, M., Katzmann, D.J., Estepa-Sabal, E.J., Meerloo, T. and Emr, S.D. 2002a. ESCRT-III: and endosome-associated heterooligomeric protein complex required for MVB sorting. *Developmental Cell.* 3: 271 – 282.
- Babst, M., Katzmann, D.J., Snyder, W.B., Wendland, B. and Emr, S. 2002b. Endosome-associated complex ESCRT-II recruits transport machinery for protein sorting at the multivesicular body. *Developmental Cell.* 3: 283 – 289.
- BAC-TO-BAC baculovirus expression system manual*, Life technologies GIBCO BRL.
- Ball, J.M., Tian, P., Zeng, C., Morris, A.P. and Estes, M.K. 1996. Age-dependent diarrhoea induced by a rotaviral non-structural glycoprotein. *Science.* 272: 101 – 104.
- Ball, J.M., Mitchell, D.M., Gibbons, T.F. and Parr, R.D. 2005. Rotavirus NSP4, A multifunctional viral enterotoxin. *Viral Immunology.* 18: 27 – 40.

- Bamford, D.H. 2000. Virus structures: those magnificent molecular machines. *Current Biology*. 10: R558 – R561.
- Bansal, O.B., Stokes, A., Bansal, A., Bishop, D. and Roy, P. 1998. Membrane organization of bluetongue virus nonstructural glycoprotein NS3. *J Virol*. 72: 3362 – 3369.
- Bassel-Duby, R., Jayasuriya, A., Chatterjee, D., Soneberg, N., Maizel, J.V. and Fields, B.N. 1985. Sequence of reovirus hemagglutinin predicts a coiled-coil structure. *Nature*. 315: 421 – 423.
- Beaton, A.R., Rodriguez, J., Reddy, Y.K. and Roy, P. 2002. The membrane trafficking protein calpactin forms a complex with bluetongue virus protein NS3 and mediates virus release. *Proc Natl Acad Sci USA*. 99: 13154 – 13159.
- Berkova, Z., Morris, A.P. and Estes, M.K. 2003. Cytoplasmic calcium measurement in rotavirus enterotoxin-enhanced green fluorescent protein (NSP4-EGFP) expressing cells loaded with fura-2. *Cell Calcium*. 34: 55 – 68.
- Berkova, Z., Crawford, S.E., Trugnan, G., Yoshimori, T., Morris, A.P. and Estes, M.K. 2006. Rotavirus NSP4 induces a novel vesicular compartment regulated by calcium and associated with viroplasm. *J. Virol*. 80: 6061 – 6071.
- Berkova, Z., Crawford, S.E., Blutt, S.E., Morris, A.P. and Estes, M.K. 2007. Expression of Rotavirus NSP4 alters the actin network organization through the actin remodelling protein cofilin. *J. Virol*. 81: 3545 – 3553.
- Bhattacharya, B., Noad, R.J. and Roy, P. 2007. Interaction between Bluetongue virus outer capsid protein VP2 and vimentin is necessary for virus egress. *Virology Journal*. 4: 7.
- Boorman, J., Mellor, P.S., Penn, M. and Jennings, M. 1975. The growth of African horse sickness virus in embryonated hen eggs and the transmission of virus by *Culicoides variipennis* Coquillett (Diptera, Ceratopogonidae). *Arch Virol*. 47: 343 – 349.
- Boyce, M. and Roy, P. 2007. Recovery of infectious Bluetongue virus from RNA. *J. Virol*. 81: 2179 – 2186.
- Bremer, C.W., Huismans, H. and Van Dijk, A.A. 1990. Characterization and cloning of the African horse sickness virus genome. *J Gen Virol*. 71: 793 – 799.

- Briggs, J.A.G., Wilk, T. and Fuller, S.D. 2003. Do lipid rafts mediate virus assembly and pseudotyping? *J. Gen. Virol.* 84: 757 – 768.
- Brignati, M.J., Loomis, J.S., Wills, J.W. and Courtney, R.J. 2003. Membrane association of VP22, a Herpes Simplex Virus type 1 tegument protein. *J. Virol.* 77: 4888 – 4898.
- Brookes, S.M., Hyatt, A.D. and Eaton, B.T. 1993. Characterization of virus inclusion bodies in bluetongue virus-infected cells. *J. Gen. Virol.* 74: 525 – 530.
- Broquet, A.H., Lenoir, C., Gardet, A., Sapin, C., Chwetzoff, S., Jouniaux, A.M., Lopez, S., Trugnan, G., Bachelet, M. and Thomas, G. 2007. Hsp 70 negatively controls rotavirus protein bioavailability in caco-2 cells infected by the rotavirus RF strain. *J. Virol.* 81: 1297 – 1304.
- Brown, D. and Breton, S. 2000. Sorting proteins to their target membranes. *Kidney International.* 57: 816 – 824.
- Bugarcic, A. and Taylor, J.A. 2006. Rotavirus non-structural glycoprotein NSP4 is secreted from the apical surfaces of polarized epithelial cells. *J Virol.* 80: 12343 – 12349.
- Burrage, T, Trevejo, R., Stone-Marschat, M. and Laegreid, W.W. 1993. Neutralizing epitopes of African horsesickness virus serotype 4 are located on VP2. *Virology.* 196: 799 – 803.
- Burroughs, J.N., O'Hara, R.S., Smale, C.J., Hamblin, C., Walton, A., Armstrong, R. and Mertens, P.P. 1994. Purification and properties of virus particles, infectious subviral particles, cores and VP7 crystals of African horsesickness virus. *J Gen Virol.* 75: 1849 – 1857.
- Caballero, S., Guix, S., Ribes, E., Bosch, A. and Pinto, R.M. 2004. Structural requirements of Astrovirus virus-like particles assembled in insect cells. *J. Virol.* 78: 13285 – 13292.
- Calisher, C.H. and Mertens, P.P. 1998. Taxonomy of African horse sickness viruses. *Arch Virol Suppl.* 14: 3 – 11.
- Carlsson, S.R., Lycksell, P.O. and Fukuda, M. 1993. Assignment of O-glycan attachment sites to the hinge-like regions of human lysosomal membrane proteins lamp-1 and lamp-2. *Arch Biochem Biophys.* 304: 65 – 73.

- Carrasco, L. 1995. Modification of membrane permeability by animal viruses. *Adv. Vir. Res.* 45: 61 – 112.
- Chalfie, M., Tu, Y., Euskirchen, G. Ward, W.W., Prasher, D.C. 1994. Green fluorescent protein as a marker for gene expression. *Science.* 263: 802 – 805.
- Chan, W.K., Au, K.S. and Estes, M.K. 1988. Topography of the simian rotavirus nonstructural glycoprotein (NS28) in the endoplasmic reticulum membrane. *Virology.* 164: 435 – 442.
- Chung, C.T. and Miller, R.H. 1988. A rapid and convenient method for the preparation and storage of competent cells. *N.A.R.* 16: 3580
- Chuma, T, Le Blois, H., Sanchez-Vizcaino, J.M., Diaz-Laviada, M. and Roy, P. 1992. Expression of the major core antigen VP7 of African horsesickness virus by a recombinant baculovirus and its use as a group-specific diagnostic reagent. *J Gen Virol.* 73: 925 – 931.
- Coetzer, J.A.W. and Erasmus, B.J. 1994. African horsesickness virus. In: *Infectious diseases of livestock with special reference to South Africa*. Edited by: J.A.W. Coetzer, G.R. Thomas and R.C. Tustin. Oxford University press. 460 - 475.
- Cowley, J.A. and Gorman, B.M. 1987. Genetic reassortants for identification of the genome segment coding for the bluetongue virus hemagglutinin. *J Virol.* 61: 2304 – 2306.
- Cuadras, M.A. and Greenberg, H.B. 2003. Rotavirus infectious particles use lipid rafts during replication for transport to the cell surface in vitro and in vivo. *Virology.* 313: 308 – 321.
- Cuadras, M.A., Bordier, B.B., Zambrano, J.L., Ludert, J.E. and Greenberg, H.B. 2006. Dissection rotavirus particle-raft interactions with small interfering RNAs: insights into rotavirus transit through the secretory pathway. *J. Virol.* 80: 3935 – 3946.
- Dalbey, R.E., Chen, M., Jiang, F. and Samuelson, J.C. 2000. Understanding the insertion of transporters and other membrane proteins. *Current Opinion in Cell Biology.* 12: 435 – 442.
- Depla, E. 2000. Interaction of viruses with annexins: a potential therapeutic target? *Curr Opin Investig Drugs.* 1: 415 – 420.

- De Waal, P.J. and Huismans, H. 2005. Characterization of the nucleic acid binding activity of inner core protein VP6 of African horsesickness virus. *Arch Virol.* 150: 2037 – 2050.
- Doms, R.W., Lamb, R.A., Rose, J.K. and Helenius, A. 1993. Folding and assembly of viral membrane proteins. *Virology.* 193: 545 – 562.
- Du Plessis, M. and Nel, L.H. 1997. Comparative sequence analysis and expression of the M6 gene, encoding the outer capsid protein VP5, of African horsesickness virus serotype nine. *Virus Res.* 47: 41 – 49.
- Eaton, B.T. and Hyatt, A.D. 1989. Association of bluetongue virus with the cytoskeleton. *Subcell. Biochem.* 15: 229 – 269.
- Eaton, B.T., Hyatt, A.D. and Brookes, S.M. 1990. The replication of bluetongue virus. *Curr. Op. Microbiol. Immunol.* 162: 89 – 118.
- Ehrhardt, D. 2003. GFP technology for live cell imaging. *Current Opinion in Plant Biology.* 6: 622 – 628.
- Els, H.J. 1973. Electron microscopy of bluetongue virus RNA. *Onderstepoort J. Vet. Res.* 40: 73 – 76.
- Estes, M.K. and Cohen, J. 1989. Rotavirus gene structure and function. *Microbiol Rev.* 53: 410 – 449.
- Fernandez-Salas, E., Steward, L.E., Ho, H., Garay, P.E., Sun, S.W., Gilmore, M.A., Ordas, J.V., Wang, J., Francis, J. and Aoki, K.R. 2004. Plasma membrane localisation signals in the light chain of botulinum neurotoxin. *PNAS.* 101: 3208 – 3213.
- Fewell, S.W., Travers, K.J., Weissman, J.S. and Brodsky, J.L. 2001. The action of molecular chaperones in the early secretory pathway. *Annu. Rev. Genet.* 35: 149 – 191.
- French, T.J., Marshall, J.J. and Roy, P. 1990. Assembly of double-shelled, viruslike particles of bluetongue virus by the simultaneous expression of four structural proteins. *J Virology.* 64: 5695 – 5700.

- French, T.J. and Roy, P. 1990. Synthesis of bluetongue virus (BTV) core-like particles by a recombinant baculovirus expressing the two major structural core proteins of BTV. *J Virol.* 64: 1530 – 1536.
- Garoff, H. 1985. Using recombinant DNA techniques to study protein targeting in eukaryotic cells. *Ann. Rev. Cell. Biol.* 1: 403 – 450.
- Ghosh, M.K., Deriaud, E., Saron, M, Lo-Man, R, Henry, T., Jiao, X., Roy, P. and Leclerc, C. 2002. Induction of protective antiviral cytotoxic T cells by a tubular structure capable of carrying large foreign sequences. *Vaccine.* 20: 1369 – 1377.
- Goepfert, P.A., Wang, G. and Mulligan, M.J. 1995. Identification of an ER retrieval signal in a retroviral glycoprotein. *Cell.* 82: 543 – 544.
- Gonzalez, R.A., Espinosa, R., Romero, P., Lopez, S. and Arias, C.F. 2000. Relative localisation of viroplasmic and endoplasmic reticulum-resident rotavirus proteins in infected cells. *Arch Virol.* 145: 1963 – 1973.
- Gonzalez, M.E. and Carrasco, L. 2003. Viroporins. *FEBS Letters.* 552: 28 – 34.
- Gosselin-Grenet, A.S., Mottet-Osman, G. and Roux, L. 2006. From assembly to virus particle budding, pertinence of the detergent resistant membranes. *Virology.* 344: 296 – 303.
- Graff, J.W., Ewen, J., Ettayebi, K. and Hardy, M.E. 2007. Zinc-binding domain of rotavirus NSP1 is required for proteasome-dependent degradation of IRF3 and autoregulatory NSP1 stability. *J. Gen. Virol.* 88: 613 – 620.
- Greenberg, M., De Tulleo, L., Rapoport, I., Skowronski, J and Kirchhausen, T. 1998. A dileucine motif in HIV-1 Nef is essential for sorting into clathrin-coated pits and for downregulation of CD4. *Curr Biol.* 8: 1239 – 1242.
- Grubman, M.J. and Lewis, S.A. 1992. Identification and characterization of the structural and nonstructural proteins of African horsesickness virus and determination of the genome coding assignments. *Virology.* 186: 444 – 451.

- Hack, N.J., Billups, B., Guthrie, P.B., Rogers, J.H., Muir, E.M., Parks, T.N. and Kater, S.B. 2000. Green fluorescent protein as a quantitative tool. *Journal of Neuroscience Methods*. 95: 177 – 184.
- Han, Z. and Harty, R.N. 2004. The NS3 protein of bluetongue virus exhibits viroporin-like properties. *J. Biol. Chem.* 279: 43092 – 43097.
- Hassan, S.S. and Roy, P. 1999. Expression and functional characterization of bluetongue virus VP2 protein: role in cell entry. *J Virol.* 73: 9832 – 9842.
- Hassan, S.H., Wirblich, C., Forzan, M. and Roy, P. 2001. Expression and functional characterization of bluetongue virus VP5 protein: role in cellular permeabilization. *J Virol.* 75: 8356 – 8367.
- Hegde, R.S. and Lingappa, V.R. 1997. Membrane protein biogenesis: regulated complexity at the endoplasmic reticulum. *Cell.* 91: 575 – 582.
- Helms, J.B. and Zurzolo, C. 2004. Lipids as targeting signals: lipid rafts and intracellular trafficking. *Traffic.* 5: 247 – 254.
- Hewat, E.A., Booth, T.F. and Roy, P. 1992a. Structure of bluetongue virus particles by cryoelectron microscopy. *J. Struct. Biol.* 109: 61 – 69.
- Hewat, E.A., Booth, T.F., Loudon, P.T. and Roy, P. 1992b. Three-dimensional reconstruction of bluetongue virus core-like particles by cryo-electron microscopy. *Virology.* 189: 10 – 20.
- House, J.A. 1993. African horse sickness. *Vet Clin North Am Equine Pract.* 9: 355 – 364.
- Howell, P.G. 1962. The isolation and identification of further antigenic types of African horse sickness virus. *Onderstepoort J. Vet. Res.* 29: 139 – 149.
- Howell, P.G. African horse sickness, in: Emerging diseases of animals, FAO, Rome FAO Agricultural studies. 61: 71 – 108.
- Huismans, H. and Els, H.J. 1979. Characterization of the tubules associated with the replication of three different orbiviruses. *Virology.* 92: 397 – 406.

- Huismans, H. and Erasmus, B.J. 1981. Identification of the serotype-specific and group-specific antigens of bluetongue virus. *Onderstepoort J. Vet. Res.* 48: 51 – 58.
- Huismans, H., Van Dijk, A.A and Els, J.H. 1987. Uncoating of parental bluetongue virus to core and subcore particles in infected L cells. *Virology.* 157: 180 – 188.
- Hyatt, A.D., Zhao, Y. and Roy, P. 1993. Release of virus-like particles from insect cells is mediated by BTV nonstructural protein NS3/NS3A. *Virology.* 193: 592 – 603.
- Jayaram, H., Estes, M.K. and Prasad, B.V.V. 2004. Emerging themes in rotavirus cell entry, genome organization, transcription and replication. *Virus Res.* 101: 67 – 81.
- Kahsay, R.Y., Gao, G., Liao, L. 2005. An improved Markov model for transmembrane protein detection and topology prediction and its application to complete genomes. *Bioinformatics.* 21: 1853 – 1858.
- Kar, A.K. and Roy, P. 2003. Defining the structure-function relationships of bluetongue virus helicase protein VP6. *J Virol.* 77: 11347 – 11356.
- Kar, A.K., Ghosh, M. and Roy, P. 2004. Mapping the assembly of Bluetongue virus scaffolding protein VP3. *Virology.* 324: 387 – 399.
- Katzmann, D.J., Babst, M. and Emr, S.D. 2001. Ubiquitin-dependent sorting into the multivesicular body pathway requires the function of a conserved endosomal protein sorting complex, ESCRT-I. *Cell.* 106: 145 – 155.
- Kawar, Z. and Jarvis, D.L. 2001. Biosynthesis and subcellular localisation of a lepidopteran insect alpha 1,2-mannosidase. *Insect Biochemistry and Molecular Biology.* 31: 289 - 297.
- Kirkwood, C.D. and Palombo, E.A. 1997. Genetic characterization of the rotavirus non-structural protein, NSP4. *Virology.* 236: 258 – 265.
- Klausner, R.D., Donaldson, J.G. and Lippincott-Schwartz, J. 1992. Brefeldin A: Insights into the control of membrane traffic and organelle structure. *J. Cell. Biol.* 116: 1071 – 1080.

- Kundu, A., Avalos, R.T., Sanderson, C.M. and Nayak, D.P. 1996. Transmembrane domain of influenza virus neuraminidase, type II protein, possesses an apical sorting signal in polarized MDCK cells. *J Virol.* 70: 6508 – 6515.
- Le Blois, H., French, T., Mertens, P.P., Burroughs, J.N. and Roy, P. 1992. The expressed VP4 protein of bluetongue virus binds GTP and is the candidate guanylyl transferase of the virus. *Virology.* 189: 757 – 761.
- Levy, J.A., Fraenkel-Conrat, H. and Owens, R.A. 1994. *Virology.* 3rd edition. Prentice Hall Inc., New Jersey, USA.
- Lin, S.L. and Tian, P. 2003. Detailed computational analysis of a comprehensive set of group A rotavirus NSP4 proteins. *Virus Genes.* 26: 271 – 282.
- Lindwasser, O.W. and Resh, M.D. 2001. Multimerization of Human Immunodeficiency Virus type 1 Gag promotes its localisation to barges, raft-like membrane microdomains. *J. Virol.* 75: 7913 – 7924.
- Lippincott-Schwartz, J. and Smith, C.L. 1997. Insights into secretory and endocytic membrane traffic using green fluorescent protein chimeras. *Current Opinion in Neurobiology* 7: 631 – 639.
- Lippincott-Schwartz, J., Presley, J.F., Zaal, K.J.M., Hirschberg, K., Miller, C. and Ellenberg, J. 1999. Monitoring the dynamics and mobility of membrane proteins tagged with green fluorescent protein. In: *Green Fluorescent proteins.* Edited by: K.F. Sullivan and S.A. Kay. Academic press. 261 - 285.
- Lodish, H., Berk, A., Matsudaira, P., Kaiser, C.A., Krieger, M., Scott, M.P., Zipursky, S.L. and Darnell, J. 2004. *Molecular Cell Biology.* W H Freeman and Company. New York. Pg 657 – 777.
- Lopez, S. and Arias, C.F. 2004. Multistep entry of rotavirus into cells: a Versaillesque dance. *TRENDS in Microbiology.* 12: 271 – 278.
- Lopez, T., Camacho, M., Zayas, M., Najera, R., Sanchez, R., Arias, C.F. and Lopez, S. 2005. Silencing the morphogenesis of rotavirus. *J. Virol.* 79: 184 – 192.

- Loudon, P.T. and Roy, P. 1991. Assembly of five bluetongue virus proteins expressed by recombinant baculoviruses: Inclusion of the largest protein VP1 in the core and virus-like particles. *Virology*. 180: 798 – 802.
- Lubroth, J. 1988. African horse sickness and the epizootic in Spain 1987. *Equine Pract.* 10: 26 – 33.
- Luckow, V.A. and Summers, M.D. 1988. Signals important for high-level expression of foreign genes in *Autographa californica* nuclear polyhedrosis virus expression vectors. *Virology*. 167: 56 – 71.
- Lymperopoulos, K., Wirblich, C., Brierley, I. And Roy, P. 2003. Sequence specificity in the interaction of bluetongue virus nonstructural protein 2 (NS2) with viral RNA. *J Biol Chem*. 278: 31722 – 31730.
- Lymperopoulos, K., Noad, R., Tosi, S., Nethisinghe, S, Brierley, I. and Roy, P. 2006. Specific binding of bluetongue virus NS2 to different viral plus-strand RNAs. *Virology. In press*.
- Maree, F.F. and Huismans, H. 1997. Characterization of tubular structures composed of non-structural protein NS1 of African horsesickness virus expressed in insect cells. *J. Gen. Virol.* 78: 1077 – 1082.
- Maree, S., Durbach, S. and Huismans, H. 1998. Intracellular production of African horsesickness virus core-like particles by expression of the two major core proteins, VP3 and VP7, in insect cells. *J. Gen. Virol.* 79: 333 – 337.
- Martin, L., Meyer, A.J., O'Hara, R.S., Fu, H., Mellor, P.S., Knowles, N.J. and Mertens, P. 1998. Phylogenetic analysis of African horse sickness virus segment 10: sequence variation, virulence characteristics and cell exit. *Arch Virol.* 14: 281 – 293.
- Martinez-Torrecuadrada, J.L. and Casal, J.I. 1995. Identification of a linear neutralization domain in the protein VP2 of African horse sickness virus. *Virology*. 210: 391 – 399.
- Martinez-Torrecuadrada, J.L., Diaz-Laviada, M., Roy, P., Sanchez, C., Vela, C., Sanchez-Vizcaino, J.M. and Casal, J.I. 1997. Serologic markers in early stages of African horse sickness virus infection. *J. Clin. Microbiol.* 35: 531 – 535.

- Martinez-Torrecuadrada, J.L., Langeveld, J.P.M., Venteo, A., Sanz, A., Dalsgaard, K., Hamilton, W.D.O., Meloen, R.H. and Casal, J.I. 1999. Antigenic profile of African horse sickness virus serotype 4 VP5 and identification of a neutralizing epitope shared with bluetongue virus and epizootic hemorrhagic disease virus. *Virology*. 257: 449 – 459.
- Matsumoto, T., Takahashi, H. and Fujiwara, H. 2004. Targeted nuclear import of open reading frame 1 protein is required for in vivo retrotransposition of a telomere-specific non-long terminal repeat retrotransposon, SART1. *Molecular and Cellular Biology*. 24: 105 – 122.
- Maurer, F.D. and McCully, R.M. 1963. African horse sickness with emphasis on pathology. *Am. J. Vet. Res.* 26: 235 – 266.
- Meiswinkel, R. 1998. The 1996 outbreak of African horse sickness in South Africa – the entomological perspective. *Arch Virol. Suppl.* 14: 69 – 83.
- Meiswinkel, R. and Paweska, J.T. 2003. Evidence for a new field *Culicoides* vector of African horsesickness in South Africa. *Preventative Veterinary Medicine*. 60: 243 – 253.
- Mellor, P.S. 1993. African horse sickness: transmission and epidemiology. *Vet Res.* 24: 199 – 212.
- Mellor, P.S. 1994. Epizootiology and vectors of African horse sickness virus. *Comp Immunol. Microbiol. Infect. Dis.* 17: 287 – 296.
- Mellor, P.S. and Boorman, J. 1995. The transmission and geographical spread of African horse sickness and bluetongue viruses. *Ann Trop Med Parasitol.* 89: 1 – 15.
- Mellor, P.S. and Hamblin, C. 2004. African horse sickness. *Vet Res.* 35: 445 – 466.
- Mertens, P. 2004. The dsRNA viruses. *Virus Res.* 101: 3 – 13.
- Mertens, P.P.C. and Diprose, J. 2004. The bluetongue virus core: a nano-scale transcription machine. *Virus Res.* 101: 29 – 43.
- Mindich, L. 1988. Bacteriophage phi 6: a unique virus having a lipid-containing membrane and a genome composed of three dsRNA segments. *Adv. Virus Res.* 35: 137 – 176.

- Mirazimi, A., Nilsson, M and Svensson, L. 1998. The molecular chaperone calnexin interacts with the NSP4 enterotoxin of rotavirus in vivo and in vitro. *J Virol.* 72: 8705 – 8709.
- Mirazimi, A., Magnusson, K.E. and Svensson, L. 2003. A cytoplasmic region of the NSP4 enterotoxin of rotavirus is involved in retention in the endoplasmic reticulum. *J. Gen. Virol.* 84: 875 – 883.
- Mirchamsy, H. and Taslimi, H. 1964. Immunisation against African horse sickness with tissue-culture-adapted neurotropic viruses. *Br. Vet. J.* 120: 481 – 486.
- Miyawaki, A., Sawano, A. and Kogure, T. 2003. Lighting up cells: labelling proteins with fluorophores. *Supplement of Nature Cell Biology.* 5: S1 – S7.
- Modrof, J., Lymeropoulos, K. and Roy, P. 2005. Phosphorylation of Bluetongue virus nonstructural protein 2 is essential for formation of viral inclusion bodies. *J. Virol.* 79: 10023 – 10031.
- Mohan, K.V., Som, I. and Atreya, C.D. 2002. Identification of a type 1 peroxisomal targeting signal in a viral protein and demonstration of its targeting to the organelle. *J. Virol.* 76: 2543 – 2547.
- Mohan, K.V.K., Muller, J. and Atreya, C.D. 2003. The N- and C-Terminal regions of rotavirus NSP5 are critical determinants for the formation of viroplasm-like structures independent of NSP2. *J Virol.* 77: 12184 – 12192.
- Monastyrskaya, K., Staeuber, N. Sutton, G. and Roy, P. 1997. Effects of domain-switching and site-directed mutagenesis on the properties and functions of the VP7 proteins of two Orbiviruses. *Virology.* 237: 217 – 227.
- Mortola, E., Noad, R. and Roy, P. 2004. Bluetongue virus outer capsid proteins are sufficient to trigger apoptosis in mammalian cells. *J Virol.* 78: 2875 – 2883.
- Moule, L. 1896. Histoire de la Medecine Veterinaire, Maulde, Paris. P 38.
- Newton, K., Meyer, J.C., Bellamy, R. and Taylor, J.A. 1997. Rotavirus non-structural glycoprotein NSP4 alters plasma membrane permeability in mammalian cells. *J Virol.* 71: 9458 – 9465.

- Nishimura, N. and Balch, W.E. 1997. A di-acidic signal required for selective export from the endoplasmic reticulum. *Science*. 277: 556 – 558.
- Owens, R.J., Limn, C. and Roy, P. 2004. Role of an arbovirus non-structural protein in cellular pathogenesis and virus release. *J Virol*. 78: 6649 – 6656.
- Parr, R.D., Storey, S.M., Mitchell, D.M., McIntosh, A.L., Zhou, M., Mir, K.D. and Ball, J.M. 2006. The rotavirus enterotoxin NSP4 directly interacts with the caveolar structural protein caveolin-1. *J. Virol*. 80: 2842 – 2854.
- Pina-Vazquez, C., De Nova-Ocampo, M., Guzman-Leon, S. and Padilla-Noriega, L. 2007. Post-translational regulation of rotavirus protein NSP1 expression in mammalian cells. *Arch Virol*. 152: 345 – 368.
- Pinto, L.H., Holsinger, L.J. and Lamb, R.A. 1992. Influenza virus M2 protein has ion channel activity. *Cell*. 69: 517 – 528.
- Ramadevi, N., Burroughs, N.J., Mertens, P.P., Jones, I.M. and Roy, P. 1998. Capping and methylation of mRNA by purified recombinant VP4 protein of bluetongue virus. *Proc. Natl. Acad. Sci. USA*. 95: 13537 – 13542.
- Raynor, C.M., Wright, J.F., Waisman, D.M. and Prydzial, E.L. 1999. Annexin II enhances cytomegalovirus binding and fusion to phospholipid membranes. *Biochemistry*. 38: 5089 – 5095.
- Rieder, C.L. and Khodjakov, A. 2003. Mitosis through the microscope: advances in seeing inside live dividing cells. *Science*. 300: 91 – 96.
- Roy, P., Fukusho, A., Ritter, G.D. and Lyon, D. 1988. Evidence for genetic relationship between RNA and DNA viruses from the sequence homology of a putative polymerase gene of bluetongue virus with that of vaccinia virus; conservation of RNA polymerase genes from diverse species. *Nucl. Acids Res*. 16: 11759 – 11767.
- Roy, P., Hirasawa, T., Fernandez, M., Blinov, V.M. and Sanchez-Vixcain Rodrique, J.M. 1991. The complete sequence of the group-specific antigen, VP7, of African horsesickness disease virus serotype 4 reveals a close relationship to bluetongue virus. *J Gen Virol*. 72: 1237 – 1241.

- Roy, P., Mertens, P.P. and Casal, I. 1994. African horsesickness virus structure. *Comp. Immune. Microbial. Infect.* 17: 243 – 273.
- Roy, P. 1996. Orbivirus structure and assembly. *Virology.* 216: 1 – 11.
- Roy, P. 2001. Orbiviruses. In: *Fields Virology*. Edited by: B.N. Fields, D.N. Knipe, P.M. Howley and D.E. Griffin. Philadelphia publisher. 1835 – 1865.
- Sanderson, C.M., McQueen, N.L. and Nayak, D.P. 1993. Sendai virus assembly: M protein binds to viral glycoproteins in transit through the secretory pathway. *J Virol.* 67: 651 – 663.
- Sambrook, J. and Russell, D.W. 2001. *Molecular Cloning, a laboratory manual*. Third edition. Cold Spring harbor Laboratory Press.
- Sapin, C., Colard, O., Delmas, O., Tessier, C., Breton, M., Enouf, V., Chwetzo, S., Ouanich, J., Cohen, J., Wolf, C. and Trugnan, G. 2002. Rafts promote assembly and atypical targeting of a nonenveloped virus, rotavirus, in Caco-2 cells. *J Virol.* 76: 4591 – 4602.
- Scheiffele, P., Rietveld, A., Wilk, T. and Simons, K. 1999. Influenza viruses select ordered lipid domains during budding from the plasma membrane. *J Biol Chem.* 274: 2038 – 2044.
- Schrag, J.D., Procopio, D.O., Cygler, M., Thomas, D.Y. and Bergeron, J.J.M. 2003. Lectin control of protein folding and sorting in the secretory pathway. *TIBS.* 28: 49 – 57.
- Shi, S.T., Polyak, S.J., Tu, H., Taylor, D.R., Gretch, D.R. and Lai, M.M.C. 2002. Hepatitis C virus NS5A colocalises with the core protein on lipid droplets and interacts with apolipoproteins. *Virology.* 292: 198 – 210.
- Silvestri, L.S. Tortorici, M.A., Carpio, R.V. and Patton, J.T. 2005. Rotavirus glycoprotein NSP4 is a modulator of viral transcription in the infected cell. *J. Virol.* 79: 15165 – 15174.
- Simons, K. and Ikonen, E. 1997. Functional rafts in cell membranes. *Nature.* 387: 569 – 572.
- Slimane, T.A. and Hoekstra, D. 2002. Sphingolipid trafficking and protein sorting in epithelial cells. *FEBS Letters.* 529: 54 – 59.

Smit, C.C. 1999. MSc. Thesis. Department of Genetics. University of Pretoria.

Stauber, N., Martinez-Costas, J., Sutton, G., Monastyrskaya, K. and Roy, P. 1997. Bluetongue virus VP6 protein binds ATP and exhibits RNA-dependent ATPase function and a helicase activity that catalyse the unwinding of double-stranded RNA substrates. *J Virol.* 71: 7220 – 7226.

Stoltz, M.A., Van der Merwe, C.F., Coetzee, J. and Huismans, H. 1996. Subcellular localisation of the non-structural protein NS3 of African horsesickness virus. *Onderstepoort. J. Vet. Res.* 63: 57 – 61.

Stone-Marschat, M.A., Moss, S.R., Burrage, T.G., Barber, M.L., Roy, P. and Laegeid, W.W. 1996. Immunization with VP2 is sufficient for protection against lethal challenge with African horsesickness virus Type 4. *Virology.* 220: 219 – 222.

Tan, B.H., Nason, E., Stauber, N., Jiang, W., Monastyrskaya, K. and Roy, P. 2001. RGD tripeptide of bluetongue virus VP7 protein is responsible for core attachment to *Culicoides* cells. *J Virol.* 75: 3937 – 3947.

Tanaka, S., Mikhailov, M. and Roy, P. 1995. Synthesis of bluetongue virus chimeric VP3 molecules and their interactions with VP7 protein to assemble into virus core-like particles. *Virology.* 214: 593 – 601.

Taraporewala, Z.F., Chen, D. and Patton, J.T. 2001. Multimers of Bluetongue virus non-structural protein, NS2, possesses nucleotidyl phosphatase activity: similarities between NS2 and rotavirus NSP2. *Virology.* 280: 221 – 231.

Taylor, J.A., Meyer, J.C., Legge, M.A., O'Brien, J.A., Street, J.E., Lord, V.J., Bergmann, C.C. and Bellamy, A.R. 1992. Transient expression and mutational analysis of the rotavirus intracellular receptor: the c-terminal methionine residue is essential for ligand binding. *J Virol.* 66: 3566 – 3572.

Taylor, J.A. O'Brien, J.A. and Yeager, M. 1996. The cytoplasmic tail of NSP4, the endoplasmic reticulum-localised non-structural glycoprotein of rotavirus, contains distinct virus binding and coiled coil domains. *The EMBO Journal.* 15: 4469 – 4476.

- Theiler, A. 1921. African horsesickness. Science Bulletin no. 19, Department of Agriculture. S.A. Pretoria.
- Thomas, C.P., Booth, T.F. and Roy, P. 1990. Synthesis of bluetongue viral-coded phosphoprotein and formation of inclusion bodies by recombinant baculoviruses in insect cells: It binds the single-stranded RNA species. *J. Gen. Virol.* 71: 2073 – 2083.
- Tian, P., Hu, Y., Schilling, W.P., Lindsay, D.A., Eiden, J. and Estes, M.K. 1994. The non-structural glycoprotein of rotavirus affects intracellular calcium levels. *J Virol.* 68: 251 – 257.
- Van der Meyden, C.H., Erasmus, B.J., Swanepoel, R. and Prozesky, O.W. 1992. Encephalitis and chorioretinitis associated with neurotropic African horsesickness virus infection in laboratory workers. Part I. Clinical and neurological observations. *S Afr Med J.* 81: 451 – 454.
- Van Niekerk, M., Smit, C., Fick, W.C., van Staden, V. and Huismans, H. 2001a. Membrane association of African horsesickness virus nonstructural protein NS3 determines its cytotoxicity. *Virology.* 279: 499 – 508.
- Van Niekerk, M., Van Staden, V., Van Dijk, A.A. and Huismans, H. 2001b. Variation of African horsesickness virus non-structural protein NS3 in southern Africa. *J. Gen. Virol.* 82: 149 – 158.
- Van Niekerk, M. 2001c. PhD. Thesis. Department of Genetics. University of Pretoria.
- Van Niekerk, M., Freeman, M., Paweska, J.T., Howell, P.G., Guthrie, A.J., Potgieter, A.C., van Staden, V. and Huismans, H. 2003. Variation in the NS3 gene and protein in South African isolates of bluetongue and equine encephalosis viruses. *J. Gen. Virol.* 84; 581 – 590.
- Van Staden, V. and Huismans, H. 1991. A comparison of the genes which encode non-structural protein NS3 of different Orbiviruses. *J. Gen. Virol.* 72: 1073 – 1079.
- Van Staden, V., Theron, J., Greyling, B.J., Huismans, H. and Nel, L.H. 1991. A comparison of cognate NS2 genes of three different orbiviruses. *Virology.* 185: 500 – 504.
- Van Staden, V. 1993. PhD. Thesis. Department of Genetics. University of Pretoria.

- Van Staden, V., Stoltz, M.A. and Huismans, H. 1995. Expression of non-structural protein NS3 of African horsesickness virus (AHSV): evidence for a cytotoxic effect of NS3 in insect cells, and characterization of the gene products in AHSV infected Vero cells. *Arch. Virol.* 140: 289 – 306.
- Van Staden, V., Smit, C.C., Stoltz, M.A., Maree, F.F. and Huismans, H. 1998. Characterization of two African horse sickness virus non-structural proteins, NS1 and NS3. *Arch Virol Suppl.* 14: 251 – 258.
- Vennema, H., Heijnen, L., Rottier, P.J., Horzinek, M.C. and Spaan, W.J. 1993. A novel glycoprotein of feline infectious peritonitis coronavirus contains a KDEL-like endoplasmic reticulum retention signal. *Adv Exp Med Biol.* 342: 209 – 214.
- Verwoerd, D.W., Els, H.J., De Villiers, E.M. and Huismans, H. 1972. Structure of the bluetongue virus capsid. *J Virol.* 10: 783 – 794.
- Verwoerd, D.W. and Huismans, H. 1972. Studies on the *in vitro* and *in vivo* transcription of the bluetongue virus genome. *Onderstepoort J. Vet. Res.* 39: 185 – 192.
- Verwoerd, D.W. and Erasmus, B.J. 1994. Bluetongue. In: *Infectious diseases of livestock with special reference to South Africa*. Edited by: J.A.W. Coetzer, G.R. Thomas and R.C. Tustin. Oxford University press. 460 - 475.
- Vogt, V.M. 2000. Ubiquitin in retrovirus assembly: actor or bystander? *PNAS.* 97: 12945 – 12947.
- Wade-Evans, A.M., Pullen, L., Hamblin, C., O'Hara, R., Burroughs, J.N. and Mertens, P.P.C. 1997. African horsesickness virus VP7 sub-unit vaccine protects mice against a lethal, heterologous serotype challenge. *J. Gen. Virol.* 78: 1611 – 1616.
- Waisman, D.M. 1995. Annexin II tetramer: structure and function. *Mol Cell Biochem.* 149 – 150: 301 – 322.
- Walter, P. and Lingappa, V.R. 1986. Mechanism of protein translocation across the endoplasmic reticulum membrane. *Annu. Rev. Cell. Biol.* 2: 499 – 516.
- Wetzel, H., Nevill, E.M. and Erasmus, B.J. 1970. Studies on the transmission of African horse sickness. *Onderstepoort J. Vet. Res.* 37: 165 – 168.

- Wirblich, C., Bhattacharya, B. and Roy, P. 2006. Nonstructural protein 3 of Bluetongue virus assists virus release by recruiting ESCRT-I protein Tsg101. *J. Virol.* 80: 460 – 473.
- Wu, W., Chen, S.Y., Iwata, H., Compans, R.W. and Roy, P. 1992. Multiple glycoproteins synthesized by the smallest RNA segment (S10) of bluetongue virus. *J Virol.* 66: 7104 – 7112.
- Xu, G., Wilson, W., Mecham, J., Murphy, K., Zhou, E.M. and Tabachnick, W. 1997. VP7: an attachment protein of bluetongue virus for cellular receptors in *Culicoides variipennis*. *J. Gen. Virol.* 78: 1617 – 1623.
- Yeagle, P.L. 1987. The membranes of cells. Academic Press. Pg 166 – 180.
- Zamyatnin, A.A., Solovyev, A.G., Sablina, A.A., Agranovsky, A.A., Vetten, H.J., Schiemann, J., Hinkkanen, A.E., Lehto, K. and Morozov, S.Y. 2002. Dual-colour imaging of membrane protein targeting directed poa semilatent virus movement protein TGBp3 in plant and mammalian cells. *J. Gen. Virol.* 83: 651 – 662.
- Zhang, M., Zeng, C.Q., Dong, Y., Ball, J.M., Saif, L.J., Morris, A.P. and Estes, M.K. 1998. Mutations in rotavirus non-structural glycoprotein NSP4 are associated with altered virus virulence. *J Virol.* 72: 3666 – 3672.
- Zhao, Y., Thomas, C., Bremer, C. and Roy, P. 1994. Deletion and mutational analysis of bluetongue virus NS2 protein indicate that the amino but not the carboxy terminus of the protein is critical for RNA-protein interactions. *J Virol.* 68: 2179 – 2185.



Appendix 1

A. Nucleotide sequence alignments of the seven fusion proteins constructed for this project. The mutation present at bp 444 of the coding region of NS3 as well as the mutations present in the hydrophobic domains of the mutants HD1-eGFP and HD2-eGFP are highlighted. Bp 444 listed here corresponds to bp 462 mentioned elsewhere, as sequences here start at the first ATG (actually bp 20), not at the first nucleotide of the noncoding region (bp 1).

	
		10	20	30	40	50
AHSV3 NS3 eGFP	ATGAGTCTAG	CTACGATCGC	CGGAAAATTA	TATGATGCAT	AATGGAGATC	
NS3-eGFP	ATGAGTCTAG	CTACGATCGC	CGGAAAATTA	TATGATGCAT	AATGGAGATC	
NS3A-eGFP	ATGAGTCTAG	CTACGATCGC	CGGAAAATTA	-ATGATGCAT	AATGGAGATC	
N11-eGFP	ATGAGTCTAG	CTACGATCGC	CGGAAAATTA	TATG	-----	
NS3ΔC-eGFP	ATGAGTCTAG	CTACGATCGC	CGGAAAATTA	TATGATGCAT	AATGGAGATC	
HD1-eGFP	ATGAGTCTAG	CTACGATCGC	CGGAAAATTA	TATGATGCAT	AATGGAGATC	
HD2-eGFP	ATGAGTCTAG	CTACGATCGC	CGGAAAATTA	TATGATGCAT	AATGGAGATC	
	NS3 start codon			NS3A start codon		
	
		60	70	80	90	100
AHSV3 NS3 eGFP	AGAGAGCAAT	TGTGCCTTAT	GCGCCGTCCC	CTTATGCGTA	TGCAAATGCT	
NS3-eGFP	AGAGAGCAAT	TGTGCCTTAT	GCGCCGTCCC	CTTATGCGTA	TGCAAATGCT	
NS3A-eGFP	AGAGAGCAAT	TGTGCCTTAT	GCGCCGTCCC	CTTATGCGTA	TGCAAATGCT	
N11-eGFP	-----	-----	-----	-----	-----	
NS3ΔC-eGFP	AGAGAGCAAT	TGTGCCTTAT	GCGCCGTCCC	CTTATGCGTA	TGCAAATGCT	
HD1-eGFP	AGAGAGCAAT	TGTGCCTTAT	GCGCCGTCCC	CTTATGCGTA	TGCAAATGCT	
HD2-eGFP	AGAGAGCAAT	TGTGCCTTAT	GCGCCGTCCC	CTTATGCGTA	TGCAAATGCT	
	
		110	120	130	140	150
AHSV3 NS3 eGFP	CCGACGCTTG	GTGGTCAAGC	GGGTGAAATG	GAGTCCATGT	CGCTTGGGAT	
NS3-eGFP	CCGACGCTTG	GTGGTCAAGC	GGGTGAAATG	GAGTCCATGT	CGCTTGGGAT	
NS3A-eGFP	CCGACGCTTG	GTGGTCAAGC	GGGTGAAATG	GAGTCCATGT	CGCTTGGGAT	
N11-eGFP	-----	-----	-----	-----	-----	
NS3ΔC-eGFP	CCGACGCTTG	GTGGTCAAGC	GGGTGAAATG	GAGTCCATGT	CGCTTGGGAT	
HD1-eGFP	CCGACGCTTG	GTGGTCAAGC	GGGTGAAATG	GAGTCCATGT	CGCTTGGGAT	
HD2-eGFP	CCGACGCTTG	GTGGTCAAGC	GGGTGAAATG	GAGTCCATGT	CGCTTGGGAT	
	
		160	170	180	190	200
AHSV3 NS3 eGFP	ACTTAATCAA	GCCATGTCAA	GTACAAC TGG	TGCAAGTCGG	GCTCTTAAGG	
NS3-eGFP	ACTTAATCAA	GCCATGTCAA	GTACAAC TGG	TGCAAGTCGG	GCTCTTAAGG	
NS3A-eGFP	ACTTAATCAA	GCCATGTCAA	GTACAAC TGG	TGCAAGTCGG	GCTCTTAAGG	
N11-eGFP	-----	-----	-----	-----	-----	
NS3ΔC-eGFP	ACTTAATCAA	GCCATGTCAA	GTACAAC TGG	TGCAAGTCGG	GCTCTTAAGG	
HD1-eGFP	ACTTAATCAA	GCCATGTCAA	GTACAAC TGG	TGCAAGTCGG	GCTCTTAAGG	
HD2-eGFP	ACTTAATCAA	GCCATGTCAA	GTACAAC TGG	TGCAAGTCGG	GCTCTTAAGG	



```

.....|.....| .....|.....| .....|.....| .....|.....| .....|.....|
          210          220          230          240          250
AHSV3 NS3 ATGAAAAAGC AGCGTTTGGT GCGATGGCGG AAGCATTACG TGATCCAGAA
eGFP -----
NS3-eGFP ATGAAAAAGC AGCGTTTGGT GCGATGGCGG AAGCATTACG TGATCCAGAA
NS3A-eGFP ATGAAAAAGC AGCGTTTGGT GCGATGGCGG AAGCATTACG TGATCCAGAA
N11-eGFP -----
NS3ΔC-eGFP ATGAAAAAGC AGCGTTTGGT GCGATGGCGG AAGCATTACG TGATCCAGAA
HD1-eGFP ATGAAAAAGC AGCGTTTGGT GCGATGGCGG AAGCATTACG TGATCCAGAA
HD2-eGFP ATGAAAAAGC AGCGTTTGGT GCGATGGCGG AAGCATTACG TGATCCAGAA

```

```

.....|.....| .....|.....| .....|.....| .....|.....| .....|.....|
          260          270          280          290          300
AHSV3 NS3 CCGATACGTC AAATAAAGAA ACATGTTGGA TTAAGAACGC TCAAGCATTT
eGFP -----
NS3-eGFP CCGATACGTC AAATAAAGAA ACATGTTGGA TTAAGAACGC TCAAGCATTT
NS3A-eGFP CCGATACGTC AAATAAAGAA ACATGTTGGA TTAAGAACGC TCAAGCATTT
N11-eGFP -----
NS3ΔC-eGFP CCGATACGTC AAATAAAGAA ACATGTTGGA TTAAGAACGC TCAAGCATTT
HD1-eGFP CCGATACGTC AAATAAAGAA ACATGTTGGA TTAAGAACGC TCAAGCATTT
HD2-eGFP CCGATACGTC AAATAAAGAA ACATGTTGGA TTAAGAACGC TCAAGCATTT

```

```

.....|.....| .....|.....| .....|.....| .....|.....| .....|.....|
          310          320          330          340          350
AHSV3 NS3 AAAGATAGAG TTGGCGTCAA TGAGACGTAG GTATGCGATA CTACGTGTAG
eGFP -----
NS3-eGFP AAAGATAGAG TTGGCGTCAA TGAGACGTAG GTATGCGATA CTACGTGTAG
NS3A-eGFP AAAGATAGAG TTGGCGTCAA TGAGACGTAG GTATGCGATA CTACGTGTAG
N11-eGFP -----
NS3ΔC-eGFP AAAGATAGAG TTGGCGTCAA TGAGACGTAG GTATGCGATA CTACGTGTAG
HD1-eGFP AAAGATAGAG TTGGCGTCAA TGAGACGTAG GTATGCGATA CTACGTGTAG
HD2-eGFP AAAGATAGAG TTGGCGTCAA TGAGACGTAG GTATGCGATA CTACGTGTAG

```

```

.....|.....| .....|.....| .....|.....| .....|.....| .....|.....|
          360          370          380          390          400
AHSV3 NS3 TGATCTTTAT GAGCGGGTGC GTAACGATGG CTACCTCGAT GGCGGGGGGG
eGFP -----
NS3-eGFP TGATCTTTAT GAGCGGGTGC GTAACGATGG CTACCTCGAT GGCGGGGGGG
NS3A-eGFP TGATCTTTAT GAGCGGGTGC GTAACGATGG CTACCTCGAT GGCGGGGGGG
N11-eGFP -----
NS3ΔC-eGFP TGATCTTTAT GAGCGGGTGC GTAACGATGG CTACCTCGAT GGCGGGGGGG
HD1-eGFP TGATCTTTAT GAGCGGGTGC CGTACGAGGG ATAAGTCGAT GGCGGGGGGG
HD2-eGFP TGATCTTTAT GAGCGGGTGC GTAACGATGG CTACCTCGAT GGCGGGGGGG

```

HD1 mutations

```

.....|.....| .....|.....| .....|.....| .....|.....| .....|.....|
          410          420          430          440          450
AHSV3 NS3 TTAACGATTA TTGATAATGA AATATATGAA GACCTTAGTG GAGATGGTTG
eGFP -----
NS3-eGFP TTAACGATTA TTGATAATGA AATATATGAA GACCTTAGTG GAGGTTGGTTG
NS3A-eGFP TTAACGATTA TTGATAATGA AATATATGAA GACCTTAGTG GAGATGGTTG
N11-eGFP -----
NS3ΔC-eGFP TTAACGATTA TTGATAATGA AATATATGAA GACCTTAGTG GAGATGGTTG
HD1-eGFP TTAACGATTA TTGATAATGA AATATATGAA GACCTTAGTG GAGATGGTTG
HD2-eGFP TTAACGATTA TTGATAATGA AATATATGAA GACCTTAGTG GAGATGGTTG

```

Mutation in NS3



```

      ....|.....| .....|.....| .....|.....| .....|.....| .....|.....|
      460          470          480          490          500
AHSV3 NS3  GCTGTCGAAG ACGATTCACG GTTTGAATTT GCTGTGTACC ACTATGTTGT
eGFP      -----
NS3-eGFP   GCTGTCGAAG ACGATTCACG GTTTGAATTT GCTGTGTACC ACTATGTTGT
NS3A-eGFP  GCTGTCGAAG ACGATTCACG GTTTGAATTT GCTGTGTACC ACTATGTTGT
N11-eGFP   -----
NS3ΔC-eGFP GCTGTCGAAG ACGATTCACG GTTTGAATTT GCTGTGTACC ACTATGTTGT
HD1-eGFP   GCTGTCGAAG ACGATTCACG GTTTGAATTT GCTGTGTACC ACTATGTTGT
HD2-eGFP   GCTGTCGAAG ACGATTCACG GTTTGAATTT GCTGTGTACC ACTAAGCGGG
                                                    HD2 mutations

```

```

      ....|.....| .....|.....| .....|.....| .....|.....| .....|.....|
      510          520          530          540          550
AHSV3 NS3  CTGCGGCTGG AAAAATATCA GATAAAATAC AGGAGGAGAT CTCACGCACA
eGFP      -----
NS3-eGFP   CTGCGGCTGG AAAAATATCA GATAAAATAC AGGAGGAGAT CTCACGCACA
NS3A-eGFP  CTGCGGCTGG AAAAATATCA GATAAAATAC AGGAGGAGAT CTCACGCACA
N11-eGFP   -----
NS3ΔC-eGFP CTGCGGCTGG AAAAATATCA GATAAAATAC AGGAGGAGAT CTCACGCACA
HD1-eGFP   CTGCGGCTGG AAAAATATCA GATAAAATAC AGGAGGAGAT CTCACGCACA
HD2-eGFP   ACGTCGCTGG AAAAATATCA GATAAAATAC AGGAGGAGAT CTCACGCACA
HD2 mutations

```

```

      ....|.....| .....|.....| .....|.....| .....|.....| .....|.....|
      560          570          580          590          600
AHSV3 NS3  AAGCGGGATA TAGCGAAGAG AGAATCATAT GTTTCGGCGG CTAGTATGTC
eGFP      -----
NS3-eGFP   AAGCGGGATA TAGCGAAGAG AGAATCATAT GTTTCGGCGG CTAGTATGTC
NS3A-eGFP  AAGCGGGATA TAGCGAAGAG AGAATCATAT GTTTCGGCGG CTAGTATGTC
N11-eGFP   -----
NS3ΔC-eGFP AAGCGGGATA TAGCGAAGAG AGAATCATAT GTTTCGGCGG CTAGTATGTC
HD1-eGFP   AAGCGGGATA TAGCGAAGAG AGAATCATAT GTTTCGGCGG CTAGTATGTC
HD2-eGFP   AAGCGGGATA TAGCGAAGAG AGAATCATAT GTTTCGGCGG CTAGTATGTC

```

```

      ....|.....| .....|.....| .....|.....| .....|.....| .....|.....|
      610          620          630          640          650
AHSV3 NS3  TTGGAGTGGG GATACGAGCG TTCTATTTAA AGAGGTAAAA TATGGCGACA
eGFP      -----
NS3-eGFP   TTGGAGTGGG GATACGAGCG TTCTATTTAA AGAGGTAAAA TATGGCGACA
NS3A-eGFP  TTGGAGTGGG GATACGAGCG TTCTATTTAA AGAGGTAAAA TATGGCGACA
N11-eGFP   -----
NS3ΔC-eGFP TTGGAGTGGG -----
HD1-eGFP   TTGGAGTGGG GATACGAGCG TTCTATTTAA AGAGGTAAAA TATGGCGACA
HD2-eGFP   TTGGAGTGGG GATACGAGCG TTCTATTTAA AGAGGTAAAA TATGGCGACA

```

```

      ....|.....| .....|.....| .....|.....| .....|.....| .....|.....|
      660          670          680          690          700
AHSV3 NS3  GCTAG-----
eGFP      ---ATGGTGAGC AAGGGCGAGG AGCTGTTTAC CGGGGTGGTG
NS3-eGFP   GC---GAATT CATGGTGAGC AAGGGCGAGG AGCTGTTTAC CGGGGTGGTG
NS3A-eGFP  GC---GAATT CATGGTGAGC AAGGGCGAGG AGCTGTTTAC CGGGGTGGTG
N11-eGFP   ---GAATT CATGGTGAGC AAGGGCGAGG AGCTGTTTAC CGGGGTGGTG
NS3ΔC-eGFP ---GAATT CATGGTGAGC AAGGGCGAGG AGCTGTTTAC CGGGGTGGTG
HD1-eGFP   GC---GAATT CATGGTGAGC AAGGGCGAGG AGCTGTTTAC CGGGGTGGTG
HD2-eGFP   GC---GAATT CATGGTGAGC AAGGGCGAGG AGCTGTTTAC CGGGGTGGTG

```

NS3 stop codon
(removed for all
fusion proteins)

EcoRI
site

eGFP
start
codon



	710	720	730	740	750
AHSV3 NS3	-----	-----	-----	-----	-----
eGFP	CCCATCCTGG	TCGAGCTGGA	CGGCGACGTA	AACGGCCACA	AGTTCAGCGT
NS3-eGFP	CCCATCCTGG	TCGAGCTGGA	CGGCGACGTA	AACGGCCACA	AGTTCAGCGT
NS3A-eGFP	CCCATCCTGG	TCGAGCTGGA	CGGCGACGTA	AACGGCCACA	AGTTCAGCGT
N11-eGFP	CCCATCCTGG	TCGAGCTGGA	CGGCGACGTA	AACGGCCACA	AGTTCAGCGT
NS3ΔC-eGFP	CCCATCCTGG	TCGAGCTGGA	CGGCGACGTA	AACGGCCACA	AGTTCAGCGT
HD1-eGFP	CCCATCCTGG	TCGAGCTGGA	CGGCGACGTA	AACGGCCACA	AGTTCAGCGT
HD2-eGFP	CCCATCCTGG	TCGAGCTGGA	CGGCGACGTA	AACGGCCACA	AGTTCAGCGT

	760	770	780	790	800
AHSV3 NS3	-----	-----	-----	-----	-----
eGFP	GTCCGGCGAG	GCGGAGGGCG	ATGCCACCTA	CGGCAAGCTG	ACCCTGAAGT
NS3-eGFP	GTCCGGCGAG	GCGGAGGGCG	ATGCCACCTA	CGGCAAGCTG	ACCCTGAAGT
NS3A-eGFP	GTCCGGCGAG	GCGGAGGGCG	ATGCCACCTA	CGGCAAGCTG	ACCCTGAAGT
N11-eGFP	GTCCGGCGAG	GCGGAGGGCG	ATGCCACCTA	CGGCAAGCTG	ACCCTGAAGT
NS3ΔC-eGFP	GTCCGGCGAG	GCGGAGGGCG	ATGCCACCTA	CGGCAAGCTG	ACCCTGAAGT
HD1-eGFP	GTCCGGCGAG	GCGGAGGGCG	ATGCCACCTA	CGGCAAGCTG	ACCCTGAAGT
HD2-eGFP	GTCCGGCGAG	GCGGAGGGCG	ATGCCACCTA	CGGCAAGCTG	ACCCTGAAGT

	810	820	830	840	850
AHSV3 NS3	-----	-----	-----	-----	-----
eGFP	TCATCTGCAC	CACCGGCAAG	CTGCCCGTGC	CCTGGCCCAC	CCTCGTGACC
NS3-eGFP	TCATCTGCAC	CACCGGCAAG	CTGCCCGTGC	CCTGGCCCAC	CCTCGTGACC
NS3A-eGFP	TCATCTGCAC	CACCGGCAAG	CTGCCCGTGC	CCTGGCCCAC	CCTCGTGACC
N11-eGFP	TCATCTGCAC	CACCGGCAAG	CTGCCCGTGC	CCTGGCCCAC	CCTCGTGACC
NS3ΔC-eGFP	TCATCTGCAC	CACCGGCAAG	CTGCCCGTGC	CCTGGCCCAC	CCTCGTGACC
HD1-eGFP	TCATCTGCAC	CACCGGCAAG	CTGCCCGTGC	CCTGGCCCAC	CCTCGTGACC
HD2-eGFP	TCATCTGCAC	CACCGGCAAG	CTGCCCGTGC	CCTGGCCCAC	CCTCGTGACC

	860	870	880	890	900
AHSV3 NS3	-----	-----	-----	-----	-----
eGFP	ACCCTGACCT	ACGGCGTGCA	GTGCTTCAGC	CGCTACCCCG	ACCACATGAA
NS3-eGFP	ACCCTGACCT	ACGGCGTGCA	GTGCTTCAGC	CGCTACCCCG	ACCACATGAA
NS3A-eGFP	ACCCTGACCT	ACGGCGTGCA	GTGCTTCAGC	CGCTACCCCG	ACCACATGAA
N11-eGFP	ACCCTGACCT	ACGGCGTGCA	GTGCTTCAGC	CGCTACCCCG	ACCACATGAA
NS3ΔC-eGFP	ACCCTGACCT	ACGGCGTGCA	GTGCTTCAGC	CGCTACCCCG	ACCACATGAA
HD1-eGFP	ACCCTGACCT	ACGGCGTGCA	GTGCTTCAGC	CGCTACCCCG	ACCACATGAA
HD2-eGFP	ACCCTGACCT	ACGGCGTGCA	GTGCTTCAGC	CGCTACCCCG	ACCACATGAA

	910	920	930	940	950
AHSV3 NS3	-----	-----	-----	-----	-----
eGFP	GCAGCACGAC	TTCTTCAAGT	CCGCCATGGC	CCGAAGGCTA	CGTCCAGGAG
NS3-eGFP	GCAGCACGAC	TTCTTCAAGT	CCGCCATGGC	CCGAAGGCTA	CGTCCAGGAG
NS3A-eGFP	GCAGCACGAC	TTCTTCAAGT	CCGCCATGGC	CCGAAGGCTA	CGTCCAGGAG
N11-eGFP	GCAGCACGAC	TTCTTCAAGT	CCGCCATGGC	CCGAAGGCTA	CGTCCAGGAG
NS3ΔC-eGFP	GCAGCACGAC	TTCTTCAAGT	CCGCCATGGC	CCGAAGGCTA	CGTCCAGGAG
HD1-eGFP	GCAGCACGAC	TTCTTCAAGT	CCGCCATGGC	CCGAAGGCTA	CGTCCAGGAG
HD2-eGFP	GCAGCACGAC	TTCTTCAAGT	CCGCCATGGC	CCGAAGGCTA	CGTCCAGGAG



```

.....|.....| .....|.....| .....|.....| .....|.....| .....|.....|
          960          970          980          990          1000
-----|-----|-----|-----|-----|
AHSV3 NS3
eGFP      CGCACCATCT TCTTCAAGGA CGACGGCAAC TACAAGACCC GCGCCGAGGT
NS3-eGFP  CGCACCATCT TCTTCAAGGA CGACGGCAAC TACAAGACCC GCGCCGAGGT
NS3A-eGFP CGCACCATCT TCTTCAAGGA CGACGGCAAC TACAAGACCC GCGCCGAGGT
N11-eGFP  CGCACCATCT TCTTCAAGGA CGACGGCAAC TACAAGACCC GCGCCGAGGT
NS3ΔC-eGFP CGCACCATCT TCTTCAAGGA CGACGGCAAC TACAAGACCC GCGCCGAGGT
HD1-eGFP  CGCACCATCT TCTTCAAGGA CGACGGCAAC TACAAGACCC GCGCCGAGGT
HD2-eGFP  CGCACCATCT TCTTCAAGGA CGACGGCAAC TACAAGACCC GCGCCGAGGT

.....|.....| .....|.....| .....|.....| .....|.....| .....|.....|
          1010         1020         1030         1040         1050
-----|-----|-----|-----|-----|
AHSV3 NS3
eGFP      GAAGTTCGAG GCGGACACCC TGGTGAACCG CATCGAGCTG AAGGGCATCG
NS3-eGFP  GAAGTTCGAG GCGGACACCC TGGTGAACCG CATCGAGCTG AAGGGCATCG
NS3A-eGFP GAAGTTCGAG GCGGACACCC TGGTGAACCG CATCGAGCTG AAGGGCATCG
N11-eGFP  GAAGTTCGAG GCGGACACCC TGGTGAACCG CATCGAGCTG AAGGGCATCG
NS3ΔC-eGFP GAAGTTCGAG GCGGACACCC TGGTGAACCG CATCGAGCTG AAGGGCATCG
HD1-eGFP  GAAGTTCGAG GCGGACACCC TGGTGAACCG CATCGAGCTG AAGGGCATCG
HD2-eGFP  GAAGTTCGAG GCGGACACCC TGGTGAACCG CATCGAGCTG AAGGGCATCG

.....|.....| .....|.....| .....|.....| .....|.....| .....|.....|
          1060         1070         1080         1090         1100
-----|-----|-----|-----|-----|
AHSV3 NS3
eGFP      ACTTCAAGGA GGACGGCAAC ATCCTGGGGC ACAAGCTGGA GTACAACCTAC
NS3-eGFP  ACTTCAAGGA GGACGGCAAC ATCCTGGGGC ACAAGCTGGA GTACAACCTAC
NS3A-eGFP ACTTCAAGGA GGACGGCAAC ATCCTGGGGC ACAAGCTGGA GTACAACCTAC
N11-eGFP  ACTTCAAGGA GGACGGCAAC ATCCTGGGGC ACAAGCTGGA GTACAACCTAC
NS3ΔC-eGFP ACTTCAAGGA GGACGGCAAC ATCCTGGGGC ACAAGCTGGA GTACAACCTAC
HD1-eGFP  ACTTCAAGGA GGACGGCAAC ATCCTGGGGC ACAAGCTGGA GTACAACCTAC
HD2-eGFP  ACTTCAAGGA GGACGGCAAC ATCCTGGGGC ACAAGCTGGA GTACAACCTAC

.....|.....| .....|.....| .....|.....| .....|.....| .....|.....|
          1110         1120         1130         1140         1150
-----|-----|-----|-----|-----|
AHSV3 NS3
eGFP      AACAGCCACA ACGTCTATAT CATGGCCGAC AAGCAGAAGA ACGGCATCAA
NS3-eGFP  AACAGCCACA ACGTCTATAT CATGGCCGAC AAGCAGAAGA ACGGCATCAA
NS3A-eGFP AACAGCCACA ACGTCTATAT CATGGCCGAC AAGCAGAAGA ACGGCATCAA
N11-eGFP  AACAGCCACA ACGTCTATAT CATGGCCGAC AAGCAGAAGA ACGGCATCAA
NS3ΔC-eGFP AACAGCCACA ACGTCTATAT CATGGCCGAC AAGCAGAAGA ACGGCATCAA
HD1-eGFP  AACAGCCACA ACGTCTATAT CATGGCCGAC AAGCAGAAGA ACGGCATCAA
HD2-eGFP  AACAGCCACA ACGTCTATAT CATGGCCGAC AAGCAGAAGA ACGGCATCAA

.....|.....| .....|.....| .....|.....| .....|.....| .....|.....|
          1160         1170         1180         1190         1200
-----|-----|-----|-----|-----|
AHSV3 NS3
eGFP      GGTGAACTTC AAGATCCGCC ACAACATCGA GGACGGCAGC GTGCAGCTCG
NS3-eGFP  GGTGAACTTC AAGATCCGCC ACAACATCGA GGACGGCAGC GTGCAGCTCG
NS3A-eGFP GGTGAACTTC AAGATCCGCC ACAACATCGA GGACGGCAGC GTGCAGCTCG
N11-eGFP  GGTGAACTTC AAGATCCGCC ACAACATCGA GGACGGCAGC GTGCAGCTCG
NS3ΔC-eGFP GGTGAACTTC AAGATCCGCC ACAACATCGA GGACGGCAGC GTGCAGCTCG
HD1-eGFP  GGTGAACTTC AAGATCCGCC ACAACATCGA GGACGGCAGC GTGCAGCTCG
HD2-eGFP  GGTGAACTTC AAGATCCGCC ACAACATCGA GGACGGCAGC GTGCAGCTCG

```



.....|.....||.....||.....||.....||.....|
1210 1220 1230 1240 1250

AHSV3 NS3

eGFP CCGACCACTA CCAGCAGAAC ACCCCCATCG GCGACGGCCC CGTGCTGCTG
NS3-eGFP CCGACCACTA CCAGCAGAAC ACCCCCATCG GCGACGGCCC CGTGCTGCTG
NS3A-eGFP CCGACCACTA CCAGCAGAAC ACCCCCATCG GCGACGGCCC CGTGCTGCTG
N11-eGFP CCGACCACTA CCAGCAGAAC ACCCCCATCG GCGACGGCCC CGTGCTGCTG
NS3ΔC-eGFP CCGACCACTA CCAGCAGAAC ACCCCCATCG GCGACGGCCC CGTGCTGCTG
HD1-eGFP CCGACCACTA CCAGCAGAAC ACCCCCATCG GCGACGGCCC CGTGCTGCTG
HD2-eGFP CCGACCACTA CCAGCAGAAC ACCCCCATCG GCGACGGCCC CGTGCTGCTG

.....|.....||.....||.....||.....||.....|
1260 1270 1280 1290 1300

AHSV3 NS3

eGFP CCCGACAACC ACTACCTGAG CACCCAGTCC GCCCTGAGCA AAGACCCCAA
NS3-eGFP CCCGACAACC ACTACCTGAG CACCCAGTCC GCCCTGAGCA AAGACCCCAA
NS3A-eGFP CCCGACAACC ACTACCTGAG CACCCAGTCC GCCCTGAGCA AAGACCCCAA
N11-eGFP CCCGACAACC ACTACCTGAG CACCCAGTCC GCCCTGAGCA AAGACCCCAA
NS3ΔC-eGFP CCCGACAACC ACTACCTGAG CACCCAGTCC GCCCTGAGCA AAGACCCCAA
HD1-eGFP CCCGACAACC ACTACCTGAG CACCCAGTCC GCCCTGAGCA AAGACCCCAA
HD2-eGFP CCCGACAACC ACTACCTGAG CACCCAGTCC GCCCTGAGCA AAGACCCCAA

.....|.....||.....||.....||.....||.....|
1310 1320 1330 1340 1350

AHSV3 NS3

eGFP CGAGAAGCGC GATCACATGG TCCTGCTGGA GTTCGTGACC GCCGCCGGGA
NS3-eGFP CGAGAAGCGC GATCACATGG TCCTGCTGGA GTTCGTGACC GCCGCCGGGA
NS3A-eGFP CGAGAAGCGC GATCACATGG TCCTGCTGGA GTTCGTGACC GCCGCCGGGA
N11-eGFP CGAGAAGCGC GATCACATGG TCCTGCTGGA GTTCGTGACC GCCGCCGGGA
NS3ΔC-eGFP CGAGAAGCGC GATCACATGG TCCTGCTGGA GTTCGTGACC GCCGCCGGGA
HD1-eGFP CGAGAAGCGC GATCACATGG TCCTGCTGGA GTTCGTGACC GCCGCCGGGA
HD2-eGFP CGAGAAGCGC GATCACATGG TCCTGCTGGA GTTCGTGACC GCCGCCGGGA

.....|.....||.....||.....||.....|
1360 1370 1380 1390

AHSV3 NS3

eGFP TCACTCTCGG CATGGACGAG CTGTACAAGT AA
NS3-eGFP TCACTCTCGG CATGGACGAG CTGTACAAGT AA
NS3A-eGFP TCACTCTCGG CATGGACGAG CTGTACAAGT AA
N11-eGFP TCACTCTCGG CATGGACGAG CTGTACAAGT AA
NS3ΔC-eGFP TCACTCTCGG CATGGACGAG CTGTACAAGT AA
HD1-eGFP TCACTCTCGG CATGGACGAG CTGTACAAGT AA
HD2-eGFP TCACTCTCGG CATGGACGAG CTGTACAAGT AA

eGFP stop
codon

B. Amino acid sequence alignments of the NS3 inserts for each of the seven fusion proteins constructed for this project. The mutation present at amino acid 148 of NS3, as well as the mutations present in the hydrophobic domains of mutants HD1-eGFP and HD2-eGFP are highlighted.

	10	20	30	40	50
AHSV3	MSLATIAENY	MMHNGNQRAI	VPYVPPPYAY	ANAPTLGGQA	GEMESMSLGI
NS3	MSLATIAENY	MMHNGNQRAI	VPYVPPPYAY	ANAPTLGGQA	GEMESMSLGI
NS3A	-----	MMHNGNQRAI	VPYVPPPYAY	ANAPTLGGQA	GEMESMSLGI
N11	MSLATIAENY	M-----	-----	-----	-----
NS3ΔC	MSLATIAENY	MMHNGNQRAI	VPYVPPPYAY	ANAPTLGGQA	GEMESMSLGI
HD1	MSLATIAENY	MMHNGNQRAI	VPYVPPPYAY	ANAPTLGGQA	GEMESMSLGI
HD2	MSLATIAENY	MMHNGNQRAI	VPYVPPPYAY	ANAPTLGGQA	GEMESMSLGI
	NS3 start codon	NS3A start codon			

	60	70	80	90	100
AHSV3	LNQAMSSTTG	ASRALKDEKA	AFGAMAEALR	DPEPIRQIKK	HVGLRTLKHL
NS3	LNQAMSSTTG	ASRALKDEKA	AFGAMAEALR	DPEPIRQIKK	HVGLRTLKHL
NS3A	LNQAMSSTTG	ASRALKDEKA	AFGAMAEALR	DPEPIRQIKK	HVGLRTLKHL
N11	-----	-----	-----	-----	-----
NS3ΔC	LNQAMSSTTG	ASRALKDEKA	AFGAMAEALR	DPEPIRQIKK	HVGLRTLKHL
HD1	LNQAMSSTTG	ASRALKDEKA	AFGAMAEALR	DPEPIRQIKK	HVGLRTLKHL
HD2	LNQAMSSTTG	ASRALKDEKA	AFGAMAEALR	DPEPIRQIKK	HVGLRTLKHL

	110	120	130	140	150
AHSV3	KIELASMRRR	YAILRVVIFM	SGCVTMATSM	AGGLTIIDNE	IYEDLSGDGW
NS3	KIELASMRRR	YAILRVVIFM	SGCVTMATSM	AGGLTIIDNE	IYEDLSG Q GW
NS3A	KIELASMRRR	YAILRVVIFM	SGCVTMATSM	AGGLTIIDNE	IYEDLSGDGW
N11	-----	-----	-----	-----	-----
NS3ΔC	KIELASMRRR	YAILRVVIFM	SGCVTMATSM	AGGLTIIDNE	IYEDLSGDGW
HD1	KIELASMRRR	YAILRVVIFM	SGC RTRDK SM	AGGLTIIDNE	IYEDLSGDGW
HD2	KIELASMRRR	YAILRVVIFM	SGCVTMATSM	AGGLTIIDNE	IYEDLSGDGW
			HD1 mutations		Mutation in NS3

	160	170	180	190	200
AHSV3	LSKTIHGLNL	LCTTMLLAAG	KISDKIQEEI	SRTKRDIAKR	ESYVSAASMS
NS3	LSKTIHGLNL	LCTTMLLAAG	KISDKIQEEI	SRTKRDIAKR	ESYVSAASMS
NS3A	LSKTIHGLNL	LCTTMLLAAG	KISDKIQEEI	SRTKRDIAKR	ESYVSAASMS
N11	-----	-----	-----	-----	-----
NS3ΔC	LSKTIHGLNL	LCTTMLLAAG	KISDKIQEEI	SRTKRDIAKR	ESYVSAASMS
HD1	LSKTIHGLNL	LCTTMLLAAG	KISDKIQEEI	SRTKRDIAKR	ESYVSAASMS
HD2	LSKTIHGLNL	LCTT KRDV AG	KISDKIQEEI	SRTKRDIAKR	ESYVSAASMS
		HD2 mutations			

	210				
AHSV3	WSGDTSVLLK	EVKYGDS			
NS3	WSGDTSVLLK	EVKYGD			
NS3A	WSGDTSVLLK	EVKYGD			
N11	-----	-----			
NS3ΔC	WSG	-----			
HD1	WSGDTSVLLK	EVKYGD			
HD2	WSGDTSVLLK	EVKYGDS			
	Dileucine motif (removed for NS3ΔC-eGFP)		NS3 stop codon (removed for all fusion proteins)		